

Response to reviewer 1

We are very grateful for the reviewer's critical comments and suggestions, which have helped us improve the paper quality substantially. We have addressed all of the comments carefully as detailed below in our point-by-point responses. Our responses start with "R:".

After a second review of Wang et al. it is evident that some improvements have been made to the manuscript. There are things remaining that need to be addressed however. Linguistics are one major obstacle. It appears that it was not thoroughly checked after the first review. Therefore, please go through this cumbersome process for your manuscript, as it sometimes hinders a correct reading of your manuscript. It also seems like some comments have been addressed with a correct response in the author's reply to the referee comments, but the necessary/appropriate change in the revised manuscript has not been done. Please check this throughout the manuscript (see also some specific examples outlined below). In the description section on the glaciers (2.1), there is still room for improvement. For example, elevations have been added for most glaciers, but I do not find any information if it is the starting point of the glaciers or the end-point. A range for where the glacier starts to the altitude where the glacier snout ends would be desired, if such information exists, as well as some estimate on the areas of the glaciers. The results section still would benefit from being synthesized in a more organized way. For example, I do not find the information on why there is no difference in ILAPs concentrations between the monsoon and non-monsoon seasons explanatory. Likewise, elevated concentrations of ILAPs in the surface of profiles would benefit from more structure, as it currently seems unorganized. Further, I did not find any comparisons of the results acquired here with other studies of ILAPs from the TP, as mentioned in the author's reply. Please see also page specific comments below.

R: We have carefully responded the following questions and concerns based on the reviewer's comments. Major changes have been listed as follows:

- (1) The introduction section is totally written (See introduction section).
- (2) We provide several new figures to give more information about the sampling locations and the topographical maps in seven glaciers (Fig. 1, Fig. 2, and Fig. S2).
- (3) We have reconstructed section 2.1, and added the necessary information about the topography of each glacier and the sampling locations (See section 2.1).

(4) A new section 3.3 is added to investigate the scavenging and washing efficiencies of the ILAPs in the vertical ice samples in the TP glaciers.

(5) We have checked the necessary changes throughout the manuscript very carefully.

We wish the reviewer could be satisfy with the significant changes in the revised manuscript.

Page specific comments

Comment 1: p. 3 lines 4-7: This is a good addition to the text. This sentence needs to be reworked however (past vs. present tense; did the reference come up with the number 30%, or where did it come from?).

R: The sentence has been deleted, and the introduction has been totally rewritten.

Comment 2: p. 3 lines 7-9: This sentence does not fit with the previous sentence. In a way it contradicts what has been said previously. Something along the lines that ILAPS have a major role in TP negative glacier mass balance, as well as temperature. This should be sorted out once the linguistics have been checked.

R: See comment 1.

Comment 3: p. 3 lines 9-10: In this sentence, BC is introduced, whereas in the previous lines ILAPs is introduced. I would urge the writers to introduce BC as a part of ILAPs (as well as the other constituents of ILAPs) before diving into BC. As it currently reads, it is confusing and jumps from one thing to another.

R: See comment 1.

Comment 4: p. 3 lines 18-20: Similar as comment above, I would introduce BC first and then provide this suitable reference to show where BC in the snow of TP comes from.

R: Changed as suggested.

Comment 5: p. 3 line 23: mineral dust (MD) has already been introduced (line 15).

R: Changed as suggested.

Comment 6: p. 4 lines 7-8: Please provide references for this statement.

R: We have provided the relative references as suggested.

Comment 7: p. 4 lines 10-14: Did all of these references provide source attribution in the snow? It is true that they reported ILAPs in snow and ice, but not source attribution.

R: We have modified this sentence as “Due to the importance of the climate effects by ILAPs, numerous snow surveys have been conducted to investigate the light absorption of ILAPs (Xu et al., 2009a, b; Doherty et al., 2010; Huang et a., 2011; Wang et al., 2013;

Dang et al., 2014), and their potential source attribution in snow and ice (Hegg et al., 2010; Zhang et al., 2013; Doherty et al., 2014; Jenkins et al., 2016; Li et al., 2016; Pu et al., 2017).”

Comment 8: p. 4 lines 22-26: This sentence needs to be reworked linguistically.

5 R: The sentence has been revised as “Doherty et al. (2014) found that the source attribution of particulate light absorption in seasonal snow is dominated by biomass/biofuel burning, soil dust and fossil fuel pollution based on the chemical and optical data from 67 North American sites.”

Comment 9: p. 4 lines 27-29: How can it be a snow survey when it was only ice sampled?

10 Also, here I think you can highlight the uniqueness of your data, for example: have all of these 7 glaciers been sampled previous for ILAPs?

R: We have changed the “snow survey” as “an ice field campaign”, and highlight the uniqueness of this large ice survey in the last paragraph of the introduction section.

Comment 10: p. 5 lines 7-10: This sentence (or possibly sentences) could be more
15 informative on what the AOD numbers imply for the areas investigated here.

R: We noted that the AOD can represent the dry aerosol deposition and its transport pathway, which could provide useful information about the possible sources of the ILAPs in the TP glaciers. As a result, we moved this sentence to the result section and reconstructed as a separate section 3.1 of “Aerosol optical depth (AOD)”.

20 Comment 11: p. 5 lines 10-12: Qiyi glacier, which classification scheme uses bucket-valley glacier? What does it actually mean with subcontinental according to physical characteristics? Please clarify what you mean ‘with an elevation of 6178 m’, highest point of glacier or lowest?

R: We have modified the description of Qiyi glacier (also see Fig. 1) and reconstructed
25 this paragraph as “Samples 1 to 19 were collected from 2013 to 2015 during the monsoon season in the center of the Qiyi glacier (QY, 39°14’ N, 97°45’ E) (Fig. 1a). The QY glacier is a small valley glacier, with the area of 2.98 km² and the length of 3.8 km. It is located in the Qilian Mountains on the north border of the TP regions. This glacier is recognized as a typical “wet island” in arid region due to its multi-land types
30 (e.g. forests, bushes, steppes and meadows).”. More information about the other glaciers could also be found in section 2.1 in the revised manuscript.

Comment 12: p. 5 lines 13-16: Xiaodongkemadi glacier, how do you know the average snowline and mean temperature there? Your own measurements or reference?

R: See comment 12, or section 2.1 in the revised manuscript.

Comment 13: p. 5 lines 16-17: Yuzhufeng glacier, is the glacier actually on top of the mountain peak? Or does it start from the peak flowing down?

5 R: See comment 12, or section 2.1 in the revised manuscript. The topography of the seven glaciers could be seen clearly in Fig. 1.

Comment 14: p. 5 line 18: Meikuang and Qiumianleiketage are located ‘in’ Kunlun Mountains not ‘over’.

R: Changed as suggested.

10 Comment 15: p. 5 lines 25-26: Hariqin and Meikuang have similar altitudes but are from different mountains? This sentence needs to be reworked. Which are the mountains?

R: See comment 12, or section 2.1 in the revised manuscript.

Comment 16: p. 5 lines 26-28: Elevation range for Gurenhekou glacier?

15 R: See comment 12, or section 2.1 in the revised manuscript. The elevation ranges for Gurenhekou glacier could also be found in Fig. 1.

Comment 17: p. 5 lines 28-30: I would argue that this sentence is added to the beginning of section 2.1 as it is an introductory statement. And is it actually enrichment of ILAPs that was studied? I would not argue that considering the results presented. How were the ice samples collected? Through drilling or?

20 R: We have moved this sentence to section 2.1, and the detailed procedure on collecting ice samples in the TP glaciers is described in section 2.1 (also see Fig. 2 and Fig. S2) as follows:

25 Wang et al. (2015) pointed out that the annual accumulation of snow/ice at the drilling site over the TP glaciers was around 2 m on average. Therefore, a 1.2-m pure clean plastic bag with a diameter of 20 cm was put into a vertical tube to collect the ice samples via wet and dry deposition during monsoon and non-monsoon seasons in each sample location from 2013 to 2015 (Fig. 2). Due to the high altitudes of these glaciers, the wet deposition in these areas were predominant by new fallen snow, while much less formed by precipitation. However, most of the samples were gathered by column
30 ice due to the multi-melting processes. Then, the column ice samples were kept frozen under -20 °C and transported to laboratory facilities at the State Key Laboratory of Cryospheric Sciences, Cold and Arid Regions Environmental and Engineering Research Institute in Lanzhou. Firstly, each sample was cut vertically into four pieces

from the top to the bottom as shown in Fig. S2, and only one of the vertical samples was cut at 10 cm resolution following clean protocols, resulting in a total of 189 samples used in this study. It should be noted that if there is a significant dirty layer inside, then, this layer will be cut and analyzed separately. Another key issue is that some of the ice samples in the top layer is not uniform due to the multi-melting processes. Therefore, several samples were cut longer or shorter than the other samples (e.g. sites 13 and 26). To minimize the losses of ILAPs to the container walls, each sample was put into a clean glass beaker and melted quickly in a microwave oven. The melted water then immediately filtered through Nuclepore filters with a pore size of 0.2- μm , as were used by Doherty et al. (2010). Further details for filtrate processing can be found in Wang et al. (2013) and Doherty et al. (2014).

Comment 18: p. 6 lines 11-14: I do not think my comments on the filters and filtering procedure in the last review (see major comments in last review) was adequately addressed in the revised manuscript section on the filtering. For example, how were the samples melted? 0.2 μm refers to what on the filter? (pore size I assume?). It is good to have the reference to previous works on how the filtering was done, but I still feel like some essential information on the filtering should be included here as suggested above.

R: See comment 18.

Comment 19: p. 7 lines 2-9: This sentence is very long, I suggest that it is shortened and it will also become more clearly what the authors did.

R: We have reconstructed this sentence as several concise sentences.

Comment 20: p. 7 lines 12-13: The definition for CBCest is not clear, please revise.

R: We have revised the definition for C_{BC}^{est} .

Comment 21: p. 8 lines 8-9: Please write out how the calculations were done, even though it is in Doherty et al. 2014, I think it would be valuable for the reader to see it how you have done it.

R: We have added the relative equation in section 2.2 as suggested.

Comment 22: p. 8 lines 9-11: Are these statements part of the optical analysis? Please place them in the appropriate section.

R: We have deleted this sentence.

Comment 23: p. 8 lines 13-14: consists of instead of ‘derived from’

R: Changed as suggested

Comment 24: p. 8 line 15: liquid instead of ‘liquor’.

R: We have deleted the relative statements of the WSOC throughout the manuscript based on two reasons. The most important novelty in this study is to investigate the mixing ratios of ILAPs and their source attributions in the TP glaciers. Another reason is that although we have confidence that our procedure on measuring WSOC in ice sample is accurate, the values of WSOC are still unexpectedly higher than those reported for the similar regions, and we can't find the possible reason yet.

5
Comment 25: p. 8 line 25-28: Please clarify what you are saying in these sentences, it is not clear what this means.

R: The sentence is irrelevant with this section, and we have deleted this sentence.

10
Comment 26: p. 8 line 30: With it mentioned here, it is unclear if the samples for ICP-MS are filtered ice samples or not?

R: We have modified this sentence more clearly as "Briefly, we acidified all melted samples directly to pH<2 with ultra-pure HNO₃, then let settle for 48h."

15
Comment 27: p. 9 line 16: What did the straightforward method entail? Would be good to provide more information on this.

R: Due to the the values are not commonly used in the seawater globally, we have deleted this sentence.

Comment 28: p. 9 line 28: What are the anthropogenic sources? You give examples of natural, so please provide it for anthropogenic also.

20
R: We have provided the relative anthropogenic sources such as fossil fuels and vehicle exhaust.

Comment 29: p. 9 line 28: Write out the EF_c abbreviation.

R: We have corrected this mistake, and revised "EF_c" as "EF".

25
Comment 30: p. 10 line 29- p. 11 line 2: You provide a higher range for glaciers in the northern TP, but not for the southern glaciers (and the lower range). Please be consistent.

R: Modified as suggested.

Comment 31: p. 11 line 3-5: This statement is not part of the results, please remove and place it elsewhere if necessary.

R: The sentences have been removed.

30
Comment 32: p. 11 lines 12-15: The way the sentence reads now, it could be interpreted that the previous studies have found that ILAPs originated from combustion sources for this glacier, whereas I believe you want to say that due to your Δ it indicates that the ILAPs come from combustion sources (and like others have indicated through their

studies on Å).

R: Because the parameter of Å is not an appropriate tracer to provide the general sources of ILAPs, we prefer to delete this sentence, and reconstructed this paragraph to illustrate the changes of the optical parameters measured by ISSW spectrophotometer.

5 Comment 33: p. 11 lines 25-29: I do not see how these statements connect with the previous sentence and how they are relevant for the results discussion.

R: We agreed with the reviewer that these sentences are irrelevant with this study, and we have deleted these sentences.

Comment 34: p. 11 line 30: Change ‘feather’ to feature.

10 R: We have corrected this mistake.

Comment 35: p. 12 lines 4-7: This statement would be more useful in the beginning of the results section, since you then talk about difference between north and south.

R: Changed as suggested

15 Comment 36: p. 12 lines 9-11: This has already been mentioned in the beginning of the results section, please add it to that.

R: Changed as suggested.

Comment 37: p. 12 lines 13-15: Is it actually local? How is that? What is the explanation for that?

R: We realized that this sentence is not reasonable, and we deleted this sentence.

20 Comment 38: p. 13 lines: 10-22: I do not see how this explains the non-existing difference between monsoon and non-monsoon seasons. Please reformulate.

R: We have reanalyzed the datasets of the BC, OC, and Fe in the glaciers during monsoon and non-monsoon seasons, and we found that there are actually significant differences in three glaciers. Therefore, we have reconstructed this paragraph as follows:

25 “Figure 6 shows the regional variations of BC, OC, and Fe concentration in each glacier during monsoon and non-monsoon seasons. Although there were significant differences between the median and average values of the ILAPs concentration in each glacier, we found that all kinds of ILAPs exhibited a similar variation from the northern QY glacier to southern GR glacier. In addition, we collected the ice samples during both monsoon
30 and non-monsoon seasons in five glaciers, only except the QY and QM glaciers. On average, the BC and OC concentrations in the HRQ, XD, and GR glacier during non-monsoon season were several orders of magnitude higher than those in monsoon seasons. The result was highly consistent with the previous study by Cong et al. (2015),

who found that although the transport pathways of air masses arriving the middle Himalayas during monsoon and non-monsoon were similar, a distinctly higher carbonaceous aerosol level was found only in the non-monsoon season. Lüthi et al. (2015) also exhibited that the atmospheric brown cloud over South Asia can climb across the Himalayan and transport of polluted air mass, which may have serious implications of the cryosphere in the TP regions. However, there appeared to be no apparent difference in the mixing ratios of ILAPs between monsoon and non-monsoon seasons in two adjacent (MK and YZF) glaciers. This can be mainly explained that, except the long-range transport of ILAPs, local air pollutants could also affect the ILAPs in the central TP regions. For instance, Huang et al. (2018) investigated that the air masses across the MK and YZF glaciers were originated from the arid western TP and Taklimakan desert regions, and the concentration of trace elements in the YZF glacier was closer to the dust sources indicating that YZF glacier was less influenced by human activities. The median values of the C_{BC}^{est} and C_{OC} (referred as the mass concentration of OC) obviously showed a slightly decreasing trend from the northern TP to the southern TP. The mass concentration of BC in northern TP glaciers was higher than that in southern TP glaciers, which showed a good agreement with Ming et al. (2013).”

Comment 39: p. 13 lines 28-30: This is valuable information that these samples were collected from the monsoon season, but I’m left wondering what it means compared to with other TP glaciers? Does it mean that your samples should be considered as high concentrations since they were collected during the monsoon? (although you have previously stated that you found no difference between seasons) Please elaborate on this for clarity.

R: See comment 39, and we also summarized the ILAPs in snow and ice in the TP glaciers by recent investigations (see Table 2 in the revised manuscript), which could provide comparable results with this study.

Comment 40: p. 14 lines 2-3: I commented on this previously. I find it confusing the way it is written now, if concentrations are increasing from the top to the bottom, or vice versa. I believe Doherty et al. (2013) found that the concentrations were highest at the surface. Please carefully review and restructure this.

R: We have revised this sentence as “This result seemed inconsistent with a previous study by Doherty et al. (2013). However, Xu et al. (2012) observed that the

concentrations of BC were higher not only at the snow surface, but also found at the bottom due to the percolation time of meltwater and superimposed ice by the temperature decline in the snowpack.”

5 Comment 41: p. 14 lines 4-6: How were the profiles more complicated compared to other profiles? In the following sentences, I do not find an explanation on this. Please add the details or take it away.

R: We have revised “complicated” to “variable”, this sentence is modified as “Fig. S7 shows that the vertical profiles of the mass mixing ratios of BC, OC, and Fe for the ice samples in the XD glacier were more variable than those for the other regions.”

10 Comment 42: p. 14 lines 11-13: This was commented on earlier and your response was sufficient. However, you have not changed this in the revised manuscript as it still reads that ILAPS are scavenged with meltwater and that leads to higher concentrations at the surface. If ILAPs are ‘washed out’ from the surface layer, it would lead to lower concentrations in the surface snow. Please review and clarify.

15 R: We have added a new section 3.3 of “Scavenging and washing efficiencies” as the reviewer suggested.

Comment 43: p. 14 lines 17-22: This discussion is interesting and is touched upon earlier in the manuscript (the argument from the previous studies for example could be introduced earlier in the manuscript. To me, it seems like there are profiles in this study
20 where the surface layer is enriched with ILAPs and then times where this is not observed. Could this information that is scattered throughout the results be collected and made into a section that is thoroughly discussed and reviewed? (possibly its own section 3.2 or something similar). I think this would only make your data stand out more and would be easier interpreted by future readers.

25 R: We agreed with the reviewer, and try to divided this discussion into a separate section 3.3 as “Scavenging and washing efficiencies”. (See section 3.3)

Comment 44: p. 14 lines 26-28: What types of samples is this based on? Please clarify.

R: We have removed the WSOC section.

30 Comment 45: p. 14 lines 28-30: The first part of the sentence almost sounds like it is part of your own results. Please rephrase this statement.

R: See comment 45.

Comment 46: p. 14 line 30- p. 15 lines 1-2: You are only referring to one study, so it is not ‘previous studies’.

R: See comment 45.

Comment 47: p. 15 lines 4-6: How do you interpret the ratios that you are presenting? Please add in the manuscript.

R: See comment 45.

5 Comment 48: p. 15 lines 7-10: I do not understand how the previous sentences lead you to this last statement in this section (3.2). Please explain this further. How are you indicating this? The last part of the statement feels more like a claim to be put in the conclusions of the manuscript.

R: See comment 45.

10 Comment 49: p. 15 lines 13-16: This was supposed to be removed and placed in your introduction according to your author's response.

R: We have modified this sentence, and then moved to the introduction section.

Comment 50: p. 15 lines 16-18: I do not see the point of this sentence in this section. Please remove.

15 R: Changed as suggested

Comment 51: p. 15 lines 18-20: I would argue that fig. S7 is more informative and sums up the results better than fig. 7. Consider changing fig. S7 to the manuscript and putting the current fig. 7 as fig. S7. If this is done

R: We have moved Fig. S7 as Fig. 7 in the revised manuscript.

20 Comment 52: please revise section 3.3 by referring to the median numbers presented in current fig. S7. Of course, specific numbers could still be highlighted in the text and then referenced to in fig. S7.

R: Changed as suggested

Comment 53: p. 16 lines 22-23: This statement should be moved to conclusions.

25 R: Changed as suggested

Comment 54: p. 18 lines 4-8: How do these statements not contradict the arguments made in the 3.3 section, where dust's role is downplayed and BC is lifted up as the major light absorber? Please clarify these statements and synchronize the results.

R: We noted the statements here are not contradictory with the previous discussion in section 3.3. The results in section 3.3 show the total light absorption of ILAPs in ice samples due to BC, OC, and MD, while the findings in section 3.5 exhibited the source attributions of the ILAPs based on the PMF receptor model.

30 Comment 55: Figure 1. The second half of the first sentence is redundant. Should not

the wavelength information (I assume it is 500 nm?) also be included?

R: We have deleted the second half of the first sentence, and modified the caption as “Spatial distribution of the averaged AOD retrieved from Aqua-MODIS at 500 nm over Tibetan Plateau from 2013 to 2015.”

5 Comment 56: Figure 2. Pictures are always good, and a nice addition to the figures. But, as the text now mentions it is ‘ice sampling locations’ how about indicating in the pictures where the samples from each glacier were taken? These pictures could be considered to be placed in the supplementary materials.

R: We have moved Fig. 1 as Fig. S1 in this revised manuscript as suggested, and a new
10 Fig. 1 is given to show the geographical maps of the seven glaciers, and their sampling locations.

15

20

25

30

Response to reviewer 2

We are very grateful for the reviewer's critical comments and suggestions, which have helped us improve the paper quality substantially. We have addressed all of the comments carefully as detailed below in our point-by-point responses. Our responses start with "R:".

Comments

After the first revision the paper has considerably improved but need more explanation before it could be accepted for publication in the journal. Some specific points have been listed below:

10 Comment 1: Still for the sampling which I am confused. The author collected "ice samples" (is it ice core?), I am not sure the authors mean supraglacial ice, granular ice or snowpits (which depends on where ice core retrieved, above ELA or ablation zone)? As in the supplementary information, depth of ice sample is more than 50 cm. For a snow pit, it is easy to dig out with 50 cm depth, but ice, you have to drill down to 50
15 cm depth manually. As my experience, drilling down to get an ice core of 50cm depth is quite hard work manually. Please clarify.

R: The equipment for collecting new snow samples was shown as follows, and a clean 1.2-m plastic bag with a diameter of 20 cm was put into the tube to collect the snow and ice samples shown in Fig. 2 in the revised manuscript. However, due to the multi-
20 melting processes in the TP regions, most of the samples were gathered as column ice samples during these field campaigns. Therefore, we prefer to use ice surveys in this study.



Figure 2. The equipment for collecting new snow samples in seven TP glaciers.

25

Comment 2: In the supplementary Table S1, for examples, in the regions 1 Qiyi glacier, are the sites from 1 to 19 located at the same latitude and longitude? The author only showed one latitude and longitude coordinates.

5 R: We feel sorry for the misleading. In order to avoid the local impacts due to human activities, we collected several snow samples at each site to better represent the regional characteristics of the ILAPs in the TP glaciers, and each of the equipment was set up for 100-300 m away from each other. As a result, the snow samples at sites 1-19 in Qiyi glacier were collected near the sample location as shown in Fig. 2a.

10 Comment 3: Page 6 line 4, “Then each ice sample was cut vertically into small pieces from the surface to the bottom”. This sentence is confused. Each ice sample means each ice core? The resolution of each pieces is not the same as shown in Table S1. Especially for the surface sample. Why you choose the surface layer is 22 cm for site 10, and 12.5cm for site 13?

15 R: We have revised the description as “Wang et al. (2015) pointed out that the annual accumulation of snow/ice at the drilling site over the TP glaciers was around 2 m on average. Therefore, a 1.2-m pure clean plastic bag with a diameter of 20 cm was put into a vertical tube to collect the ice samples via wet and dry deposition during monsoon and non-monsoon seasons in each sample location from 2013 to 2015 (Fig. 2). Due to the high altitudes of these glaciers, the wet deposition in these areas were predominant
20 by new fallen snow, while much less formed by precipitation. However, most of the samples were gathered by column ice due to the multi-melting processes. Then, the column ice samples were kept frozen under -20 °C and transported to laboratory facilities at the State Key Laboratory of Cryospheric Sciences, Cold and Arid Regions Environmental and Engineering Research Institute in Lanzhou. Firstly, each sample was cut vertically into four pieces from the top to the bottom as shown in Fig. S2, and
25 only one of the vertical samples was cut at 10 cm resolution following clean protocols, resulting in a total of 189 samples used in this study. It should be noted that if there is a significant dirty layer inside, then, this layer will be cut and analyzed separately. Another key issue is that some of the ice samples in the top layer is not uniform due to
30 the multi-melting processes. Therefore, several samples were cut longer or shorter than the other samples (e.g. sites 13 and 26). To minimize the losses of ILAPs to the container walls, each sample was put into a clean glass beaker and melted quickly in a microwave oven. The melted water then immediately filtered through Nuclepore filters

with a pore size of 0.2- μm , as were used by Doherty et al. (2010). Further details for filtrate processing can be found in Wang et al. (2013) and Doherty et al. (2014).”

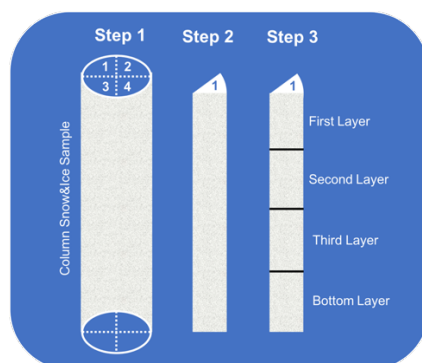


Figure S2. The cutting processes of the column ice samples collected in each glacier following clean protocols.

Comment 4: WSOC measurements: In the previous studies of WSOC from the glaciers, precipitation and river waters in the Tibetan Plateau, e.g., Li Xiangying et al. (2018), Hu Zhaofu et al. (20187), Liu Yanmei et al. (2016), Li Chaoliu et al. (2018), Qu Bin et al. (2017), the concentrations of WSOC is much lower than the data the author measured. What kind of bottles (or vials) did the authors use to collect ice samples in this study? Any pretreatment? Any blanks of WSOC measurements? When the author cut the ice pieces, any pretreatment to shaving the outer layer (avoiding contamination) where contacted with the plastic bags? Dose the author mean the pretreatment as same as that for ice core? Any explanation for the very higher WSOC concentrations in this study?

R: Due to the dataset the WSOC concentrations is unexpectedly higher than the previous studies, and this scope mainly focuses on the ILAPs in the TP glaciers, we decide to delete this section of WSOC in this study. However, although we delete the dataset of WSOC concentration in this study, we have fully confidence that the procedure on measuring WSOC in ice samples is accurate.

Comment 5: The author mentioned “10 ml refers to the amount of sample solution after filtration that used to measure the WSOC concentration,” what kind of filters used to filter the WSOC samples?

R: See comments 4.

Comment 6: For Fe analysis, dose the author use the bulk sample or the filtered sample? How many days you used for acidifying the samples?

R: We use the bulk sample to analyze the concentration of Fe, and at least 48 hours were used for acidifying the samples.

5 Comment 7: In the response to Reviewer 2, the author declared that “we referred to attribute the major industrial pollution and biomass burning sources to the anthropogenic emission sources.” As an important biomass burning, how does the author to eliminate the impact of forest fire (natural source)?

R: Agreed, we can’t separate the forest fire into natural and anthropogenic sources by using the PMF receptor model in this study. Therefore, we have revised the relative statements in this revised manuscript.

10 Comment 8: For the MD data (average concentration is 241 ± 452 ng g⁻¹ on TP glaciers in the abstract) in this study, I can’t see the AI concentrations, but I think the unit should be ppm rather than ppb as compared with previous studies from glaciers in the Tibetan Plateau. AI concentrations may be much higher than that of Fe in glaciers, thus calculation should be larger the current data.

15 R: We have added the dataset of AI in Table S1, and convert the unit of ng g⁻¹ to ppm for AI and Fe. We also noted the concentration of MD in this study is calculated by using the AI concentration based on equation 5 in the revised manuscript.

20 Comment 9: In the conclusion, “The lower absorption Ångström exponent ($A_{\text{tot}} < 2$) suggested that the sites 30, 51, and 56-58, 65 were primarily influenced by fossil fuel emission, whereas the rest of the sites were heavily influenced by mineral dust and biomass burning.” Sites 30, 5a, and 56-58, 65, were corresponding to which glacier and which season? Why for the same glacier, the influence of fossil fuel emission, mineral dust and biomass burning are difference? Any reasons? In the conclusion, I prefer to see the clear summary of region rather than different sites.

25 R: We have reconstructed the conclusion section for the regional averages rather than different sites.

30

Reference

1. Cong, Z., Kang, S., Kawamura, K., Liu, B., Wan, X., Wang, Z., Gao, S., and Fu, P.: Carbonaceous aerosols on the south edge of the Tibetan Plateau: concentrations, seasonality and sources, *Atmos. Chem. Phys.*, 15, 1573-1584, 10.5194/acp-15-1573-2015, 2015.
2. Dang, C., and Hegg, D. A.: Quantifying light absorption by organic carbon in Western North American snow by serial chemical extractions, *J. Geophys. Res.-Atmos.*, 119, 10.1002/2014jd022156, 2014.
3. Doherty, S. J., Dang, C., Hegg, D. A., Zhang, R. D., and Warren, S. G.: Black carbon and other light-absorbing particles in snow of central North America, *J. Geophys. Res.-Atmos.*, 119, 12807-12831, 10.1002/2014JD022350, 2014.
4. Doherty, S. J., Grenfell, T. C., Forsstrom, S., Hegg, D. L., Brandt, R. E., and Warren, S. G.: Observed vertical redistribution of black carbon and other insoluble light-absorbing particles in melting snow, *J. Geophys. Res.-Atmos.*, 118, 5553-5569, 10.1002/Jgrd.50235, 2013.
5. Doherty, S. J., Warren, S. G., Grenfell, T. C., Clarke, A. D., and Brandt, R. E.: Light-absorbing impurities in Arctic snow, *Atmos. Chem. Phys.*, 10, 11647-11680, 10.5194/acp-10-11647-2010, 2010.
6. Hegg, D. A., Warren, S. G., Grenfell, T. C., Doherty, S. J., and Clarke, A. D.: Sources of light-absorbing aerosol in arctic snow and their seasonal variation, *Atmos. Chem. Phys.*, 10, 10923-10938, 10.5194/acp-10-10923-2010, 2010.
7. Huang, J. P., Fu, Q. A., Zhang, W., Wang, X., Zhang, R. D., Ye, H., and Warren, S. G.: Dust and Black Carbon in Seasonal Snow across Northern China, *Bull. Amer. Meteor. Soc.*, 92, 175-181, 10.1175/2010bams3064.1, 2011.
8. Huang, J., Li, Y., Li, Z., and Xiong, L.: Spatial variations and sources of trace elements in recent snow from glaciers at the Tibetan Plateau. *Environmental Science and Pollution Research*, 25(8), 7875–7883, 10.1007/s11356-017-0904-3, 2018.
9. Jenkins, M., Kaspari, S., Kang, S. C., Grigholm, B., and Mayewski, P. A.: Tibetan Plateau Geladaindong black carbon ice core record (1843-1982): Recent increases due to higher emissions and lower snow accumulation, *Adv Clim Chang Res*, 7, 132-138, 10.1016/j.accre.2016.07.002, 2016.
10. Li, C. L., Bosch, C., Kang, S. C., Andersson, A., Chen, P. F., Zhang, Q. G., Cong,

- Z. Y., Chen, B., Qin, D. H., and Gustafsson, O.: Sources of black carbon to the Himalayan-Tibetan Plateau glaciers, *Nat. Commun.*, 7, ARTN 12574, 10.1038/ncomms12574, 2016.
- 5 11. Lüthi, Z. L., Škerlak, B., Kim, S.-W., Lauer, A., Mues, A., Rupakheti, M., and Kang, S.: Atmospheric brown clouds reach the Tibetan Plateau by crossing the Himalayas, *Atmos. Chem. Phys.*, 15, 6007-6021, <https://doi.org/10.5194/acp-15-6007-2015>, 2015.
- 10 12. Ming, J., Xiao, C. D., Du, Z. C., and Yang, X. G.: An overview of black carbon deposition in High Asia glaciers and its impacts on radiation balance, *Adv. Water Res.*, 55, 80-87, 10.1016/j.advwatres.2012.05.015, 2013.
- 13 13. Pu, W., Wang, X., Wei, H. L., Zhou, Y., Shi, J. S., Hu, Z. Y., Jin, H. C., and Chen, Q. L.: Properties of black carbon and other insoluble light-absorbing particles in seasonal snow of northwestern China, *Cryosphere*, 11, 1213-1233, 10.5194/tc-11-1213-2017, 2017.
- 15 14. Wang, M., Xu, B., Cao, J., et al: Carbonaceous aerosols recorded in a southeastern Tibetan glacier: analysis of temporal variations and model estimates of sources and radiative forcing, *Atmos. Chem. Phys.*, 15, 1191-1204, 10.5194/Acp-15-1191-2015, 2015.
- 20 15. Wang, X., Doherty, S. J., and Huang, J. P.: Black carbon and other light-absorbing impurities in snow across Northern China, *J. Geophys. Res.-Atmos.*, 118, 1471-1492, 10.1029/2012jd018291, 2013.
- 25 16. Xu, B. Q., Cao, J. J., Hansen, J., Yao, T. D., Joswia, D. R., Wang, N. L., Wu, G. J., Wang, M., Zhao, H. B., Yang, W., Liu, X. Q., and He, J. Q.: Black soot and the survival of Tibetan glaciers, *Proc. Nat. Acad. Sci.*, 106, 22114-22118, 10.1073/pnas.0910444106, 2009a.
17. Xu, B. Q., Wang, M., Joswiak, D. R., Cao, J. J., Yao, T. D., Wu, G. J., Yang, W., and Zhao, H. B.: Deposition of anthropogenic aerosols in a southeastern Tibetan glacier, *J. Geophys. Res.-Atmos.*, 114, 10.1029/2008jd011510, 2009b.
- 30 18. Xu, B. Q., Cao, J. J., Joswiak, D. R., Liu, X. Q., Zhao, H. B., and He, J. Q.: Post-depositional enrichment of black soot in snow-pack and accelerated melting of Tibetan glaciers, *Environ. Res. Lett.*, 7, 10.1088/1748-9326/7/1/014022, 2012.
19. Zhang, R., Hegg, D. A., Huang, J., and Fu, Q.: Source attribution of insoluble light-absorbing particles in seasonal snow across northern China, *Atmos. Chem. Phys.*,

13, 6091-6099, 10.5194/acp-13-6091-2013, 2013.

Quantifying light absorption and its source attribution of insoluble light-absorbing particles in Tibetan Plateau glaciers from 2013-2015

Xin Wang^{1,*}, Hailun Wei¹, Jun Liu¹, Baiqing Xu^{1,2,*}, Mo Wang², Mingxia Ji¹, and Hongchun Jin³

¹ Key Laboratory for Semi-Arid Climate Change of the Ministry of Education, College of Atmospheric Sciences, Lanzhou University, Lanzhou, 730000, China

² Key Laboratory of Tibetan Environment Changes and Land Surface Processes, Institute of Tibetan Plateau Research, Chinese Academy of Sciences, Beijing 100085, China

³ [KuWeather Science and Technology, Haidian, Beijing, 100085, China](#)

Correspondence to: X. Wang (wxin@lzu.edu.cn), and B. Xu (baiqing@itpcas.ac.cn)

带格式的: 左侧: 3.17 厘米, 右侧: 3.17 厘米

带格式的: 两端对齐

删除的内容: and

带格式的: 上标

带格式的: 两端对齐

带格式的: fontstyle01, 字体: (默认) 宋体, (中文) + 中文正文 (DengXian), 小四

带格式的: fontstyle01, 字体: 宋体

带格式的: fontstyle01

删除的内容:)^d

带格式的: 两端对齐

Abstract. Amounts of insoluble light-absorbing particles (ILAPs) deposited on the surface of snow and ice can significantly reduce the snow albedo and accelerate the snow melting process. In this study, 67 ice samples were collected in seven glaciers over the Tibetan Plateau (TP) from May 2013 to October 2015. The mixing ratio of black carbon (BC), organic carbon (OC), and mineral dust (MD) was measured using an integrating sphere/integrating sandwich spectrophotometer (ISSW) system associated with the chemical analysis by assuming that the light absorption of mineral dust is due to iron oxide. The results indicated that the mass mixing ratios of BC, OC, and MD showed a large variation of 10-3100 ng g⁻¹, 10-17000 ng g⁻¹, 10-3500 ng g⁻¹, with mean values of 220±400 ng g⁻¹, 1360±2420 ng g⁻¹, 240±450 ng g⁻¹ on TP glaciers during the entire ice field campaign, respectively. Although the mineral dust was assumed to be the highest contributor to the mass loading of ILAPs, we noted that the averaged light absorption of BC (50.7%) and OC (33.2%) was largely responsible for the measured light absorption in the TP glaciers at the wavelengths of 450-600 nm. The chemical elements and the selected carbonaceous particles were also analyzed for the source attributions of the particulate light absorption based on a positive matrix factorization (PMF) receptor model. On average, the industrial pollution (33.1%), biomass/biofuel burning (29.4%), and mineral dust (37.5%) were the major sources of the ILAPs in TP glaciers.

删除的内容: 7 high mountain

删除的内容: regions

删除的内容: IS

删除的内容: a

删除的内容: 218

删除的内容: 397

删除的内容: 1357

删除的内容: 2417

删除的内容: 241

删除的内容: 452

删除的内容: of

删除的内容: Although the mineral dust assumed to be the highest contributor to the mass loading of ILAPs, we noted that the averaged light absorption of BC (50.7%) and ISOC (33.2%) was largely responsible for the measured light absorption in the high mountain glaciers at the wavelengths of 450-600 nm.

带格式的: 两端对齐

删除的内容: ¶

1 Introduction

Ample evidence indicated that the snow albedo at visible wavelengths is largely dominant by black carbon (BC) (Warren and Wiscombe, 1980, 1985; Brandt et al., 2011; Hadley and Kirchstetter, 2012). For instance, a mixing ratio of 10 ng g⁻¹ of BC in snow can reduce snow albedo by 1%, which has a similar effect to that of 500 ng g⁻¹ of dust at 500 nm (Warren and Wiscombe, 1980; Warren, 1982; Wang et al., 2017). Chylek et al. (1984) indicated that the absorbing efficiency of BC is higher in snow than in the atmosphere due to more sunlight scattering in snow. Conway et al. (1996) measured a snow albedo reduction of 0.21 and a 50% increase in the ablation rate of natural snow attributed to 500 ng g⁻¹ BC contamination. Liou et al. (2011) developed a geometric-optics surface-wave approach to demonstrate the snow albedo reduction by as much as ~5–10% due to small amounts of BC internally mixed with snow grains. Totally, BC accounts for 85% of absorption by all insoluble light-absorbing impurities (ILAPs) in snow at the wavelength of 400-700 nm (Bond et al., 2013). Due to the impact of BC on snow and ice albedos, the “efficacy” of this BC-snow forcing is twice as effective as CO₂, and may have contributed to global warming of the past century in the Northern Hemisphere (Hansen and Nazarenko, 2004).

The Tibetan Plateau (TP), known as the highest plateau in the world and its surrounding areas, contains the largest store of snow and ice outside the polar regions (Qin et al., 2006). However, ~82% of the plateau's glaciers have retreated, and 10% of its permafrost has degraded in the past decade (Qiu, 2008; Yao et al., 2012). Xu et al. (2009a, b) indicated that the BC deposited in snow and ice potentially lead the melting seasons earlier, and the large retreat of these glaciers across the TP regions may affect the atmospheric circulation and ecosystem at regional and global scales in multiple ways (Qian et al., 2011; Skiles et al., 2012; Sand et al., 2013). Therefore, the BC content is considered one of the major absorbers to lead great decrease in length and area of TP glaciers (Xu et al., 2006, 2009a; Qian et al., 2015; Li et al., 2016).

In addition to BC, organic carbon (OC) and mineral dust (MD) recognized as the other types of ILAPs that substantially contribute to springtime snowmelt and surface warming through the snow darkening effects (Painter et al., 2010, 2012; Huang et al., 2011; Kaspari

已下移 [1]: The Tibetan Plateau (TP), known as the highest plateau in the world, and its surrounding areas contain the largest snow and ice mass outside the polar regions (Qin et al., 2006).

删除的内容: The Tibetan Plateau (TP), known as the highest ... [1]

删除的内容: evidence has indicated

删除的内容: the deposition of

删除的内容: insoluble light-absorbing particles (ILAPs) ... [2]

删除的内容: The unusual increase in temperature over the ... [3]

删除的内容: example

删除的内容: mineral

删除的内容: on the albedo of snow and ice

删除的内容: wavelength

带格式的: 字体: 小四, 字体颜色: 文字 1

删除的内容: .

带格式的: 字体: 小四, 字体颜色: 文字 1

带格式的: 字体: 小四, 字体颜色: 文字 1, 下标

带格式的: 字体: 小四, 字体颜色: 文字 1

带格式的 ... [4]

带格式的: 字体: (默认) Times, 字体颜色: 黑色

带格式的: 两端对齐, 缩进: 首行缩进: 0 字符, 无孤行控制

删除的内容: also

删除的内容: Yasunari et al., 2015;

删除的内容: ;Painter et al., 2010;

et al., 2014; Wang et al., 2013, 2014; Yasunari et al., 2015). However, the optical properties of OC in snow are still absent due to limited small-scale field campaigns and technical limitations. For instance, the OC concentrations extracted at Antarctic sites are unexpectedly higher ranging from 80 to 360 ng g⁻¹ than those reported for Greenland (10–40 ng g⁻¹) and Alpine (45–98 ng g⁻¹) for pre-industrial ice (Federer et al., 2008; Preunkert et al., 2011). Furthermore, there are still significant uncertainties in estimating the light absorption by different types of OC associated with both the chemical and optical analyses from snow samples across western North America (Dang et al., 2014). Although the contribution of OC to the global warming is generally lower than BC, but still significant mainly over southeastern Siberia, northeastern East Asia, and western Canada (Yasunari et al., 2015). As summarized by Flanner et al. (2009), consideration of OC in snow is a key approach for better estimating the climate effects in global models due to the absorption of solar radiation by other ILAPs from the ultraviolet to visible wavelengths.

It is well known that the light absorption capacity of MD mainly depends on the iron oxides (hereafter referred to Fe) (Alfaro et al., 2004; Lafon et al., 2004, 2006; Moosmuller et al., 2012). Fe (primarily hematite and goethite) imparted a yellow-red color is a major component, which affects the ability of mineral dust to absorb sunlight at short wavelengths, then alters the dust's radiative properties and may influence the climate (Takahashi et al., 2011; Jeong et al., 2012; Zhou et al., 2017). Cong et al. (2018) indicated that the goethite was predominant form of Fe (81% to 98 % in mass fraction) among the glaciers in the TP regions. Painter et al. (2007) pointed out that snow cover duration in a seasonally snow-covered mountain was shortened by 18 to 35 days due to the deposition of disturbed desert dust. Wang et al. (2013) revealed that the light absorption was major dominated by OC across the grassland of Inner Mongolia across northern China, while the snow particulate light absorption was mainly contributed by local soil and desert dust at the northern boundary of the TP regions.

Due to the importance of the climate effects by ILAPs, numerous snow surveys have been conducted to investigate the light absorption of ILAPs (Xu et al., 2009a, b; Doherty et al., 2010; Huang et al., 2011; Wang et al., 2013; Dang et al., 2014), and their potential source attribution in snow and ice (Hegg et al., 2010; Zhang et al., 2013a; Doherty et al., 2014

删除的内容: Wang et al., 2013;Huang et al., 2011

带格式的: 字体: 小四

带格式的: 两端对齐

删除的内容: Lafon et al., 2006

带格式的: 字体: 小四

带格式的: 字体: 小四, 字体颜色: 文字 1

带格式的: 字体: 小四, 字体颜色: 文字 1

带格式的: 字体: 小四, 字体颜色: 文字 1

删除的内容: (Jeong et al., 2012)

带格式的: 字体颜色: 自动设置

删除的内容: . The Tibetan Plateau (TP), known as the highest plateau in the world, and its surrounding areas contain ... [6]

已移动(插入) [1]

Jenkins et al., 2016; Li et al., 2016; Pu et al., 2017), Hegg et al. (2009) indicated that the light absorption by ILAPs in Arctic snow is mainly originated from biomass burning, pollution, and marine sources based on a positive matrix factorization (PMF) receptor model. Doherty et al. (2014) found that the source attribution of particulate light absorption in seasonal snow is dominated by biomass/biofuel burning, soil dust, and fossil fuel pollution based on the chemical and optical data from 67 North American sites. Up to now, the light absorption and emission sources of ILAPs remain poorly understood. Increasing the in-situ measurements of ILAPs in snow and ice is the most urgent task to explore the glacier retreat, especially in the TP regions. Here, we performed a large survey on collecting column ice samples on seven glaciers in the TP regions during the monsoon and non-monsoon seasons from 2013-2015. By using an integrating sphere/integrating sandwich spectrophotometer (ISSW) system associated with the chemical analysis, the particulate light absorption by BC, OC, and MD in TP glaciers was evaluated. Finally, the relative contributions of their emission sources in these glaciers was explored based on a PMF receptor model.

2 Site description and methods

2.1 Site description and sample collection

According to the second Chinese glacier inventory dataset, Fig. 1 exhibits the topographical maps in each glacier associated with the sampling locations (Liu et al., 2014). Fig. S1 shows the pictures of the sampling locations in all seven glaciers, and all these glaciers are arranged from north to south according to their latitude and longitude in this study. Basically, the sampling locations are selected to be at least 50 km apart from the main road and the cities to minimize the effects of local sources. ~67 column ice samples were gathered during monsoon and non-monsoon seasons along a south-north transect over the TP regions from 2013-2015. It is worth noting that the seven glaciers can represent different climate and land surface types gradually from the dry area to wet area along the northern to the southern over the TP regions.

Samples 1 to 19 were collected from 2013 to 2015 during the monsoon season in the center of the Qiyi glacier (QY, 39°14' N, 97°45' E) (Fig. 1a). The QY glacier is a small valley glacier, with the area of 2.98 km² and the length of 3.8 km. It is located in the Qilian

删除的内容: 4

Recently, Li et al. (2016) exhibited that similar contributions from fossil fuel (46±11%) and biomass (54±11%) combustion of the BC sources based on the dual-carbon isotopes technique from aerosol and snowpit samples in the TP regions. Bond et al. (2013) indicated that the best estimate of climate forcing from BC deposition on snow and sea ice in

带格式的

已移动(插入) [2]

已上移 [2]: Due to the importance of the climate effects by

删除的内容: For instance,...Hegg et al. (2009) found

带格式的: 两端对齐

删除的内容: present ...erformed a snow ...large survey on

带格式的: 字体: (默认) Times New Roman, 字体颜色: 自动设置

删除的内容: 4

带格式的: 字体: (默认) Times New Roman, (中文) 华文宋体, 字体颜色: 文字 1

带格式的

已移动(插入) [5]

删除的内容: To investigate the enrichment of ILAPs via wet

已下移 [6]: As shown in Fig. 1, the spatial distribution of

已移动(插入) [4]

删除的内容: Therefore, the ice samples numbered in

带格式的: 两端对齐

带格式的

删除的内容: Qiyi

带格式的: 非突出显示

删除的内容: ...lacier (39°14' N, 97°45' E)

带格式的: 字体: 小四, 字体颜色: 文字 1

删除的内容: eastern part

Mountains on the north border of the TP regions. This glacier is recognized as a typical “wet island” in arid region due to its multi-land types (e.g. forests, bushes, steppes and meadows).

Samples 20 to 22 were collected during the non-monsoon season in the southeast Qiumianleiketage glacier (QM, 36°70' N, 90°73' E), which is originated from the Kunlun Mountains of the Qinghai-Tibet Plateau (Fig. 1b). The length of the QM glacier is 2.6 km, and the area is 1.73 km².

Samples 23-32 were collected in the northern Meikuang glacier during both monsoon and non-monsoon season (MK, 35°42' N, 94°12' E). The MK glacier is located in the eastern Kunlun Mountains, where is characterized by alluvial deposits and sand dunes. The MK glacier is 1.8 km in length with an area of 1.1 km² (Fig. 1c).

As shown in Fig. 1d, samples 33-44 were collected in the southwest Yuzhufeng glacier (YZF, 35°38' N, 94°13' E). The YZF glacier is adjacent to MK glacier with the highest peak of 6178 m across the eastern Kunlun Mountains at the northern margin of the TP regions. The glacier is surrounded by a small quantity of ferns, forests and some bushes due to the high altitude as well as the cold and arid climate.

Samples 45-49 were collected in the center of Hariqin glacier (HRQ, 33°14' N, 92°09' E), which is located at the headwaters of the Dongkemadi river on the northern slope of the Tanggula Mountains in the central region of the Qinghai-Tibetan Plateau (Fig. 1e). The HRQ glacier face north, with a mountain peak of 5820 m a.s.l. to its terminus of 5400 m a.s.l.

Samples 50-60 were collected in the southern Xiaodongkemadi glacier (XD, 33°04' N, 92°04' E). The XD glacier is adjacent to HRQ glacier, with an area of 1.767 km² and 2.8 km in length (Fig. 1f). The elevations of the glacier from the peak to its terminus are 5900 and 5500 m a.s.l., respectively. It has a cold steppe landscape, mainly surrounded by tundra.

Samples 61-67 were collected in the eastern Gurenhekou glacier (GR, 30°19' N, 90°46' E). The GR glacier is relatively small and cold alpine-type valley glacier, in the central part of the southern TP, which is seated about 90 km northwest of Lhasa, the capital city of Tibet (Fig. 1g). The glacier area is 1.4 km², with a length and width of 2.5 km and 0.6 km, and the elevation is in the range of 5600 and 6000 m a.s.l. Kang et al. (2009) and Bolch et al.

删除的内容: ...f the ... [16]
带格式的: 非突出显示

删除的内容: ,
带格式的 ... [17]

删除的内容: with an elevation of 6178 m. It is classified bucket-valley glaciers according to its shape, and is classified subcontinental glacier according to the physical characteristics of glacier.

带格式的 ... [18]

带格式的 ... [19]

带格式的 ... [20]

带格式的 ... [21]

带格式的 ... [22]

带格式的: 非突出显示
删除的内容: The

带格式的 ... [23]

删除的内容: located

带格式的 ... [24]

删除的内容: in the central Qinghai-Tibetan Plateau... It is 2.8 km in length and the average snowline is 5560 m a.s.l.... The elevations of the glacier from the peak to its terminus are 5900 and 5500 m a.s.l., respectively. The annual ... [25]

带格式的: 字体: 小四, 字体颜色: 文字 1

删除的内容: ...The surrounding region is ... [26]

带格式的: 两端对齐, 无孤行控制

带格式的: 非突出显示

删除的内容: The Yuzhufeng glacier (35°38' N, 94°13' E) is ... [27]

带格式的 ... [28]

删除的内容: located

带格式的 ... [29]

删除的内容: on the south-eastern margin of the Nyenchen ... [30]

带格式的 ... [31]

(2010) indicated that the Gurenhekou glacier is mainly influenced by both the continental climate of central Asia and the Indian monsoon system.

Wang et al. (2015) pointed out that the annual accumulation of snow/ice at the drilling site over the TP glaciers was around 2 m on average. Therefore, a 1.2-m pure clean plastic bag with a diameter of 20 cm was put into a vertical tube to collect the ice samples via wet and dry deposition during monsoon and non-monsoon seasons in each sample location from 2013 to 2015 (Fig. 2). Due to the high altitudes of these glaciers, the wet deposition in these areas were predominant by new fallen snow, while much less formed by precipitation. However, most of the samples were gathered by column ice due to the multi-melting processes. Then, the column ice samples were kept frozen under -20 °C and transported to laboratory facilities at the State Key Laboratory of Cryospheric Sciences, Cold and Arid Regions Environmental and Engineering Research Institute in Lanzhou. Firstly, each sample was cut vertically into four pieces from the top to the bottom as shown in Fig. S2, and only one of the vertical samples was cut at 10 cm resolution following clean protocols, resulting in a total of 189 samples used in this study. It should be noted that if there is a significant dirty layer inside, then, this layer will be cut and analyzed separately. Another key issue is that some of the ice samples in the top layer is not uniform due to the multi-melting processes. Therefore, several samples were cut longer or shorter than the other samples (e.g. sites 13 and 26). To minimize the losses of ILAPs to the container walls, each sample was put into a clean glass beaker and melted quickly in a microwave oven. The melted water then immediately filtered through Nuclepore filters with a pore size of 0.2- μm , as were used by Doherty et al. (2010). Further details for filtrate processing can be found in Wang et al. (2013) and Doherty et al. (2014).

2.2 Optical analysis

An updated integrating sphere/integrating sandwich spectrophotometer (ISSW) was used to calculate the mass mixing ratio of BC in the ice samples, which is similar with the instrument developed by Grenfell et al. (2011). Compared with the ISSW spectrophotometer developed by Grenfell et al. (2011), the major difference is that we used two integrating spheres instead of the integrating sandwich diffuser to reduce the diffuse radiation during the measuring process. This ISSW spectrophotometer measures the light

已上移 [5]: To investigate the enrichment of ILAPs via wet and dry deposition on glaciers, we collected 67 ice samples in seven glaciers on the Tibetan Plateau from May 2013 to October 2015 (Fig. 2).

删除的内容: To investigate the enrichment of ILAPs via wet and dry deposition on glaciers, we collected 67 ice samples in seven glaciers on the Tibetan Plateau from May 2013 to October 2015 (Fig. 2). The collected ice samples were preserved in 0.5-m pure clean plastic bag with a diameter of 20 cm, and kept frozen at the State Key Laboratory of Cryospheric Sciences, Cold and Arid Regions Environmental and Engineering Research Institute in Lanzhou.

带格式的: ... [32]

带格式的: 两端对齐, 段落间距段后: 0 磅, 行距: 单倍行距

删除的内容: ...e column ice samples were kept frozen under -20 °C and transported to laboratory facilities at the State Key Laboratory of Cryospheric Sciences, Cold and Arid ... [33]

已上移 [4]: Therefore, the ice samples numbered in chronological order from 1 to 19 was in the Qiye glacier, while sites 20-22, 23-32, 33-44, 45-49, 50-60, and 61-67 in

删除的内容: The ...ice samples were filtered at laboratories in Lanzhou University. The ...amples...wasere...put into a clean glass beaker and quickly ...elted quickly in a ... [34]

删除的内容: Additional ...urther details on ...or filtrate processingthe ice filtration processes...have ...an be found been previously reported (...n Wang et al. (2013)Doherty et ... [35]

带格式的: 两端对齐

删除的内容: is ...as used to calculate the mass mixing ratio of BC in the ice samplesnow... which is similar with the instrument developed by Grenfell et al. (2011). Compared ... [36]

attenuation spectrum from 400 to 700 nm. The total light attenuation spectrum is extended over the full spectral range by linear extrapolation from 400 to 300 and from 700 to 750 nm. Light attenuation is nominally only sensitive to ILAPs on the filter because of the diffuse radiation field and the sandwich structure of two integrated spheres in the ISSW (Doherty et al., 2014). Briefly, the transmitted light detected by the system for an ice sample, $S(\lambda)$, is compared with the signal detected for a blank filter, $S_0(\lambda)$, and the relative attenuation (A_{tn}) is expressed as:

$$A_{tn} = \ln[S_0(\lambda)/S(\lambda)] \quad (1)$$

The MACs and the absorption Ångström exponents (\AA) for BC, OC, and Fe used in this study could be found in Wang et al. (2013). By using this technique, we can estimate the following parameters included equivalent BC (C_{BC}^{equiv}), maximum BC (C_{BC}^{max}), estimated BC (C_{BC}^{est}), fraction of light absorption by non-BC ILAPs (f_{non-BC}^{est}), the absorption Ångström exponent of non-BC ILAPs (\AA_{non-BC}) and the total absorption Ångström exponent (\AA_{tot}). These parameters are defined as follows:

1. C_{BC}^{max} (ng g⁻¹): maximum BC is the maximum possible BC mixing ratio in snow by assuming that all light absorption is due to BC at the wavelengths of 650-700 nm.
2. C_{BC}^{est} (ng g⁻¹): estimated BC is the estimated true mass of BC in snow derived by separating the spectrally resolved total light absorption and non-BC fractions.
3. C_{BC}^{equiv} (ng g⁻¹): equivalent BC is the amount of BC that would be needed to produce absorption of solar energy by all insoluble particles in snow for the wavelength-integrated from 300-750 nm.
4. \AA_{tot} : absorption Ångström exponent is calculated for all insoluble particles deposited on the filter between 450 and 600 nm.
5. \AA_{non-BC} : non-BC absorption Ångström exponent is derived from the light absorption by non-BC components of the insoluble particles in snow between 450-600 nm.
6. f_{non-BC}^{est} (%): fraction of light absorption by non-BC light absorbing particles is the integrated absorption due to non-BC light absorbing particles, which is weighted by the down-welling solar flux at the wavelengths of 300-750 nm.

It is well known that the aerosol composition and the size distribution are key parameters that affect the absorption Ångström exponent. Doherty et al. (2010) reported that the value

删除的内容: (Grenfell et al., 2011)

删除的内容: are

带格式的: 字体: 小四, 字体颜色: 文字 1

带格式的: 字体: 小四, 字体颜色: 文字 1

删除的内容: The following measured parameters included equivalent BC (C_{BC}^{equiv}), maximum BC (C_{BC}^{max}), estimated BC (C_{BC}^{est}), fraction of light absorption by non-BC ILAPs (f_{non-BC}^{est}), the non-BC absorption Ångström exponent (\AA_{non-BC}) and the absorption Ångström exponent of all ILAPs (\AA_{tot}), were calculated by using the wavelength dependence of the measured spectral light absorption and by assuming that the MACs of the BC, OC, and Fe are 6.3, 0.3, and 0.9 m² g⁻¹, respectively, at 550 nm and that the absorption Ångström exponents (\AA or AAE) for BC, OC, and Fe are 1.1, 6, and 3, respectively (Doherty et al., 2010, 2014; Grenfell et al., 2011; Wang et al., 2013). These parameters are defined as follows: ↓

删除的内容: snow

删除的内容: mixing ratio

删除的内容: .

带格式的: 字体: 小四

删除的内容: ↓

删除的内容: defined

删除的内容: as

删除的内容: from snow

带格式的: 两端对齐, 定义网格后自动调整右缩进, 调整中文与西文文字的间距, 调整中文与数字的间距

of the absorption Ångström exponent of OC was close to 5, which is consistent with previous studies with values ranging from 4-6 (Kirchstetter et al., 2004). Several studies indicated that the absorption Ångström exponent of mineral dust ranged from 2 to 5 (Fialho et al., 2005; Lafon et al., 2006; Zhou et al., 2017; Cong et al., 2018). The variation of the absorption Ångström exponents for urban and industrial fossil fuel emissions is typically in the range of 1.0-1.5 (Millikan, 1961; Bergstrom et al., 2007), which is slightly lower than that of biomass burning aerosols, which primarily falls in the range of 1.5-2.5 (Kirchstetter et al., 2004; Bergstrom et al., 2007). In this study, we noted that the absorption Ångström exponent (\hat{A}_{tot}) is due to the mix state of BC and non-BC impurities on the filters, and the calculations of \hat{A}_{tot} and \hat{A}_{non-BC} could be found in the study of Doherty et al. (2014). The \hat{A}_{non-BC} is calculated as a linear combination of contributions to light absorption due to OC and Fe, and the equation is listed as follows:

$$\hat{A}_{non-BC} = F_{OC} \times \hat{A}_{OC} + F_{Fe} \times \hat{A}_{Fe} \quad (2)$$

2.3 Chemical analysis

The major metallic elements (Al, Cr, Mn, Fe, Ni, Cu, Zn, Cd, Pb) were analyzed by an inductively coupled plasma-mass spectrometry (ICP-MS, X-7 Thermo Elemental) at the Institute of Tibetan Plateau Research in Beijing. The detection limits are Al, 0.238 ng ml⁻¹; Cr, 0.075 ng ml⁻¹; Mn, 0.006 ng ml⁻¹; Fe, 4.146 ng ml⁻¹; Ni, 0.049 ng ml⁻¹; Cu, 0.054 ng ml⁻¹; Zn, 0.049 ng ml⁻¹; Cd, 0.002 ng ml⁻¹; Pb, 0.002 ng ml⁻¹. Briefly, we acidified all melted samples directly to pH<2 with ultra-pure HNO₃, then let settled for 48h. The relative deviation between most of the measured values and the standard reference values is within 10%. Details on these procedures are given in Li et al. (2009) and Cong et al. (2010).

Meanwhile, for the filtrated water samples, we measured the major anions (Cl⁻, NO₂⁻, NO₃⁻, SO₄²⁻) and cations (Na⁺, NH₄⁺, K⁺, Mg²⁺, Ca²⁺) with an ion chromatograph (Dionex 320; Dionex, Sunnyvale, CA) using a CS12 column for cations and an AS11 column for anions at the Institute of Tibetan Plateau Research in Beijing. All the detection limit of the ions was 1 μg · l⁻¹. In addition, except for the anions and cations and trace elements, CI salt, MD, and biosmoke K (K_{Biosmoke}) were determined to assess the mass contributions of the major components in the ice samples. CI salt was estimated as follows

删除的内容: in ... f the absorption Ångström exponents for urban and industrial fossil fuel emissions is typically in the range of 1.0-1.5 (Millikan, 1961; Bergstrom et al., 2007), which is slightly lower than that of biomass burning aerosols, which primarily falls in the range of 1.5-2.5 (Kirchstetter et al., 2004; Bergstrom et al., 2007). Although the source attribution of the insoluble light-absorbing particles in the samples is not a dominant determinant of the value of the absorption Ångström exponent, fossil fuel burning may have a lower absorption Ångström exponent (<2) than 2-5 (Millikan, 1961; Fialho et al., 2005). ... n this study, we noted that the absorption Ångström exponent (\hat{A}_{tot}) is due to a ... he mix state of BC and non-BC impurities on our ... he filters, and the calculations of \hat{A}_{tot} and \hat{A}_{non-BC} could be found in the study of Doherty et al. (2014). The OC mixing ratio was also ... [37]

带格式的 ... [38]

带格式的 ... [39]

带格式的: 两端对齐

删除的内容: ... [40]

带格式的: 字体颜色: 黑色

删除的内容: Previous studies on these parameters have ... [41]

带格式的: 字体颜色: 自动设置

带格式的 ... [42]

删除的内容: Generally speaking, we acidified all ice samples ... [43]

删除的内容: The instrument adopted national standard ... [44]

删除的内容: ice

删除的内容: μg l⁻¹

删除的内容: Cl_{salt} M

删除的内容: D

删除的内容: Cl_{salt}

in accordance with Pio et al. (2007), by adding to sodium, chloride, and sea-salt contributions of sodium, magnesium, calcium, potassium, and sulfate, as follows:

$$CL_{\text{salt}} = Na_{\text{SS}}^+ + Cl^- + Mg_{\text{SS}}^{2+} + Ca_{\text{SS}}^{2+} + K_{\text{SS}}^+ + SO_{4\text{SS}}^{2-}$$

$$= Na_{\text{SS}}^+ + Cl^- + 0.12Na_{\text{SS}}^+ + 0.038Na_{\text{SS}}^+ + 0.038Na_{\text{SS}}^+ + 0.25Na_{\text{SS}}^+$$

5 $Na_{\text{SS}} = Na_{\text{Total}} - Al \cdot (Na/Al)_{\text{Crust}}$ (3)

Where $(Na/Al)_{\text{Crust}} = 0.33$, and represents the Na/Al ratio in the dust materials (Wedepohl, 1995). (4)

The MD content was calculated by a straightforward method, and the Al concentration in dust was estimated as 7% (Zhang et al., 2013b):

10 $MD = Al / 0.07$ (5)

We determined K_{Biosmoke} as follows (Pu et al., 2017):

$$K_{\text{Biosmoke}} = K_{\text{Total}} - K_{\text{Dust}} - K_{\text{SS}}$$

$$K_{\text{Dust}} = Al \cdot (K/Al)_{\text{Crust}}$$

$$K_{\text{SS}} = Na_{\text{SS}} \cdot 0.038$$

15 Where $(K/Al)_{\text{Crust}}$ is 0.37, which represents the K/Al ratio in the dust materials (Wedepohl, 1995) and Na_{SS} is estimated by Eq. (4). (6)

2.4 Enrichment factor (EF)

To evaluate the relative contributions of trace elements from natural (e.g., mineral and soil dust) versus anthropogenic sources (e.g., fossil fuels and vehicle exhaust), an inter-annual comparison of EF values, which represent the enrichment of a given element relative to its concentration in the crust of the earth. The primary uncertainty in these calculations is attributed to the differences between chemical compositions in the snow and the reference crustal composition. The EF is defined as the concentration ratio of a given metal to that of Al, which is a reliable measure of crustal dust, normalized to the same concentration ratio characteristic of the upper continental crust (Wedepohl, 1995), calculated with the following equation:

20
$$EF = \frac{(X/Al)_{\text{snow}}}{(X/Al)_{\text{crust}}}$$
 (7)

2.5 Source apportionment

删除的内容: 2

删除的内容: 3

删除的内容:

带格式的: 两端对齐, 段落间距段后: 0 磅

删除的内容: With 0.12, 0.038, 0.038, and 0.25 being the mass ratios in seawater of magnesium to sodium, calcium to sodium, as well as potassium to sodium and sulfate to sodium, respectively.

删除的内容: t

删除的内容: 4

带格式的: 两端对齐

删除的内容: 5

删除的内容: 6

删除的内容: 7

删除的内容: and

删除的内容: 3

删除的内容: d

删除的内容: EF_c

删除的内容:

删除的内容: 8

删除的内容: d

The Positive Matrix Factorization (PMF 5.0) is considered as a generally accepted receptor model to determine source apportionment of the ILAPs when source emission profiles are unknown (Paatero and Tapper, 1994). Details of the PMF procedure used in this study are similar to the previous work as discussed in Hegg et al. (2009, 2010). Generally, the mass concentration and the uncertainties of the chemical species were used as the input. The final data set used for the PMF analysis contained 189 samples with 18 elements whereby only elements that have high recovery were used. The uncertainty value of each variable in each sample was estimated from an empirical equation. The PMF model was run for 3 to 6 factors with 6 random seeds, but only a three-factor solution could provide the most meaningful results of the ILAPS in TP glaciers. The Q values (modified values) for the 3-factor solution (both robust and true) were closest to the theoretical Q value of any of the factor numbers for which the model was run, suggesting that the 3-factor solution was optimal.

3. Results and Discussion

3.1 Aerosol optical depth (AOD)

As shown in Fig. 3, the QY, QM, MK, YZF glaciers are located in the northern part of Tibetan Plateau, while XD, HRQ, GR glaciers are located in the southern part of Tibetan Plateau. It worth noting that the aerosol optical depth (AOD) can represent the dry aerosol deposition and its transport pathway, which could provide useful information about the possible sources of the ILAPs in the TP glaciers. Therefore, the spatial distribution of the averaged AOD at 500 nm derived from Aqua-MODIS were retrieved over the TP regions and its adjacent areas from 2013 to 2015. Following the work of Ramanathan et al. (2007), the anthropogenic AOD, which is also called as atmospheric brown clouds (ABC), was larger than 0.3 on the southern side of the Himalayas. Therefore, AOD (500 nm) values >0.3 and <0.1 are considered to present the anthropogenic haze and background conditions, respectively. We found that the AOD was much larger across the western TP than that in the central part of TP regions. As a result, the AOD values in the QY, QM, MK, and YZF glaciers were in the range of 0.25 to 0.3 could be highly influenced by human activities. The high values of AOD might thus contribute to the retreat of Himalayan glaciers (Engling and Gelencser, 2010). In contrast, the lower values of AOD (<0.125)

删除的内容: also

删除的内容: of

删除的内容: and the uncertainty

删除的内容: of the ILAPs in TP glaciers

带格式的: 字体: 非加粗

删除的内容: 。

删除的内容: 1

带格式的: 字体: 小四, 字体颜色: 文字 1

带格式的: 字体: 小四, 字体颜色: 文字 1

带格式的: 字体: 小四, 字体颜色: 文字 1

带格式的: 字体颜色: 文字 1

were observed near the HRQ, XD, and GR glaciers. However, the AOD over the TP regions was much lower than that over Southern Asia, especially over the Indo-Gangetic Plain during the cold season. This is close to previous measurements over the TP regions (Cong et al., 2009; Ming et al., 2010; Yang et al., 2012; Lüthi et al., 2015).

3.2 Regional averages of the optical parameters

The general information of C_{BC}^{est} , C_{BC}^{max} , C_{BC}^{equiv} , f_{non-BC}^{est} , \hat{A}_{tot} , and \hat{A}_{non-BC} of the ice samples are given in Table 1 for each glacier. The lower median values of C_{BC}^{est} could be 23 ng g⁻¹, 26 ng g⁻¹ during the monsoon season in the HRQ and GR glaciers on the south of the TP regions, while the higher values of 187 ng g⁻¹ and 165 ng g⁻¹ found in the MK and YZF glaciers on the central part of the TP regions. Compared with the monsoon season, the concentration of C_{BC}^{est} increased very significantly in all seven glaciers than those values during the non-monsoon season. We found that the lowest concentration of BC in the ice samples is found in the XD glacier, with a value of $C_{BC}^{est} \sim 10$ ng g⁻¹. In contrast, the highest values of C_{BC}^{est} , C_{BC}^{max} , and C_{BC}^{equiv} were 3100 ng g⁻¹, 3600 ng g⁻¹, and 4700 ng g⁻¹, respectively, taken in the GR glacier. Generally, the median of \hat{A}_{tot} exceeded 1.0 at all locations (Fig. 4, and Table 1). \hat{A}_{tot} and \hat{A}_{non-BC} for all ice samples were in the range of 1.4-3.7 and 1.9-5.8, respectively (Table S1). As shown in Fig. 4a, the median values of \hat{A}_{tot} were 2.62, 2.64, 2.18, and 2.46 in the QY, MK, XD, and GR glaciers, associated with the estimated contributions to absorption by non-BC ILAPs in these regions were ~41%, 44%, 36%, and 48%, respectively. Compared with these glaciers, the higher values of median \hat{A}_{tot} were found in the QM (2.76), YZF (2.95), and HRQ (2.87) glaciers. Correspondingly, the estimated f_{non-BC}^{est} values in those regions is ~44%, 48%, and 48%, respectively. Except the HRQ glacier, the other glaciers showed an increased trend of the \hat{A}_{non-BC} from the south to north regions in the TP regions (Fig. 4b). Histograms of the \hat{A}_{tot} by regions are shown in Fig. 5. We found that there was a large variation of \hat{A}_{tot} in the XD glacier, not only in the higher values (~2-4), but also for the lower values (<2). The broadness of the \hat{A}_{tot} distribution is indicative of the complicated sources of particulate light absorption. For instance, Wang et al. (2013) indicated that the higher values of \hat{A}_{tot} (~3.5-4.5) was highly correlated with the local soil source, while fossil fuel burning may have an absorption Ångström exponent lower than 2 (Millikan, 1961; Fialho et al., 2005). Therefore, a

带格式的: 字体: (中文) 宋体, 小四, 字体颜色: 文字 1

带格式的 ... [45]

带格式的: 字体: (中文) 宋体, 小四, 字体颜色: 文字 1

带格式的: 字体颜色: 文字 1, 非突出显示

删除的内容: (Cong et al., 2009; Yang et al., 2012)

带格式的: 字体: 非加粗

带格式的: 两端对齐

已移动(插入) [7]

删除的内容: Based on our sampling locations shown in Fig. 1, the Qiyi, Qiumianleiketage, Meikuang, Yuzhufeng glaciers were located in the northern part of Tibetan Plateau, while Xiaodongkemadi, Hariqin, Gurenhekou glaciers were located in the southern part of Tibetan Plateau.

67 ice samples were collected at 7 sites from 2013 to 2015 across the Tibetan plateau field campaign. As shown in Fig. 1, the spatial distribution of aerosol optical depth (AOD) retrieved from Moderate-resolution Imaging Spectrometer (MODIS) sensors are ranging from 0.1 to 0.4 from south to north near the high mountain glacier regions over TP regions from 2013-2015.

已移动(插入) [6]

带格式的: 非上标/下标

删除的内容: found...during the monsoon season in the Xiaodongkemadi, Hariqin...RQ...and Gurenhekou ...R ... [46]

删除的内容: Details of the vertical profiles of all ice samples ... [47]

删除的内容: are ...ere 3100 ng g⁻¹, 3600 ng g⁻¹, and 4700 ng ... [48]

已移动(插入) [9]

删除的内容: 3a...a, the lowest...median ... [49]

删除的内容: (~2.1) is found in the Xiaodongkemadi glacier ... [50]

已上移 [9]: \hat{A}_{tot} and \hat{A}_{non-BC} for all ice samples were in the

删除的内容: absorption Ångström exponent ... by regions are ... [51]

significant fraction of the total absorption was not only attributed to BC (49%, shown in Fig. 7), but also contributed by non-BC absorbers (accounting for 51%) due to OC and MD in the XD glacier. In contrast, a common feature in the other regions was that the major dominated values of \hat{A}_{tot} range from 2 to 3. The \hat{A}_{non-BC} and \hat{A}_{tot} in each site are also given as red dots and blue triangles, respectively, in Fig. S3.

Figure 6 shows the regional variations of BC, OC, and Fe concentration in each glacier during monsoon and non-monsoon seasons. Although there were significant differences between the median and average values of the ILAPs concentration in each glacier, we found that all kinds of ILAPs exhibited a similar variation from the northern QY glacier to southern GR glacier. In addition, we collected the ice samples during both monsoon and non-monsoon seasons in five glaciers, only except the QY and QM glaciers. On average, the BC and OC concentrations in the HRQ, XD, and GR glacier during non-monsoon season were several orders of magnitude higher than those in monsoon seasons. The result was highly consistent with the previous study by Cong et al. (2015), who found that although the transport pathways of air masses arriving the middle Himalayas during monsoon and non-monsoon were similar, a distinctly higher carbonaceous aerosol level was found only in the non-monsoon season. Lüthi et al. (2015) also exhibited that the atmospheric brown cloud over South Asia can climb across the Himalayan and transport of polluted air mass, which may have serious implications of the cryosphere in the TP regions. However, there appeared to be no apparent difference in the mixing ratios of ILAPs between monsoon and non-monsoon seasons in two adjacent (MK and YZF) glaciers. This can be mainly explained that, except the long-range transport of ILAPs, local air pollutants could also affect the ILAPs in the central TP regions. For instance, Huang et al. (2018) investigated that the air masses across the MK and YZF glaciers were originated from the arid western TP and Taklimakan desert regions, and the concentration of trace elements in the YZF glacier was closer to the dust sources indicating that YZF glacier was less influenced by human activities. The median values of the C_{BC}^{est} and C_{OC} (referred as the mass concentration of OC) obviously showed a slightly decreasing trend from the northern TP to the southern TP. The mass concentration of BC in northern TP glaciers was

删除的内容: that the ILAPs are not only dominated by BC in these regions ...ut also influenced ...ontributed by non-BC absorbers (accounting for 51%) such as ...ue to OC and mineral dust...D in the XD glacier. In contrast, a common feature in the other regions is ...as that they ...he major dominated values show a less variable ...f \hat{A}_{tot} the absorption Ångström exponent,...angeing...from ...rom 2.5...to - ... [52]

带格式的: 字体颜色: 文字 1

删除的内容: BC and other ILAPs are integrated into the snowpack and ice surface by dry and wet deposition, such as gravity, turbulence, and precipitation. For instance, Flanner et al. (2012) indicated that BC nucleates ice very poorly via direct deposition of vapor, so most relevant mechanisms involve liquid water. Therefore, the investigation of the mixing ratios of ILAPs in each glacier ...igure 6 shows the regional variations of BC, OC, and Fe concentration in each glacier during monsoon and non-monsoon seasons could be ... [53]

带格式的

已移动(插入) [11]

删除的内容: We noted that several reasons could lead this ... [55]

带格式的: 非突出显示

删除的内容: can

带格式的: 非突出显示

删除的内容: in the glacier via wet and dry deposition...n the ... [56]

带格式的: 非突出显示

删除的内容: the Fossil fuel contributions of BC is much ... [57]

带格式的

已上移 [7]: Based on our sampling locations shown in Fig. 1,

删除的内容: Based on our sampling locations shown in Fig. ... [59]

删除的内容: $ISOC$...referred as the mass concentration of ... [60]

higher than that in southern TP glaciers, which showed a good agreement with Ming et al. (2013).

To quantify the regional status of ILAPs in each glacier, the statistics of the ILAPs in snow and ice in the studied TP glaciers and other related glaciers by previous studies are shown in Table 2. During this field campaign, twelve ice samples were collected in the YZF glacier. The depths of these ice samples collected in the YZF glacier were ranging from 15 to 45 cm (Table S1). As shown in Fig. S4, most values of C_{BC}^{est} in this region ranged from ~100-1000 ng g⁻¹, with a few values lower than 100 ng g⁻¹. One notable feature is that the highest concentrations of C_{BC}^{max} and C_{OC} for the surface layer were 1600 ng g⁻¹ and 9160 ng g⁻¹ at site 41. We pointed out that the light absorption in the surface glacier at site 41 was not only influenced by BC, but also possibly related to the OC and MD due to the high value of f_{non-BC}^{est} (0.56). In the YZF glacier, A_{tot} generally varied between ~2 and 3.7, and the average value of f_{non-BC}^{est} was close to 50%, so these results also revealed that the ILAPs in ice samples are heavily influenced by anthropogenic air pollutants. Large variations of C_{OC} were also observed, with values ranging from ~10 to 17000 ng g⁻¹. Except site 23, the values of C_{BC}^{est} in the MK glacier were much lower than those in the YZF glacier, which were in the ranges of ~20-670 ng g⁻¹, with a median value of 130 ng g⁻¹ (Fig. S5). The median C_{OC} was ~600 ng g⁻¹ in the MK glacier. The fraction of total particulate light absorption due to non-BC constituents was typically ~16-62%, and A_{non-BC} (5.12) in this region was highly similar to that found in the YZF glacier (5.06).

In the QY glacier (Fig. S6), the C_{BC}^{est} were much similar with those in the MK glacier, with values ranging from ~20-720 ng g⁻¹, which did not include the highest value of 1900 ng g⁻¹ at site 13. The fraction of total particulate light absorption due to non-BC constituent f_{non-BC}^{est} was typically ~20-70%, with a median value of 41%. This information along with the lower A_{tot} (2.6) indicated that BC played the dominant role in influencing the light absorption in this region. Compared with the other TP glaciers, we noted that the vertical profiles of ILAPs in the QY glacier were collected in the monsoon season from 2014 to 2015 (Table S1). The mixing ratios of OC and Fe ranged from 80-10100 ng g⁻¹ and 20-340 ng g⁻¹, respectively. Fig. S7 shows that the vertical profiles of the mass mixing ratios of BC, OC, and Fe for the ice samples in the XD glacier were more variable than those for

删除的内容: s...a good agreement with Ming et al. (2013).

Comparing with Hariqin, Xiaodongkemadi and Gurenhekou glaciers, the relative higher values of the C_{BC}^{est} and C_{ISOC} [61]

已下移 [10]: The Yuzhufeng glacier is located in the northern part of the Loess Plateau, close to the Meikuang glacier.

Twelve ice samples were collected in the Yuzhufeng glacier.

The depth of these ice samples collected in the Yuzhufeng

删除的内容: in the Qiyi, Qiumianleiketage, Yuzhufeng, and ... [62]

已上移 [11]: We noted that several reasons could lead this

带格式的: 字体颜色: 文字 1

带格式的: 突出显示

带格式的: 突出显示

带格式的: 两端对齐, 定义网格后不调整右缩进, 不调整西文与中文之间的空格, 不调整中文和数字之间的空格

已移动(插入) [10]

删除的内容: The Yuzhufeng glacier is located in the ... [63]

删除的内容: IS

删除的内容: OC...for the surface layer are...ere 1600 ng g⁻¹ ... [64]

删除的内容: w... pointed out that the light absorption in the ... [65]

删除的内容: The large variation of the absorption Ångström ... [66]

删除的内容: is...as close to 50%, so these results also ... [67]

删除的内容: OC (measured by ISSW) and WSOC...are...ere ... [68]

删除的内容: Meikuan...Kg...glacier are...ere much lower ... [69]

带格式的: 非上标/下标

删除的内容: value of the mass concentration of ... [70]

带格式的: 字体颜色: 黑色

删除的内容: Qiyi ...Y glacier (Fig. S4 ... [71]

删除的内容: are...ere much similar withthan...those in the ... [72]

删除的内容: is...as typically ~20-70%, with a median value ... [73]

the other regions. With the exception of the surface layer at sites 53 and 54, most values of C_{BC}^{est} ranged from 10 to 280 ng g⁻¹ in the XD glacier; therefore, this glacier was the cleanest region among all the studied glaciers. At sites 56-58, f_{non-BC}^{est} was lower than 38%, and A_{tot} ranged from 1-2.5. These results were consistent with the fossil fuel combustion source due to industrial activities.

3.3 Scavenging and washing efficiencies

Previous studies have illustrated that the ILAPs could become trapped and integrated at the surface of the snowpack due to melting and sublimation to enrich the surface concentrations (Conway et al., 1996; Painter et al., 2012; Doherty et al., 2013). For instance, Doherty et al. (2013) found that the ILAPs could be scavenged with the snow meltwater to lead to a much higher concentration of BC in the surface snow. Flanner et al. (2007, 2009) indicated that the melt amplification due to concentrated BC in melted snow would amplify snow-albedo reduction, and therefore provide a positive feedback to radiative forcing. However, it still remains unclear what happens to the vertical ILAPs in the deeper layer of snow and ice during the multi-melting processes due to limited in-situ observations.

In this study, the mixing ratios of ILAPs in most of the ice samples increased remarkably from the top to the bottom in QY glacier. This result seemed inconsistent with a previous study by Doherty et al. (2013). However, Xu et al. (2012) observed that the concentrations of BC were higher not only at the snow surface, but also found at the bottom due to the percolation time of meltwater and superimposed ice by the temperature decline in the snowpack. Another notable feature was that the surface mixing ratios of C_{BC}^{est} at sites 52-54 in the XD glacier were significantly larger than those in the sub-surface layers, possibly because of the accumulation of BC via dry/wet deposition on the surface samples. We found that the mechanism of the ILAPs in the vertical ice samples in the QY and XD glacier could be difference. The ice samples in the QY glacier were collected in the monsoon season. Due to the higher temperature in the monsoon season, the strong melting processes could wash out the ILAPs in ice samples to lead a higher concentration in the bottom layer in QY glaciers. In contrast, the ice samples were collected in XD glacier in both monsoon and monsoon seasons. Therefore, it can be seen clearly that a decreasing trend of the ILAPs in the ice samples was found from the top to the bottom in XD glacier due to the high

已移动(插入) [12]

删除的内容: are

带格式的: 字体颜色: 黑色

带格式的: 字体: 加粗

已移动(插入) [13]

删除的内容: also

带格式的: 字体: (默认) Times New Roman, (中文) 宋体, 小四

带格式的: 字体: (默认) Times New Roman, (中文) 宋体, 小四

带格式的: 字体: (默认) Times New Roman, (中文) 宋体, 小四

带格式的: 字体: (默认) Times New Roman, (中文) 宋体, 小四

带格式的: 字体: (默认) Times New Roman, (中文) 宋体, 小四

带格式的: 两端对齐, 行距: 最小值 13 磅

删除的内容: Compared with the other TP glaciers, we noted that the vertical profiles of ILAPs in the Qiyi glacier were collected in the monsoon season from 2014 to 2015 (Table S1). In the monsoon season, the mixing ratios of ISOC and Fe ... [74]

删除的内容: T

删除的内容: is

删除的内容: highly

删除的内容: Fig. S5 shows that the vertical profiles of the ... [75]

删除的内容: a

删除的内容: is

删除的内容: are

删除的内容: Doherty et al. (2013) also found that the ILAPs ... [76]

带格式的: 字体颜色: 自动设置

已上移 [12]: At sites 56-58, f_{non-BC}^{est} was lower than 38%,

带格式的: 字体颜色: 自动设置

带格式的: 字体颜色: 自动设置

带格式的: 字体颜色: 自动设置

带格式的: 字体颜色: 自动设置

scavenging effect during the non-monsoon season (Fig. S7a-S7f, only except Fig. S7e and S7g), while a opposite trend due to the washing effect during the monsoon season (Fig. S7h and Fig. S7j). Because the single layer samples are not shown, the vertical profiles of C_{BC}^{est} are plotted in Fig. S8 for all ice samples, which were collected in the QM, HRQ, and GR glaciers. Except for the sites in Fig. S8d, S8e, S8i, and S8h, the other sites revealed the trapping and scavenging effects of a higher mass concentration of BC in the surface layer due to the melting processes.

3.4 Contributions to particulate light absorption by ILAPs

The fractional contributions to total absorption by BC, OC, and Fe (assumed to be in the form of goethite) at 450 nm in each glacier, are shown in Fig. 7, and further details of the concentrations of BC, OC, and Fe are given in Table S1. BC played a dominant role in particulate light absorption with average values ranging from ~44%-54% in all glacier regions. OC was the second highest absorber in glacier regions, and there are large variations of light absorption of OC during the field campaign (~25%-46% on average). The contributions to total absorption due to BC and OC were relatively comparable in the QY, YZF and HRQ, which are located in the eastern TP regions. The highest fraction of BC was accounting for 54% in the QM glaciers, which is located in the western TP regions. So the light absorption due to ILAPs in the TP glacier regions was not only from BC and OC, but also with a small contribution from Fe. The average fraction of total light absorption due to Fe was ~11%-31% in all seven glaciers, with the highest light absorption of Fe in the GR glacier. The relative contributions to total light absorption by BC, OC, and Fe for surface ice samples in each sampling location are also shown in Fig. S9 and Table 1. This result was an indication that mineral dust played a key role in affecting the spectral absorption properties of ILAPs in ice samples from the TP glaciers.

3.5 Enrichment factor (EF)

Briefly, the EF values ranging from 0.1 to 10 indicate significant input from crustal sources. Conversely, EF values that larger than 10 exhibit a major contribution from anthropogenic activities. Referring to the EF analysis (Fig. 8), the mean EF of Fe < 5 in each glacier can be assumed to customarily originate from crustal sources. Recent studies have also indicated that light-absorbing particles in snow are dominated by local soil dust in some

带格式的 ... [77]

删除的内容: S6 ... 8 for all ice samples, which were collected in the Qiumianleiketage...M, Hariqin...RQ, and Gurenhekou ...R glaciers. Except for the sites in Fig. S6d...8d, S6e...8e, S6i...8i, and S6h ... [78]

已上移 [13]: Previous studies have also illustrated that the ILAPs could become trapped and integrated at the surface of the snowpack due to melting and sublimation to enrich the surface concentrations (Conway et al., 1996; Painter et al., 2012; Doherty et al., 2013).

删除的内容: 4

删除的内容: 3.2 Water-soluble organic carbon
It is well known that the WSOC component has a large variation ranging from 20% to 99% of total carbonaceous particles (Saxena and Hildemann, 1996; Mayol-Bracero et al., 2002). There is a very large fraction representing the average WSOC (>80%) to TOC, which can absorb solar light and enhance cloud formation through their direct and indirect climate effects (Ram et al., 2010). These results are highly consistent with previous studies showing that fossil fuel combustion plays a key role in leading to the higher fraction ... [79]

带格式的: 两端对齐

删除的内容: 3

删除的内容: BC and OC were mainly emitted from biomass burning and biofuel and fossil fuel combustion, while mineral ... [80]

带格式的 ... [81]

删除的内容: ...his result was an indication that mineral dust played a key role in affecting the spectral absorption ... [82]

删除的内容: 4

带格式的: 两端对齐

typical regions over northern China (Wang et al., 2013), and northern America (Doherty et al., 2014). Comparable with Fe, the other trace metals with the mean EF of ≥ 5.0 were moderately to highly enriched from anthropogenic emissions (Hsu et al., 2010). For example, Pacyna and Pacyna (2001) reported that fossil fuel combustion is a major source of Cr. Cu primarily originates from emissions from fossil fuel combustion and industrial processes, while Pb and Zn are known to be drawn from the traffic-related activities and coal burning (Christian et al., 2010; Contini et al., 2014). Hence, the high EF values observed for Cu, Zn, and Cd in our ice samples clearly suggested that the TP glaciers have already been polluted by human activities, such as biomass burning, fossil fuel burning, and the coal burning.

3.6. Source apportionment

Given the importance of the climate effect in our understanding of the ILAPs in TP glaciers, we applied a PMF receptor model to analyze the source attribution of ILAPs light absorption in these glaciers. In this study, the mass concentrations of the chemical components and the ILAPs in ice associated with the uncertainty datasets were used to run the PMF 5.0 model. The details of the techniques have already been illustrated by Hegg et al. (2009, 2010) and Pu et al. (2017). The factor loadings (apportionment of species mass to individual factors) for the 3-factor solution of the source profiles based on the PMF 5.0 model are given in Fig. 9 (in both measured mass concentration and the % total mass allocated to each factor). It was evident that the first factor (top panel) was obviously characterized by high loadings of Cl^- , Cl salt, SO_4^{2-} , and NO_3^- , which are well known markers for the urban or local industrial pollutions (Alexander et al., 2015). Although Cl^- to Na^+ are usually considered as a potential product of emission source of sea salt, but also a high loading of Cl^- to Cl salt reflecting another source in addition to sea salt such as industrial emission and coal combustion (Hailin et al., 2008; Kulkarni, 2009). Additionally, the highest loading of NH_4^+ is also suggested as an indicator of coal combustion (Pang et al., 2007). Compared with the first factor, Al (90.3%) and Fe (87.3%) usually regarded as major indicators for the urban or regional mineral dust (Pu et al., 2017). Therefore, the second factor was easily interpretable as a natural mineral dust source. It was notable that C_{BC}^{max} showed a high mass loading in this factor, K^+ and $\text{K}_{\text{Biosmoke}}$ are the major

删除的内容: predominantly

删除的内容: Together with

已下移 [8]: Therefore, we concluded that the natural dust source and anthropogenic emission source are both non-negligible to the ILAPs in the TP glaciers. ^d

删除的内容: For instance, high level of Pb and Cr have demonstrated a link to coal combustion (Zhang et al., 2013a, ... [83])

删除的内容: 5

删除的内容: present

删除的内容: two datasets including

删除的内容: and the

删除的内容: is

删除的内容: Cl_{salt}

删除的内容: Cl_{salt}

删除的内容: indicated another source in addition to sea salt ... [84]

删除的内容: the highest loading of

删除的内容: are well-known

删除的内容: markers

删除的内容: or source profile is

删除的内容: But a

删除的内容: feature is

删除的内容: the relative high mass loading of

删除的内容: (76.4%)

删除的内容: to that of the previously identified mineral dust ... [85]

删除的内容: It is well known that

indicators of biomass burning (Zhang et al., 2013a). Therefore, it was easily interpretable that the highest loadings of K^+ and K_{Biosmoke} were well representative for the biomass burning source (Fig. 9c). However, the lowest mass loading of C_{BC}^{max} in this factor is a bit unexpected. Indeed, the C_{BC}^{max} is not only attributed to the biomass burning emission, but also associated with the industrial activities associated with the local mineral dust (Bond et al., 2006). Therefore, we interpreted the third factor normally considered a predominantly biomass burning product.

Finally, the chemical composition and mean source apportionment of the ILAPs to the three sources in the TP glaciers were given in Fig. 10. Note that the apportionment was of the light absorption by insoluble particles in the surface glaciers. On average, the source apportionment of the ILAPs in all TP glaciers by mineral dust was close to 37.5%, while the industrial emission and biomass burning contributed 33% and 29.4%, respectively. Specifically, the largest biomass burning contribution of the light-absorption of ILAPs was found in the QY glacier, which is close to the human activity regions (Guan et al., 2009; Li et al., 2016). In the MK, QM, GR, and XD glaciers, the mineral dust contribution of light absorption was much larger (>47.9%) than that of industrial pollution and biomass burning, especially in the MK glacier. In these regions, the percent of the light absorption due to soil dust ranged from 20.4-31.1%, while the light absorption by biomass burning was in the range of 18.5-35.8%. Industrial pollution constituted a major fraction in the YZF glacier. Chemical analysis showed that the percentages of the chemical species in the YZF and MK glaciers were much similar. The attribution of the total anions by chloride, nitrate, and sulphate were higher than the other chemical species in the YZF and MK glaciers. In the HRQ glacier, the largest contribution of the sulphate was up to 45.4%. As shown in Fig. 10, the source of the light absorption by insoluble particles in the surface glaciers was dominated by mineral dust and the industrial pollution in most glaciers. The only exception was the YZF glacier where a large fraction of the light absorption was due to biomass burning in the YZF glacier. These results were highly consistent with the previous studies (Andersson et al., 2015). They found that the contributions of coal-combustion-sourced BC are the most significant for the TP glaciers.

4 Conclusions

删除的内容: source ...Zhang et al., 2013a). Therefore, it is ... [86]

删除的内容: are ...ere well representative for the biomass burning source (Fig. 9c). However, it is also important to note that ... [87]

删除的内容: However, the major emission of BC in TP glaciers originated from the local mineral dust source instead of the biomass burning and industrial pollution than previous studies (Zhang et al., 2013a; Pu et al., 2017).

删除的内容: is ...as of the light absorption by insoluble particles in the surface glaciers. On average, the source apportionment of the ILAPs in all TP glaciers by mineral dust is ...as close to 37.5%, while the industrial emission and biomass burning contributed...33% and 29.4%, respectively. Specifically, the largest biomass burning contribution of the light-absorption of ILAPs was found in the Qiyi ...Y glacier, which is close to the human activity regions (Guan et al., 2009; Li et al., 2016). In the Meikuang...K, Qiumianleiketage...M, Gurenhekou...R, and Xiaodongkemadi ...D glaciers, the mineral dust contribution of light absorption is ...as much larger (>47.9%) than that of industrial pollution and biomass burning, especially in the Meikuang ...K glacier. In these regions, the percent of the MD ...light absorption due to soil dust is ...angedging...from 20.4-31.1%, while the light absorption by biomass burning is ...as in the range of 18.5-35.8%. Industrial pollution constitutes ...onstituted a major fraction in the Yuzhufeng ...ZF glacier. Chemical analysis showed...that the percentages of the chemical species in the Yuzhufeng ...ZF and Meikuang ...K glaciers are ...ere much similar. The attribution of the total anions by chloride, nitrate, ... [88]

In this study, the ILAPs observations in seven glacier regions across the Tibetan Plateau were presented using the ISSW technique along with chemical analysis. 67 vertical profiles of ice samples collected during the monsoon and non-monsoon seasons from 2013-2015 were analyzed. On average, the BC and OC concentrations in the HRQ XD, and GR glacier during non-monsoon season were several orders of magnitude higher than those in monsoon seasons. However, it remains unclear that the ILAPs in the MK and YZF glaciers were comparable during the monsoon and non-monsoon seasons, which could be investigated by future survey studies across these regions. By excluding some of the highest ILAPs values in the ice samples, the mass concentration of BC, OC, and Fe ranged from 100-1000 ng g⁻¹, 10-2700 ng g⁻¹, and 10-1000 ng g⁻¹, respectively. Among the samples, the lower concentrations of BC were found in the XD, HRQ and GR glaciers, with the median concentrations of 33 ng g⁻¹, 24 ng g⁻¹, and 28 ng g⁻¹, respectively. We found that the ILAPs in the ice samples was decreased from the top to the bottom in XD glacier due to the scavenging effect during the non-monsoon season, while a opposite trend due to the washing effect by high temperature during the monsoon season. BC played a dominant role in particulate light absorption with average values ranging from ~44%-54% in these glaciers, while ~25%-46% for OC. By using a PMF receptor model, we found that the ILAPs across the northern glaciers is heavy polluted due to human activities, but the major emissions of the light absorption by insoluble particles in TP glaciers originated from the local mineral dust and industrial pollution sources, followed by the biomass burning source. Therefore, the natural mineral dust source and anthropogenic emission source are both non-negligible to the ILAPs in the TP glaciers.

5 Data availability

All datasets and codes used to produce this study can be obtained by contacting Xin Wang (wxin@lzu.edu.cn).

删除的内容: 7

删除的内容: are

删除的内容: are analyzed

删除的内容: There are no apparent differences in the mixing ... [89]

带格式的: 字体颜色: 黑色

删除的内容: .

带格式的: 字体颜色: 黑色

带格式的: 字体: (中文) 宋体, 小四, 字体颜色: 黑色

带格式的: 字体: (中文) 宋体, 小四, 字体颜色: 黑色

删除的内容: The results indicate that the variations of A_{tot} ... [90]

删除的内容: values

删除的内容: C_{BC}^{est} , C_{ISOC} and C_{Fe}

带格式的: ... [91]

删除的内容:

删除的内容: Xiaodongkemadi

删除的内容: Hariqin

删除的内容: Gurenhekou

删除的内容: ... [92]

带格式的: 字体颜色: 自动设置

删除的内容: to analyze the source attributions of ILAPs in ... [93]

删除的内容: W

删除的内容: anthropogenic air pollution

删除的内容: much

删除的内容: across the northern glaciers

删除的内容: We note that the C_{BC}^{max} is not only attributed to ... [94]

已移动(插入) [8]

删除的内容: Therefore, we concluded that the natural dust ... [95]

带格式的: 两端对齐

Competing interests. The authors declare that they have no conflicts of interest.

Acknowledgements. This research was supported by the Foundation for Innovative Research Groups of the National Natural Science Foundation of China (41521004), the
5 National Natural Science Foundation of China under grant (41775144 and 41522505), and the Fundamental Research Funds for the Central Universities (lzujbky-2018-k02).

Table 1. Statistics of the JLAPs in each glacier measured using an ISSW spectrophotometer associated with the chemical analysis.

Region	Latitude	Longitude		C_{BC}^{equiv}	C_{BC}^{max}	C_{BC}^{est}	f_{non-BC}^{est}	A_{tot}	OC	AI	Fe
	(N)	(E)		(ng g ⁻¹)	(ng g ⁻¹)	(ng g ⁻¹)	(%)		(ppm)	(ppm)	(ppm)
Qiyi glacier	39°14'28"	97°45'27"	average	414	299	238 (116, 313)	42 (15, 66)	2.59	1.21	0.19	0.18
			median	176	128	94 (29, 124)	41 (17, 70)	2.62	0.66	0.08	0.09
			minimum	26	29	25 (13, 35)	21 (—, 53)	0.8	0.08	0.01	0.02
			maximum	2651	2230	1877 (1182, 2109)	73 (41, —)	3.73	11.59	3.35	2.41
Qiumianleiketage	36°41'47"	90°43'44"	average	421	296	238 (139, 402)	44 (24, 81)	2.80	1.43	0.21	0.23
			median	307	215	172 (64, 218)	44 (24, 81)	2.76	1.06	0.15	0.18
			minimum	139	93	62 (19, 93)	37 (12, 64)	2.45	0.54	0.09	0.11
			maximum	995	662	558 (143, 678)	56 (27, 86)	3.08	3.97	0.55	0.63
Meikuang glacier	35°40'24"	94°11'10"	average	493	328	260 (119, 331)	42 (15, 37)	2.65	2.14	0.19	0.22
			median	197	156	133 (76, 153)	44 (16, 69)	2.64	0.61	0.09	0.13
			minimum	24	23	19 (17, 24)	16 (—, 17)	1.37	0.13	0.02	0.03
			maximum	4696	2817	2292 (109, 2938)	62 (23, 85)	3.56	16.89	1.36	1.22
Yuzhufeng glacier	35°38'43"	94°13'36"	average	457	312	233 (94, 295)	51 (—, 37)	2.84	1.51	0.17	0.44
			median	317	201	160 (116, 204)	48 (26, 87)	2.95	1.02	0.10	0.21
			minimum	52	35	24 (8, 35)	15 (—, 37)	1.82	0.07	0.02	0.05
			maximum	2630	1608	1169 (72, 1603)	110 (6, 49)	3.7	9.16	0.81	3.51
Hariqin glacier	33°08'23"	92°05'34"	average	476	327	256 (100, 385)	48 (26, 82)	2.79	1.59	0.17	0.17
			median	54	37	23 (9, 30)	48 (26, 82)	2.87	0.22	0.04	0.05
			minimum	36	24	13 (4, 22)	19 (—, 41)	1.96	0.08	0.01	0.03
			maximum	3990	2702	2131 (682, 2784)	64 (32, 84)	3.52	9.64	1.11	1.05
Xiaodongkemadi	33°04'08"	92°04'24"	average	253	171	152 (76, 177)	37 (15, 63)	2.28	0.95	0.13	0.17

Region	Latitude	Longitude	C_{BC}^{equiv}	C_{BC}^{max}	C_{BC}^{est}	f_{non-BC}^{est}	A_{tot}	ISOC	Al_e	Fe_e	
	(N)	(E)	(ng g ⁻¹)	(ng g ⁻¹)	(ng g ⁻¹)	(%)		(ppm)	(ppm)	(ppm)	
Gurenhekou glacier	30°11'17"	90°27'23"	median	62	47	53 (37, 65)	36 (13, 59)	2.18	0.19	0.03	0.06
			minimum	13	12	9 (6, 18)	8 (—, 19)	1.08	0.01	0.01	0.01
			maximum	2770	1849	1637 (596, 2031)	86 (25, 90)	3.63	6.97	2.40	2.13
			average	382	292	247 (212, 591)	46 (16, 71)	2.42	0.62	0.15	0.18
			median	61	46	30 (19, 44)	48 (18, 75)	2.46	0.13	0.05	0.10
			minimum	28	23	15 (10, 24)	27 (7, 52)	1.34	0.02	0.01	0.03
			maximum	4674	3634	3080 (1876, 3884)	61 (26, 85)	2.92	5.22	1.35	0.91

- 删除的内容: WSOC
- 删除的内容: Fe
- 带格式的: 两端对齐
- 删除的内容: (ppm)
- 删除的内容: (ppb)
- 带格式的: 两端对齐
- 删除的内容: 1.41
- 删除的内容: 62.08
- 带格式的: 两端对齐
- 删除的内容: 0.45
- 删除的内容: 10.22
- 带格式的: 两端对齐
- 删除的内容: 5.91
- 删除的内容: 2129
- 带格式的: 两端对齐
- 带格式的: 两端对齐
- 删除的内容: 1.21
- 删除的内容: 182.1
- 删除的内容: 0.85
- 删除的内容: 97.99
- 带格式的: 两端对齐
- 删除的内容: 0.41
- 删除的内容: 31.51
- 带格式的: 两端对齐
- 删除的内容: 4.65
- 删除的内容: 911.2
- 带格式的: 两端对齐

Table 2. Statistics of the ILAPs in snow and ice in the studied TP glaciers and other related glaciers.

<u>Glacier name</u>	<u>Sampling time</u>	<u>Season</u>	<u>Altitude/ m a.s.l.</u>	<u>BC (ng g⁻¹)</u>	<u>OC (ng g⁻¹)</u>	<u>MD (ug g⁻¹)</u>	<u>Sample type</u>	<u>References</u>
Qiyi	2005.7	Monsoon	4850	22+2	==	==	Snow pit	Ming et al., 2009
	2001.7-8	Monsoon	4600	6.65+3.3	87.52+37.59	==	Fresh snow	Xu et al., 2006
	2001.7-8	Monsoon	4600	52.64+17.83	195.5+85	==	Aged snow	Xu et al., 2006
	2013.8-9	Monsoon	4700	238+349	1210+2023	1.42+1.17	Ice	This study
Qiumianleiketage	2014.5	Non-monsoon	5300	238+168	1431+1130	2.92+2.09	Ice	This study
Meikuang	2001.7-8	Monsoon	5200	446	124	==	Surface snow	Xu et al., 2006
	2015.10	Monsoon	5050	290+241	3745+5100	5.27+6.81	Ice	This study
	2015.5	Non-monsoon	5050	250+468	1718+3639	1.85+2.38	Ice	This study
Yuzhufeng	2014,2015.10	Monsoon	5350	265+270	1596+2052	2.93+3.19	Ice	This study
	2014.5	Non-monsoon	5350	213+188	1421+1173	1.9+1.77	Ice	This study
Hariqin	2015.10	Monsoon	5650	91+126	930+1880	1.23+1.77	Ice	This study
	2015.5	Non-monsoon	5650	1077+1489	4860+6759	8.38+10.59	Ice	This study
Xiaodongkemadi	2014.8-2015.7	Monsoon	5400-5750	41.77+6.36	157.97+42.3	1.89+0.92	Fresh snow	Li et al., 2017
		Monsoon	5400-5750	246.84+118.3	611.45+467.7	39.43+24.35	Aged snow	Li et al., 2017
		Monsoon	5400-5750	3335+3767	9857+10923	880+1038	Granular ice	Li et al., 2017
	2015.10	Monsoon	5600	57+37	250+233	0.68+0.3	Ice	This study

带格式的: 字体: (默认) Times New Roman, (中文) 宋体, 加粗, 字体颜色: 自动设置

带格式的: 字体: (默认) Times New Roman, (中文) 宋体, 加粗, 字体颜色: 自动设置

	<u>2013-2015.5</u>	<u>Non- monsoon</u>	<u>5600</u>	<u>178+381</u>	<u>1174+2014</u>	<u>2.18+6.15</u>	<u>Ice</u>	<u>This study</u>
<u>Gurenhekou</u>	<u>2015.10</u>	<u>Monsoon</u>	<u>5610</u>	<u>85+177</u>	<u>330+648</u>	<u>1.17+1.49</u>	<u>Ice</u>	<u>This study</u>
	<u>2014.5</u>	<u>Non-monsoon</u>	<u>5610</u>	<u>1116+1700</u>	<u>2148+2668</u>	<u>7.7+9.99</u>	<u>Ice</u>	<u>This study</u>
<u>Palong-Zanbu-</u>	<u>1998-2005</u>	<u>Monsoon</u>	<u>4800-5600</u>	<u>5.27+2.23</u>	<u>70.8+39.3</u>	<u>====</u>	<u>Ice core</u>	<u>Xu et al., 2009a</u>
<u>No. 4</u>		<u>Non-monsoon</u>	<u>4800-5600</u>	<u>11.51+4.7</u>	<u>97.5+49.9</u>	<u>====</u>	<u>Ice core</u>	<u>Xu et al., 2009a</u>
<u>Zuoqiupu</u>	<u>1956-2006</u>	<u>Monsoon</u>	<u>5100-5400</u>	<u>2.37+1.55</u>	<u>11.55+11.5</u>	<u>====</u>	<u>Ice core</u>	<u>Xu et al., 2009b</u>
		<u>Non-monsoon</u>	<u>5100-5400</u>	<u>8.33+3.29</u>	<u>26.71+13.74</u>	<u>====</u>	<u>Ice core</u>	<u>Xu et al., 2009b</u>
<u>Zhadang</u>	<u>2012.8</u>	<u>Monsoon</u>	<u>5500-5800</u>	<u>51.9+7.2</u>	<u>====</u>	<u>6.38+1.54</u>	<u>Snow pit</u>	<u>Qu et al., 2014</u>
<u>---</u>	<u>2014.6</u>	<u>Monsoon</u>	<u>5800</u>	<u>79</u>	<u>515.08</u>	<u>====</u>	<u>Snow pit</u>	<u>Li et al., 2016</u>
<u>---</u>	<u>2015.5</u>	<u>Non-monsoon</u>	<u>5790</u>	<u>303</u>	<u>822</u>	<u>====</u>	<u>Snow pit</u>	<u>Li et al., 2018</u>
<u>-</u>	<u>2015.6-9</u>	<u>Monsoon</u>	<u>5570-5790</u>	<u>281</u>	<u>743</u>	<u>====</u>	<u>Surface snow</u>	<u>Li et al., 2018</u>
<u>Urumqi No.1</u>	<u>2004.7-8</u>	<u>Monsoon</u>	<u>4130</u>	<u>500</u>	<u>1200</u>	<u>====</u>	<u>Surface snow</u>	<u>Xu et al., 2012</u>
	<u>2013.8</u>	<u>Monsoon</u>	<u>3800-4100</u>	<u>30+5</u>	<u>====</u>	<u>17+6</u>	<u>Fresh snow</u>	<u>Ming et al., 2016</u>
<u>Muji</u>	<u>2012.6-10</u>	<u>Monsoon</u>	<u>4700-5500</u>	<u>375+3</u>	<u>175+15</u>	<u>====</u>	<u>Snow pit</u>	<u>Yang et al., 2015</u>
<u>Qiangyong</u>	<u>2001</u>	<u>====</u>	<u>5400</u>	<u>43.1</u>	<u>117.3</u>	<u>====</u>	<u>Surface snow</u>	<u>Xu et al., 2006</u>
<u>Kangwure</u>	<u>2001</u>	<u>====</u>	<u>6000</u>	<u>21.8</u>	<u>161.1</u>	<u>====</u>	<u>Surface snow</u>	<u>Xu et al., 2006</u>
<u>Namunani</u>	<u>2004</u>	<u>====</u>	<u>5780-6080</u>	<u>4.4+2.1</u>	<u>51.1+20.6</u>	<u>====</u>	<u>Surface snow</u>	<u>Xu et al., 2006</u>
<u>Demula</u>	<u>2014.5</u>	<u>Non-monsoon</u>	<u>5404</u>	<u>17</u>	<u>185</u>	<u>====</u>	<u>Snow pit</u>	<u>Li et al., 2016</u>
<u>Yulong</u>	<u>2015.5</u>	<u>Non-monsoon</u>	<u>4400-4800</u>	<u>372+58</u>	<u>2003+308</u>	<u>9.47+2.36</u>	<u>Aged snow</u>	<u>Niu et al., 2017</u>
	<u>2015.8</u>	<u>Monsoon</u>	<u>4400-4800</u>	<u>2309+125</u>	<u>3211+168</u>	<u>97.12+50.78</u>	<u>Aged snow</u>	<u>Niu et al., 2017</u>

<u>Laohugou No. 12</u>	<u>2015.8</u>	<u>Monsoon</u>	<u>4400-4800</u>	<u>2198±1004</u>	<u>2190±1203</u>	<u>114±67</u>	<u>Aged snow</u>	<u>Zhang et al., 2017</u>
	<u>2015.10</u>	<u>Non-monsoon</u>	<u>4400-4800</u>	<u>1218±212</u>	<u>504±50</u>	<u>63±2</u>	<u>Aged snow</u>	<u>Zhang et al., 2017</u>

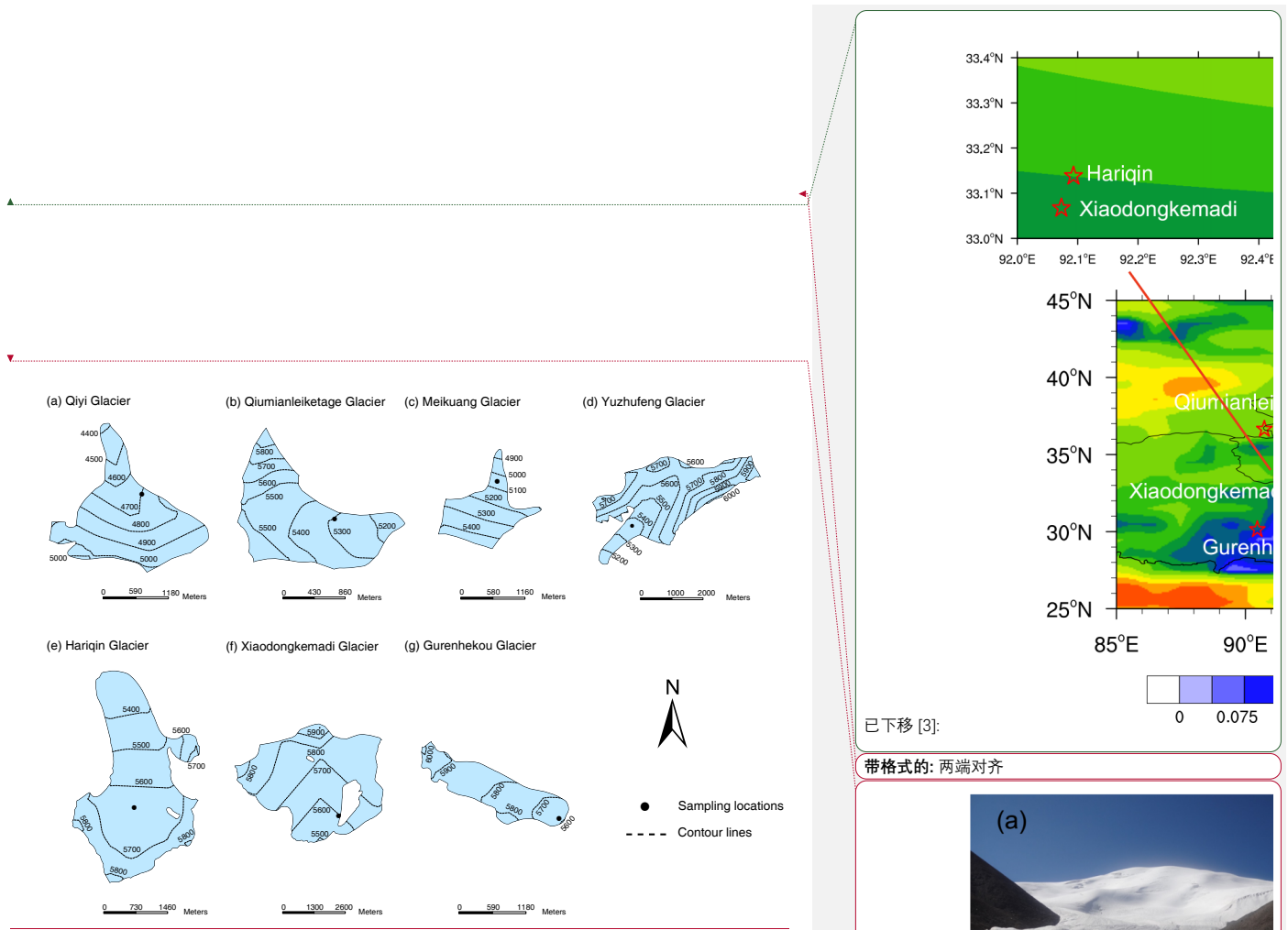


Figure 1. Geographical locations of (a) Qiyi glacier (97.76° E, 39.24° N), (b) Qiumianleiketage glacier (90.73° E, 36.70° N), (c) Meikuang glacier (94.19° E, 35.67° N), (d) Yuzhufeng glacier (94.23° E, 35.65° N), (e) Hariqin glacier (92.09° E, 33.14° N), (f) Xiaodongkemadi glacier (92.07° E, 33.07° N), (g) Gurenhekou glacier (90.46° E, 30.19° N). The black dot is the sampling locations.

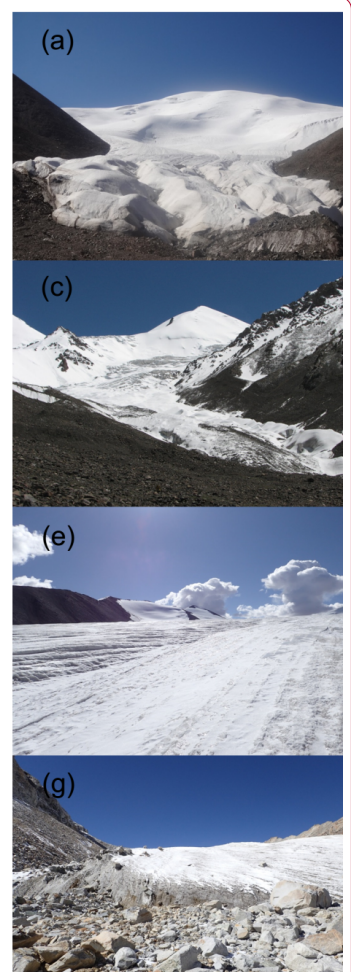




Figure 2. The equipment for collecting new snow samples in seven TP glaciers.

带格式的: 居中

带格式的: 字体: (默认) Times New Roman, (中文) 宋体, 五号, 字体颜色: 自动设置

带格式的: 字体: (默认) Times New Roman, (中文) 宋体, 五号, 字体颜色: 自动设置

带格式的: 字体: 加粗

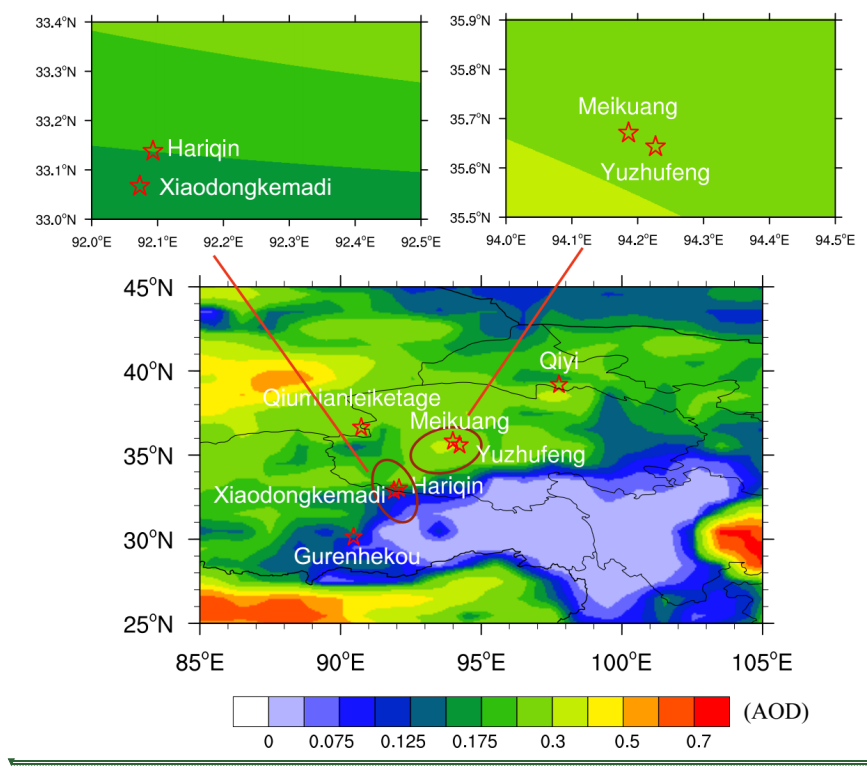


Figure 3. Spatial distribution of the averaged AOD retrieved from Aqua-MODIS at 500 nm over Tibetan Plateau from 2013 to 2015. The red stars are the sampling locations (see also Table 1):

已移动(插入) [3]
带格式的: 两端对齐

删除的内容: 1

删除的内容: , and larger values represent higher optical depth and smaller values represent smaller optical depth

删除的内容: 1, Qiyi glacier (97.76° E, 39.24° N, 4850 m a.s.l); 2, Qimianleiketage glacier (90.73° E, 36.70° N, 5240 m a.s.l); 3, Meikuang glacier (94.19° E, 35.67° N, 4983 m a.s.l); 4, Yuzhufeng glacier (94.23° E, 35.65° N, 5200 m a.s.l); 5, Hariqin glacier (92.09° E, 33.14° N, 5100 m a.s.l); 6, Xiaodongkemadi glacier (92.07° E, 33.07° N, 5600 m a.s.l); 7, Gurenhekou glacier (90.46° E, 30.19° N, 5655 m a.s.l).

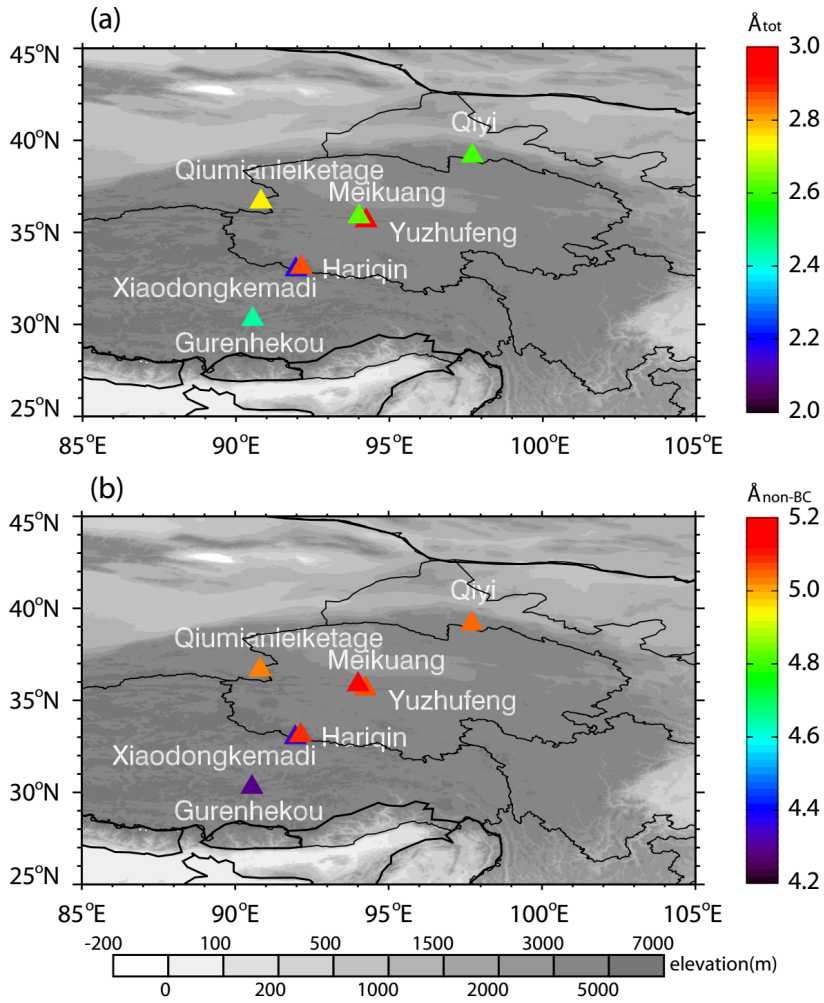


Figure 4. The spatial distribution of the median absorption Ångström exponent for (a) total particulate constituents (\bar{A}_{tot}), and (b) non-BC particulate constituents (\bar{A}_{non-BC}) in each glacier.

带格式的: 两端对齐

删除的内容: 3

删除的内容: (see Fig. 1)

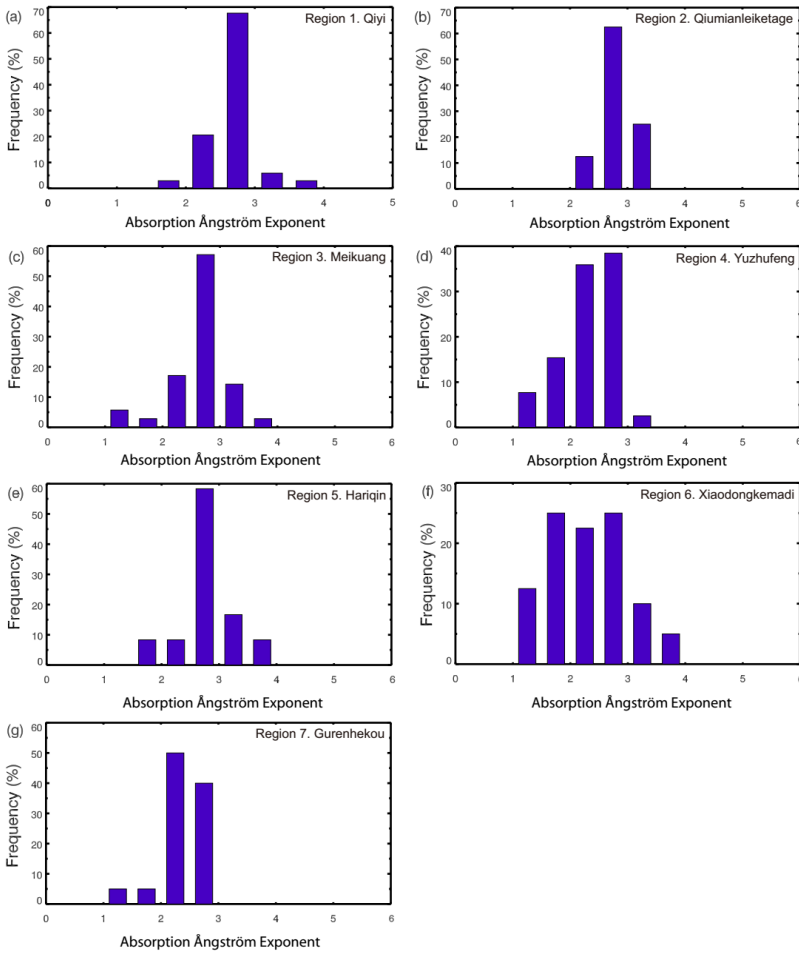


Figure 5. Histograms of the frequency of \hat{A}_{tot} (450-600 nm) for ice samples in each of the glacier region. Samples from all vertical profiles are included.

带格式的: 两端对齐

删除的内容: 4

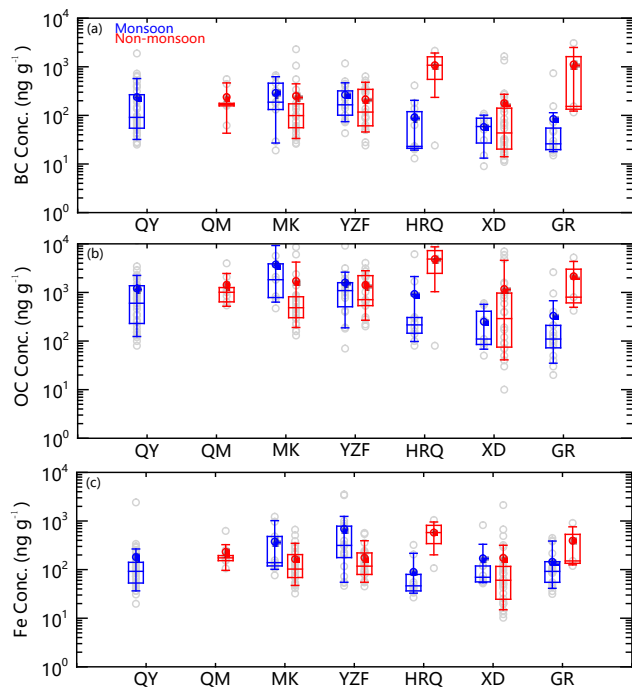
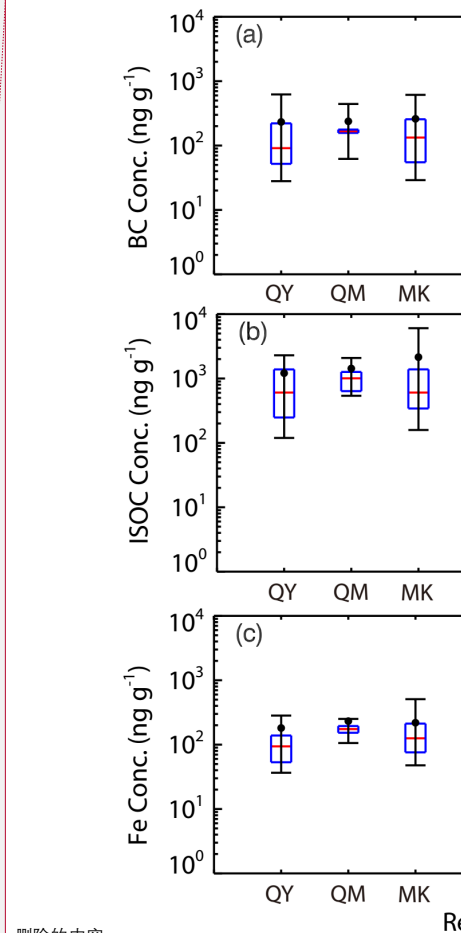


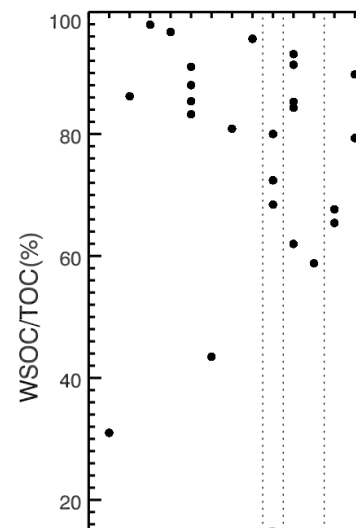
Figure 6. Box plots of the regional variations in (a) BC concentration, (b) ISOC concentration, and (c) Fe concentration of the seven glaciers. Error bars are 10th, 25th, median, 75th, and 90th percentiles of the data. The dot symbol represents the average concentrations of the ILAPs in ice samples in each glacier.



删除的内容:

带格式的: 两端对齐

删除的内容: 5... Box plots of the regional variations in (a) BC concentration, (b) ISOC concentration, and (c) Fe concentration of the seven glaciers. QY, QM, MK, YZF, HRQ, XD, and GR represent the following glaciers: Qiye, Qiumianleiketage, Meikuang, Yuzhufeng, Hariqin, Xiaodongkemadi, Gurenhekou glaciers, respectively. ... [126]



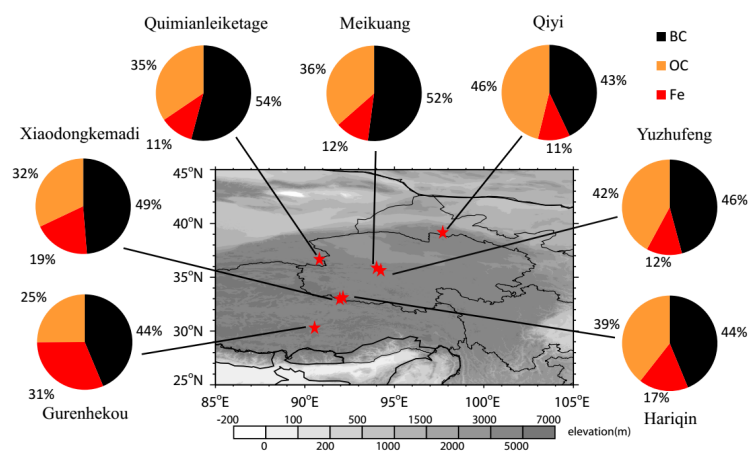


Figure 7. The median of relative contributions to total light absorption by BC, OC, and Fe for ice samples in each glacier.

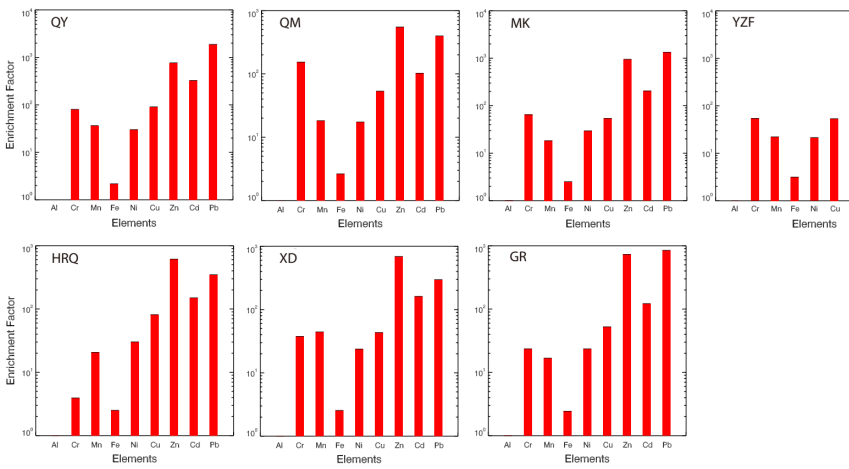
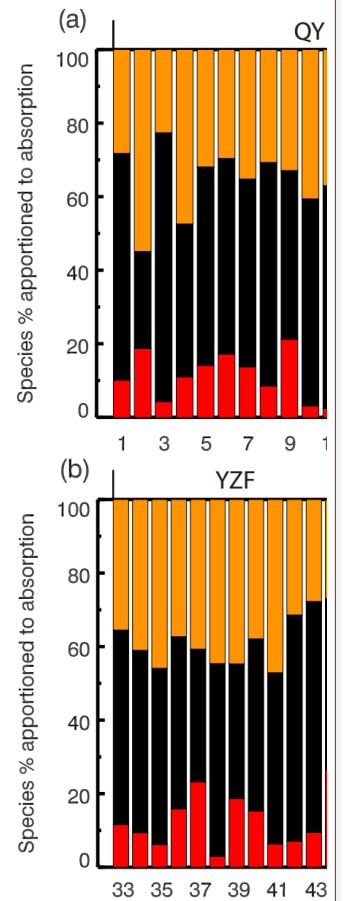


Figure 8. Average enrichment factors of trace metals in surface ice samples at each region.



删除的内容:

Figure 7. Relative contributions to total light absorption by BC, ISOC, and Fe oxide (assumed to be in the form of goethite) for surface ice samples in each sampling site (See Table 1).

带格式的: 两端对齐

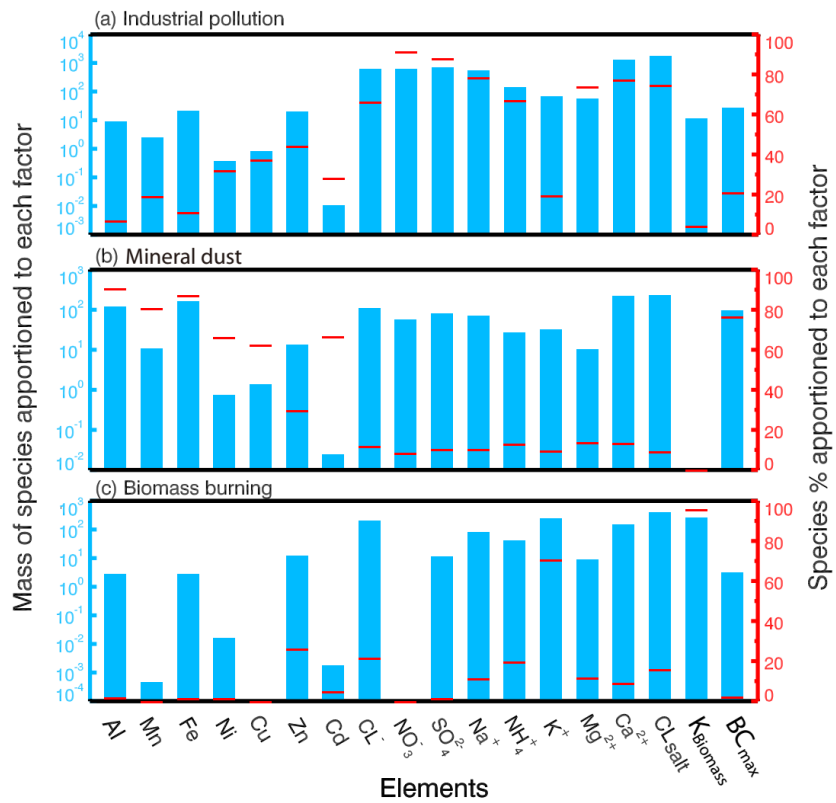


Figure 9. Source profiles for the three factors/sources that were resolved by the PMF 5.0 model.

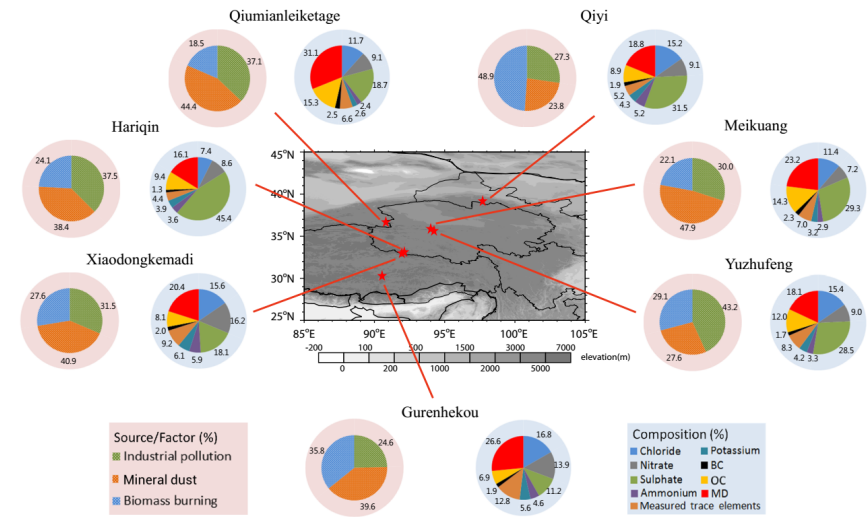
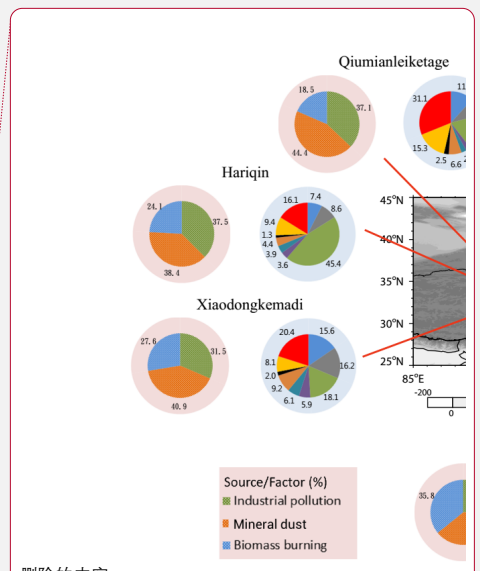


Figure 10. Chemical composition and source apportionment for the seven glaciers in the TP regions. Note that the apportionment is of the light absorption by insoluble particles in the surface glaciers.



删除的内容:

带格式的: 缩进: 左侧: 0 厘米, 首行缩进: 0 厘米

删除的内容: ↓

删除的内容: ↓

带格式的: 两端对齐

References

- Alexander, B., and Mickley, L. J.: Paleo-perspectives on potential future changes in the oxidative capacity of the atmosphere due to climate change and anthropogenic emissions, *Current Pollution Reports*, 1, 57-69, 2015.
- Alfaro, S. C., Lafon, S., Rajot, J. L., Formenti, P., Gaudichet, A., and Maille, M.: Iron oxides and light absorption by pure desert dust: An experimental study, *J. Geophys. Res.-Atmos.*, 109, Artn D08208, 10.1029/2003jd004374, 2004.
- Bergstrom, C.: Measuring the value and prestige of scholarly journals, *College and Research Libraries News*, 68, 314-316, 2007.
- Bolch, T., Yao, T., Kang, S., Buchroithner, M. F., Scherer, D., Maussion, F., Huintjes, E., and Schneider, C.: A glacier inventory for the western Nyainqentanglha Range and the Nam Co Basin, Tibet, and glacier changes 1976–2009, *The Cryosphere*, 4, 419-433, <https://doi.org/10.5194/tc-4-419-2010>, 2010.
- Bond, T. C., and Bergstrom, R. W.: Light absorption by carbonaceous particles: An investigative review, *Aerosol Sci. Technol.*, 40, 27-67, 2006.
- Bond, T. C., Doherty, S. J., Fahey, D. W., et al.: Bounding the role of black carbon in the climate system: A scientific assessment, *J. Geophys. Res.-Atmos.*, 118, 5380-5552, 2013.
- Brandt, R. E., Warren, S. G., and Clarke, A. D.: A controlled snowmaking experiment testing the relation between black carbon content and reduction of snow albedo, *J. Geophys. Res.-Atmos.*, 116, Artn D08109, 10.1029/2010jd015330, 2011.
- Christian, T. J., Yokelson, R. J., Cárdenas, B., Molina, L. T., Engling, G., and Hsu, S. C.: Trace gas and particle emissions from domestic and industrial biofuel use and garbage burning in Central Mexico, *Atmos. Chem. Phys.*, 10, 565-584, 2010.
- Chylek, P., Ramaswamy, V. & Srivastava, V.: Graphitic carbon content of aerosols, clouds and snow, and its climatic implications, *Sci. Total Environ.*, 36, 117–120, 1984.
- Cong, Z., Gao, S., Zhao, W., Wang, X., Wu, G., Zhang, Y., Kang, S., Liu, Y., and Ji, J.: Iron oxides in the cryoconite of glaciers on the Tibetan Plateau: abundance, speciation and implications, *The Cryosphere*, 12, 3177-3186, 10.5194/tc-12-3177-2018, 2018.
- Cong, Z. Y., Kang, S. C., Smirnov, A., and Holben, B.: Aerosol optical properties at Nam Co, a remote site in central Tibetan Plateau, *Atmos. Res.*, 92, 42-48,

[10.1016/J.Atmosres.2008.08.005](https://doi.org/10.1016/J.Atmosres.2008.08.005), 2009.

[Cong, Z. Y., Kang, S. C., Zhang, Y. L., and Li, X. D.: Atmospheric wet deposition of trace elements to central Tibetan Plateau, *Appl. Geochem.*, 25, 1415-1421, 2010.](#)

[Cong, Z., Kang, S., Kawamura, K., Liu, B., Wan, X., Wang, Z., Gao, S., and Fu, P.: Carbonaceous aerosols on the south edge of the Tibetan Plateau: concentrations, seasonality and sources, *Atmos. Chem. Phys.*, 15, 1573-1584, 2015.](#)

[Contini, D., Cesari, D., Genga, A., Siciliano, M., Ielpo, P., and Guascito, M. R.: Source apportionment of size-segregated atmospheric particles based on the major water-soluble components in Lecce \(Italy\), *Sci. Total Environ.*, 472, 248-261, 2014.](#)

[Conway, H., Gades, A., and Raymond, C. F.: Albedo of dirty snow during conditions of melt, *Water Resour. Res.*, 32, 1713-1718, \[10.1029/96wr00712\]\(https://doi.org/10.1029/96wr00712\), 1996.](#)

[Dang, C., and Hegg, D. A.: Quantifying light absorption by organic carbon in Western North American snow by serial chemical extractions, *J. Geophys. Res.-Atmos.*, 119, \[10.1002/2014jd022156\]\(https://doi.org/10.1002/2014jd022156\), 2014.](#)

[Doherty, S. J., Warren, S. G., Grenfell, T. C., Clarke, A. D., and Brandt, R. E.: Light-absorbing impurities in Arctic snow, *Atmos. Chem. Phys.*, 10, 11647-11680, 2010.](#)

[Doherty, S. J., Grenfell, T. C., Forsström, S., Hegg, D. L., Brandt, R. E., and Warren, S. G.: Observed vertical redistribution of black carbon and other insoluble light-absorbing particles in melting snow, *J. Geophys. Res.-Atmos.*, 118, 5553-5569, 2013.](#)

[Doherty, S. J., Dang, C., Hegg, D. A., Zhang, R. D., and Warren, S. G.: Black carbon and other light-absorbing particles in snow of central North America, *J. Geophys. Res.-Atmos.*, 119, 12807-12831, 2014.](#)

[Engling, G. and Gelencser, A.: Atmospheric Brown Clouds: From Local Air Pollution to Climate Change, *Elements*, 6, 223-228, 2010.](#)

[Federer, U., Kaufmann, P. R., Hutterli, M., Schüpbach, S., and Stocker, T. F.: Continuous flow analysis of total organic carbon in polar ice cores, *Environ. Sci. Technol.*, 42, 8039-8043, 2008.](#)

[Fialho, P., Hansen, A. D. A., and Honrath, R. E.: Absorption coefficients by aerosols in remote areas: a new approach to decouple dust and black carbon absorption coefficients using seven-wavelength Aethalometer data, *J. Aerosol Sci.*, 36, 267-282, 2005.](#)

- [Flanner, M. G., Zender, C. S., Randerson, J. T., and Rasch, P. J.: Present-day climate forcing and response from black carbon in snow, J. Geophys. Res.-Atmos., 112, D11202, doi: 10.1029/2006jd008003, 2007.](#)
- [Flanner, M. G., Zender, C. S., Hess, P. G., Mahowald, N. M., Painter, T. H., Ramanathan, V., and Rasch, P. J.: Springtime warming and reduced snow cover from carbonaceous particles, Atmos. Chem. Phys., 9, 2481-2497, 2009.](#)
- [Grenfell, T. C., Doherty, S. J., Clarke, A. D., and Warren, S. G.: Light absorption from particulate impurities in snow and ice determined by spectrophotometric analysis of filters, Appl. Opt., 50, 2037-2048, 2011.](#)
- [Guan, X., Huang, J., Guo, N., Bi, J., and Wang, G.: Variability of soil moisture and its relationship with surface albedo and soil thermal parameters over the Loess Plateau, Adv. Atmos. Sci., 26, 692-700, 2009.](#)
- [Hadley, O. L., and Kirchstetter, T. W.: Black-carbon reduction of snow albedo, Nat. Clim. Change, 2, 437-440, 2012.](#)
- [Hansen, J., and Nazarenko, L.: Soot climate forcing via snow and ice albedos, P. Natl. Acad. Sci. USA, 101, 423-428, 2004.](#)
- [Hegg, D. A., Warren, S. G., and Grenfell, T. C.: Source attribution of black carbon in Arctic snow, Environ. Sci. Technol., 43, 4016-4021, 2009.](#)
- [Hegg, D. A., Warren, S. G., and Grenfell, T. C.: Sources of light-absorbing aerosol in arctic snow and their seasonal variation, Atmos. Chem. Phys., 10, 10923-10938, 2010.](#)
- [Hsu, S. C., Liu, S. C., Arimoto, R., et al.: Effects of acidic processing, transport history, and dust and sea salt loadings on the dissolution of iron from Asian dust, J. Geophys. Res.-Atmos., 115, 2010.](#)
- [Huang, J., Li, Y. F., Li, Z., and Xiong, L. F.: Spatial variations and sources of trace elements in recent snow from glaciers at the Tibetan Plateau, Environ. Sci. Pollut. R., 25, 7875-7883, 2018.](#)
- [Huang, J. P., Fu, Q., Zhang, W., Wang, X., Zhang, R. D., Ye, H., and Warren, S. G.: Dust and Black Carbon in Seasonal Snow across Northern China, Bull. Amer. Meteor. Soc., 92, 175-181, 2011.](#)
- [Jenkins, M., Kaspari, S., Kang, S. C., Grigholm, B., and Mayewski, P. A.: Tibetan plateau geladaindong black carbon ice core record \(1843-1982\): recent increases due to higher](#)

- [emissions and lower snow accumulation, *Advances in Climate Change Research*, 7\(3\), 132-138, 2016.](#)
- [Jeong, D., Kim, K., and Choi, W.: Accelerated dissolution of iron oxides in ice, *Atmos. Chem. Phys.*, 12, 11125-11133, 10.5194/acp-12-11125-2012, 2012.](#)
- [Kang, S., Chen, F., Gao, T., Zhang, Y., Yang, W., Yu, W., and Yao, T.: Early onset of rainy season suppresses glacier melt: a case study on Zhadang glacier, Tibetan Plateau, *J. Glaciol.*, 55\(192\), 755–758, 2009.](#)
- [Kaspari, S., Painter, T. H., Gysel, M., Skiles, S. M., and Schwikowski, M.: Seasonal and elevational variations of black carbon and dust in snow and ice in the Solu-Khumbu, Nepal and estimated radiative forcings, *Atmos. Chem. Phys.*, 14, 8089-8103, 2014.](#)
- [Kirchstetter, T. W., Novakov, T., Hobbs, P. V.: Evidence that the spectral dependence of light absorption by aerosols is affected by organic carbon, *J. Geophys. Res.-Atmos.*, 109, D21, 10.1029/2004JD004999, 2004.](#)
- [Kulkarni, S.: Assessment of source-receptor relationships of aerosols: an integrated forward and backward modeling approach, *Dissertations and Theses-Gradworks*, 2009.](#)
- [Lafon, S., Rajot, J. L., Alfaro, S. C., and Gaudichet, A.: Quantification of iron oxides in desert aerosol, *Atmos. Environ.*, 38, 1211-1218, 10.1016/J.Atmosenv.2003.11.006, 2004.](#)
- [Lafon, S., and Lee, A. B.: Diffusion maps and coarse-graining: a unified framework for dimensionality reduction, graph partitioning and data set parameterization, *IEEE T. Pattern anal.*, 28, 1393-1403, 2006.](#)
- [Li C. L., Kang S. C., Zhang Q.: Elemental composition of Tibetan Plateau top soils and its effect on evaluating atmospheric pollution transport, *Environ. Pollut.*, 157, 8-9, 2009.](#)
- [Li, C. L., Bosch, C., Kang, S. C., Andersson, A., Chen, P. F., Zhang, Q. G., Cong, Z. Y., Chen, B., Qin, D. H., and Gustafsson, O.: Sources of black carbon to the Himalayan-Tibetan Plateau glaciers, *Nat. Commun.*, 7, 12574, 10.1038/ncomms12574, 2016.](#)
- [Li, X. F., Kang, S. C., He, X. B., Qu, B., Tripathee, L., Jing, Z. F., Paudyal, R., Li, Y., Zhang, Y. L., Yan, F. P., Li, G., and Li, C. L.: Light-absorbing impurities accelerate glacier melt in the Central Tibetan Plateau, *Sci. Total Environ.*, 587, 482-490, 2017.](#)

- Li, X. F., Kang, S. C., Zhang, G. S., Qu, B., Tripathee, L., Paudyal, R., Jing, Z. F., Zhang, Y. L., Yan, F. P., Li, G., Cui, X. Q., Xu, R., Hu, Z. F., and Li, C. L.: Light-absorbing impurities in a southern Tibetan Plateau glacier: Variations and potential impact on snow albedo and radiative forcing, *Atmos. Res.*, 200, 77-87, 2018.
- Liou, K. N., Takano, Y., and Yang, P.: Light absorption and scattering by aggregates: Application to black carbon and snow grains, *J. Quant. Spectrosc. Ra.*, 112, 1581-1594, 10.1016/J.jqsrt.2011.03.007, 2011.
- Liu S. Y., Guo, W. Q., Xu J. L., et al.: The Second Glacier Inventory Dataset of China (Version 1.0), Cold and Arid Regions Science Data Center at Lanzhou, 10.3972/glacier.001.2013.db, 2014.
- Lüthi, Z. L., Škerlak, B., Kim, S.-W., Lauer, A., Mues, A., Rupakheti, M., and Kang, S.: Atmospheric brown clouds reach the Tibetan Plateau by crossing the Himalayas, *Atmos. Chem. Phys.*, 15, 6007-6021, <https://doi.org/10.5194/acp-15-6007-2015>, 2015.
- Millikan, R. C.: Optical properties of soot, *J. Opt. Soc. Am.*, 51, 698-699, 1961.
- Ming, J., Xiao, C. D., Cachier, H., Qin, D. H., Qin, X., Li, Z. Q., and Pu, J. C.: Black Carbon (BC) in the snow of glaciers in west China and its potential effects on albedos, *Atmos. Res.*, 92, 114-123, 2009.
- Ming, J., Xiao, C. D., Du, Z. C., and Yang, X. G.: An overview of black carbon deposition in High Asia glaciers and its impacts on radiation balance, *Adv. Water Resour.*, 55, 80-87, 2013.
- Ming, J., Xiao, C. D., Sun, J. Y., Kang, S. C., and Bonasoni, P.: Carbonaceous particles in the atmosphere and precipitation of the Nam Co region, central Tibet, *J. Environ. Sci.*, 22, 1748-1756, 10.1016/S1001-0742(09)60315-6, 2010.
- Ming, J., Xiao, C. D., Wang, F. T., Li, Z. Q., and Li, Y. M.: Grey Tianshan Urumqi Glacier No.1 and light-absorbing impurities, *Environ. Sci. Pollut. R.*, 23, 9549-9558, 2016.
- Moosmuller, H., Engelbrecht, J. P., Skiba, M., Frey, G., Chakrabarty, R. K., and Arnott, W. P.: Single scattering albedo of fine mineral dust aerosols controlled by iron concentration, *J. Geophys. Res.-Atmos.*, 117, Artn D11210, 10.1029/2011jd016909, 2012.

- Niu, H. W., Kang, S. C., Zhang, Y. L., Shi, X. Y., Shi, X. F., Wang, S. J., Li, G., Yan, X. G., Pu, T., and He, Y. Q.: Distribution of light-absorbing impurities in snow of glacier on Mt. Yulong, southeastern Tibetan Plateau, Atmos. Res., 197, 474-484, 2017.
- Paatero, P., and Tapper, U.: Positive matrix factorization: a non-negative factor model with optimal utilization of error estimates of data values, Environmetrics, 5, 111-126, 1994.
- Pacyna, J. M. and Pacyna, E. G.: An assessment of global and regional emissions of trace metals to the atmosphere from anthropogenic sources worldwide, Environ. Rev., 9, 269-298, 2001.
- Painter, T. H., Barrett, A. P., Landry, C. C., Neff, J. C., Cassidy, M. P., Lawrence, C. R., McBride, K. E., and Farmer, G. L.: Impact of disturbed desert soils on duration of mountain snow cover, Geophys. Res. Lett., 34, L12502, 10.1029/2007gl030284, 2007.
- Painter, T. H., Deems, J. S., Belnap, J., Hamlet, A. F., Landry, C. C., and Udall, B.: Response of Colorado River runoff to dust radiative forcing in snow, P. Natl. Acad. Sci. USA, 107, 17125-17130, 2010.
- Painter, T. H., Bryant, A. C., and Skiles, S. M.: Radiative forcing by light absorbing impurities in snow from MODIS surface reflectance data, Geophys. Res. Lett., 39, L17502, 10.1029/2012gl052457, 2012.
- Pang, H., He, Y., Theakstone, W. H., and Zhang, D. D.: Soluble ionic and oxygen isotopic compositions of a shallow firn profile, Baishui glacier No. 1, southeastern Tibetan Plateau, Ann. Glaciol., 46, 325-330, 2007.
- Pio, C. A., Legrand, M., Oliveira, T., Afonso, J., Santos, C., Caseiro, A., Fialho, P., Barata, F., Puxbaum, H., Sanchez-Ochoa, A., Kasper-Giebl, A., Gelencser, A., Preunkert, S., and Schock, M.: Climatology of aerosol composition (organic versus inorganic) at nonurban sites on a west-east transect across Europe, J. Geophys. Res., 112, D23S02, 10.1029/2006JD008038, 2007.
- Preunkert, S., Legrand, M., Stricker, P., Bulat, S., Alekhina, I., Petit, J. R., Hoffmann, H., May, B., and Jourdain B.: Quantification of Dissolved Organic Carbon at very low levels in natural ice samples by a UV induced oxidation method, Environ. Sci. Technol., 45, 673-678, 2011.
- Pu, W., Wang, X., Wei, H. L., Zhou, Y., Shi, J. S., Hu, Z. Y., Jin, H. C., and Chen, Q. L.: Properties of black carbon and other insoluble light-absorbing particles in seasonal

- [snow of northwestern China, *The Cryosphere*, 11, 1213-1233, 2017.](#)
- [Qian, Y., Flanner, M. G., Leung, L. R., and Wang, W.: Sensitivity studies on the impacts of Tibetan Plateau snowpack pollution on the Asian hydrological cycle and monsoon climate, *Atmos. Chem. Phys.*, 11, 1929-1948, 2011.](#)
- [Qian, Y., Yasunari, T. J., Doherty, S. J., Flanner, M. G., Lau, W. K. M., & Jing, M.: Light-absorbing particles in snow and ice: measurement and modeling of climatic and hydrological impact, *Adv. Atmos. Sci.*, 32, 64-91, 2015.](#)
- [Qin, D. H., Liu, S. Y., and Li, P. J.: Snow cover distribution, variability, and response to climate change in western China, *J. Climate*, 19, 1820-1833, 2006.](#)
- [Qiu, J.: The third pole, *Nature*, 454, 393-396, 10.1038/454393a, 2008.](#)
- [Qu, B., Ming, J., Kang, S. C., Zhang, G. S., Li, Y. W., Li, C. D., Zhao, S. Y., Ji, Z. M., and Cao, J. J.: The decreasing albedo of the Zhadang glacier on western Nyainqentanglha and the role of light-absorbing impurities, *Atmos. Chem. Phys.*, 14, 11117-11128, 2014.](#)
- [Ramanathan, V., Li, F., Ramana, M. V., et al.: Atmospheric brown clouds: Hemispherical and regional variations in long-range transport, absorption, and radiative forcing, *J. Geophys. Res.*, 112, D22S21, 10.1029/2006JD008124, 2007.](#)
- [Sand, M., Berntsen, T. K., Seland, O., and Kristjansson, J. E.: Arctic surface temperature change to emissions of black carbon within Arctic or midlatitudes, *J. Geophys. Res.-Atmos.*, 118, 7788-7798, 10.1002/Jgrd.50613, 2013.](#)
- [Skiles, S. M., Painter, T. H., Deems, J. S., Bryant, A. C., and Landry, C. C.: Dust radiative forcing in snow of the Upper Colorado River Basin: 2. Interannual variability in radiative forcing and snowmelt rates, *Water Resour. Res.*, 48, 10.1029/2012wr011986, 2012.](#)
- [Takahashi, Y., Higashi, M., Furukawa, T., and Mitsunobu, S.: Change of iron species and iron solubility in Asian dust during the long-range transport from western China to Japan, *Atmos. Chem. Phys.*, 11, 11237-11252, 10.5194/acp-11-11237-2011, 2011.](#)
- [Wang, M., Xu, B., Cao, J., et al.: Carbonaceous aerosols recorded in a southeastern Tibetan glacier: analysis of temporal variations and model estimates of sources and radiative forcing, *Atmos. Chem. Phys.*, 15, 1191-1204, 10.5194/Acp-15-1191-2015, 2015.](#)
- [Wang, X., Doherty, S. J., and Huang, J. P.: Black carbon and other light-absorbing](#)

- [impurities in snow across Northern China, *J. Geophys. Res.-Atmos.*, 118, 1471-1492, 2013.](#)
- [Wang, X., Xu, B. Q., and Ming, J.: An overview of the studies on Black Carbon and Mineral Dust deposition in Snow and Ice Cores in East Asia, *J. Meteorol. Res.*, 28, 354-370, 2014.](#)
- [Wang, X., Pu, W., Ren, Y., Zhang, X., Zhang, X., Shi, J., Jin, H., Dai, M., and Chen, Q.: Observations and model simulations of snow albedo reduction in seasonal snow due to insoluble light-absorbing particles during 2014 Chinese survey, *Atmos. Chem. Phys.*, 17, 2279-2296, 2017.](#)
- [Warren, S. G., and Wiscombe, W. J.: A Model for the Spectral Albedo of Snow. II: Snow Containing Atmospheric Aerosols, *J. Atmos. Sci.*, 37, 2734-2745, 1980.](#)
- [Warren, S. G.: Optical-Properties of Snow, *Rev. Geophys.*, 20, 67-89, 1982.](#)
- [Warren, S. G., and Wiscombe, W. J.: Dirty Snow after Nuclear-War, *Nature*, 313, 467-470, 10.1038/313467a0, 1985.](#)
- [Wedepohl, K. H.: The Composition of the Continental-Crust, *Geochim. Cosmochim. Ac.*, 59, 1217-1232, 1995.](#)
- [Xu, B. Q., Yao, T. D., Liu, X. Q., and Wang, N. L.: Elemental and organic carbon measurements with a two-step heating-gas chromatography system in snow samples from the Tibetan Plateau, *Ann. Glaciol.*, 43, 257-262, 2006.](#)
- [Xu, B. Q., Cao, J. J., Hansen, J., Yao, T. D., Joswiak, D. R., Wang, N. L., Wu, G. J., Wang, M., Zhao, H. B., Yang, W., Liu, X. Q., and He, J. Q.: Black soot and the survival of Tibetan glaciers, *P. Natl. Acad. Sci. USA*, 106, 22114-22118, 2009a.](#)
- [Xu, B. Q., Wang, M., Joswiak, D. R., Cao, J. J., Yao, T. D., Wu, G. J., Yang, W., and Zhao, H. B.: Deposition of anthropogenic aerosols in a southeastern Tibetan glacier, *J. Geophys. Res.-Atmos.*, 114, D17209, 10.1029/2008jd011510, 2009b.](#)
- [Xu, B. Q., Cao, J. J., Joswiak, D. R., Liu, X. Q., Zhao, H. B., and He, J. Q.: Post-depositional enrichment of black soot in snow-pack and accelerated melting of Tibetan glaciers, *Environ. Res. Lett.*, 7, 014022, 10.1088/1748-9326/7/1/014022, 2012.](#)
- [Yang, K., Ding, B., Qin, J., Tang, W., Lu, N., and Lin, C.: Can aerosol loading explain the solar dimming over the Tibetan Plateau?, *Geophys. Res. Lett.*, 39,](#)

[10.1029/2012GL053733, 2012.](#)

[Yang, S., Xu, B. Q., Cao, J. J., Zender, C. S., and Wang, M.: Climate effect of black carbon aerosol in a Tibetan Plateau glacier, *Atmos. Environ.*, 111, 71-78, 2015.](#)

[Yao, T. D., Thompson, L., Yang, W., Yu, W. S., Gao, Y., Guo, X. J., Yang, X. X., Duan, K. Q., Zhao, H. B., Xu, B. Q., Pu, J. C., Lu, A. X., Xiang, Y., Kattel, D. B., and Joswiak, D.: Different glacier status with atmospheric circulations in Tibetan Plateau and surroundings, *Nat. Clim. Change*, 2, 663-667, 2012.](#)

[Yasunari, T. J., Koster, R. D., Lau, W. K. M., and Kim, K. M.: Impact of snow darkening via dust, black carbon, and organic carbon on boreal spring climate in the Earth system, *J. Geophys. Res.-Atmos.*, 120, 5485-5503, 2015.](#)

[Zhang, R., Hegg, D. A., Huang, J., and Fu, Q.: Source attribution of insoluble light-absorbing particles in seasonal snow across northern China, *Atmos. Chem. Phys.*, 13, 6091-6099, 2013a.](#)

[Zhang, R., Jing, J., Tao, J., Hsu, S. C., Wang, G., Cao, J., Lee, C. S. L., Zhu, L., Chen, Z., Zhao, Y., and Shen, Z.: Chemical characterization and source apportionment of PM_{2.5} in Beijing: seasonal perspective, *Atmos. Chem. Phys.*, 13, 7053-7074, 2013b.](#)

[Zhang, Y. L., Kang, S. C., Li, C. L., Gao, T. G., Cong, Z. Y., Sprenger, M., Liu, Y. J., Li, X. F., Guo, J. M., Sillanpaa, M., Wang, K., Chen, J. Z., Li, Y., and Sun, S. W.: Characteristics of black carbon in snow from Laohugou No. 12 glacier on the northern Tibetan Plateau, *Sci. Total Environ.*, 607, 1237-1249, 2017.](#)

[Zhou, Y., Wang, X., Wu, X., Cong, Z., Wu, G., and Ji, M.: Quantifying light absorption of iron oxides and carbonaceous aerosol in seasonal snow across northern China, *Atmosphere*, 8, 63, 10.3390/atmos8040063, 2017.](#)

带格式的: 两端对齐, 缩进: 左侧: 0 厘米, 悬挂缩进: 2.36 字符, 首行缩进: -2.36 字符

删除的内容: **References**

Agarwal, S., Aggarwal, S. G., Okuzawa, K., and Kawamura, K.: Size distributions of dicarboxylic acids, ketoacids, α -dicarbonyls, sugars, wsoc, oc, ec and inorganic ions in atmospheric particles over northern japan: implication for long-range transport of siberian biomass burning and east asian polluted aerosols, *Atmos. Chem. Phys.*, 10, 5839-5858, 2010.

Akagi, S. K., Yokelson, R. J., Wiedinmyer, C., and Alvarado, M. J.: Emission factors for open and domestic biomass burning for use in atmospheric models, *Atmos. Chem. Phys.*, 11, 27523-27602, 2011.

Alexander, B., Allman, D. J., Amos, H. M., Fairlie, T. D., Dachs, J., and Hegg, D. A.: Isotopic constraints on the formation pathways of sulfate aerosol in the marine boundary layer of the subtropical northeast atlantic ocean, *J. Geophys. Res.-Atmos.*, 117, D06304, doi: 10.1029/2011JD016773, 2012.

Alexander, B., and Mickley, L. J.: Paleo-perspectives on potential future changes in the oxidative capacity of the atmosphere due to climate change and anthropogenic emissions, *Current Pollution Reports*, 1, 57-69, 2015.

Andersson, A., Deng, J., Du, K., Zheng, M., Yan, C., and Sköld, M.: Regionally-varying combustion sources of the January 2013 severe haze events over eastern China, *Environ. Sci. Technol.*, 49, 2038-2043, 2015.

Andreae, M. O., and Rosenfeld, D.: Aerosol-cloud-precipitation interactions. Part 1. The nature and sources of cloud-active aerosols, *Earth-Sci. Rev.*, 8, 13-41, 2008. ... [128]

带格式的: 字体: 非加粗

Quantifying light absorption and its source attribution of insoluble light-absorbing particles in Tibetan Plateau glaciers from 2013-2015

Xin Wang^{1,*}, Hailun Wei¹, Jun Liu¹, Baiqing Xu^{1,2,*}, ~~and~~ Mo Wang², [Mingxia Ji¹](#), and [Hongchun Jin³](#)

5 ¹ Key Laboratory for Semi-Arid Climate Change of the Ministry of Education, College of Atmospheric Sciences, Lanzhou University, Lanzhou, 730000, China

² Key Laboratory of Tibetan Environment Changes and Land Surface Processes, Institute of Tibetan Plateau Research, Chinese Academy of Sciences, Beijing 100085, China

³ [KuWeather Science and Technology, Haidian, Beijing, 100085, China](#)

10

Correspondence to: X. Wang (wxin@lzu.edu.cn), and B. Xu (baiqing@itpcas.ac.cn)

†

15

20

Abstract. Amounts of insoluble light-absorbing particles (ILAPs) deposited on the surface of snow and ice can significantly reduce the snow albedo and accelerate the snow melting process. In this study, 67 ice samples were collected in ~~7 high mountain seven~~ glaciers over the Tibetan Plateau (TP) ~~regions~~ from May 2013 to October 2015. The mixing ratio of black carbon (BC), organic carbon (OC), and mineral dust (MD) was measured using an integrating sphere/integrating sandwich spectrophotometer (ISSW) system associated with the chemical analysis by assuming that the light absorption of mineral dust is due to iron oxide. The results indicated that the mass mixing ratios of BC, ~~ISOC~~, and MD showed a large variation of 10-3100 ng g⁻¹, 10-17000 ng g⁻¹, 10-3500 ng g⁻¹, with ~~a~~ mean values of ~~218220±400397~~ ng g⁻¹, ~~13571360±2417-2420~~ ng g⁻¹, ~~241240±452-450~~ ng g⁻¹ on TP glaciers during the entire ice field campaign, respectively. Although the mineral dust was assumed to be the highest contributor to the mass loading of ILAPs, we noted that the averaged light absorption of BC (50.7%) and OC (33.2%) was largely responsible for the measured light absorption in the TP glaciers at the wavelengths of 450-600 nm. The chemical elements and the selected carbonaceous particles were also analyzed ~~of for~~ the source attributions of the particulate light absorption based on a positive matrix factorization (PMF) receptor model. On average, the industrial pollution (33.1%), biomass/biofuel burning (29.4%), and mineral dust (37.5%) were the major sources of the ILAPs in TP glaciers. ~~Although the mineral dust assumed to be the highest contributor to the mass loading of ILAPs, we noted that the averaged light absorption of BC (50.7%) and ISOC (33.2%) was largely responsible for the measured light absorption in the high mountain glaciers at the wavelengths of 450-600 nm.~~

5

1 Introduction

~~The Tibetan Plateau (TP), known as the highest plateau in the world, and its surrounding areas contain the largest snow and ice mass outside the polar regions (Qin et al., 2006).~~

10 ~~Ample~~ The Tibetan Plateau (TP), known as the highest plateau in the world, and its surrounding areas contain the largest snow and ice mass outside the polar regions (Qin et al., 2006). ~~Ample evidence indicated~~ evidence has indicated ~~that the deposition of the snow albedo at visible wavelengths is largely dominant by black carbon (BC) (Warren and~~
15 ~~Wiscombe, 1980, 1985; Brandt et al., 2011; Hadley and Kirchstetter, 2012) insoluble light-~~
~~absorbing particles (ILAPs) was one of the major factors (up to 30%) to lead the greatest~~
~~decrease in length and area of negative mass balance in the TP glaciers over the past decade~~
~~(Xu et al., 2006, 2009a; Yao et al., 2012; Qian et al., 2015; Li et al., 2017). The unusual~~
~~increase in temperature over the TP is now considered one of the major contributors to~~
~~glacial shrinkage (Ding et al., 2006). Climate models indicated that black carbon (BC) heats~~
20 ~~the troposphere by absorbing solar radiation (Jacobson, 2001; Ji et al., 2016; Yang et al.,~~
~~2017), and BC reduces snow and ice albedos when it is deposited on their surface, thus~~
~~leading to the acceleration of snowmelt (Hansen and Nazarenko, 2004; Flanner et al., 2007,~~
~~2009; Hadley and Kirchstetter, 2012; Yasunari et al., 2015; Schmale et al., 2017; Zhang et~~
~~al., 2017, 2018).~~ For example instance, a mixing ratio of 10 ng g⁻¹ of BC in snow can reduce
25 snow albedo by 1%, which has a similar effect to that of 500 ng g⁻¹ of ~~mineral dust on the~~
~~albedo of snow and ice at 500 nm wavelength~~ (Warren and Wiscombe, 1980; Warren, 1982;
Wang et al., 2017). Chylek et al. (1984) indicated that the absorbing efficiency of BC is
higher in snow than in the atmosphere due to more sunlight scattering in snow. Conway et
al. (1996) measured a snow albedo reduction of 0.21 and a 50% increase in the ablation
30 rate of natural snow attributed to 500 ng g⁻¹ BC contamination. Liou et al. (2011) developed

5 a geometric-optics surface-wave approach to demonstrate the snow albedo reduction by as much as ~5–10% due to small amounts of BC internally mixed with snow grains. Totally, BC accounts for 85% of absorption by all insoluble light-absorbing impurities (ILAPs) in snow at the wavelength of 400-700 nm (Bond et al., 2013). Due to the impact of BC on snow and ice albedos, the “efficacy” of this BC-snow forcing is twice as effective as CO₂, and may have contributed to global warming of the past century in the Northern Hemisphere (Hansen and Nazarenko, 2004).

10 The Tibetan Plateau (TP), known as the highest plateau in the world and its surrounding areas, contains the largest store of snow and ice outside the polar regions (Qin et al., 2006). However, ~82% of the plateau's glaciers have retreated, and 10% of its permafrost has degraded in the past decade (Qiu, 2008; Yao et al., 2012). Xu et al. (2009a, b) indicated that the BC deposited in snow and ice potentially lead the melting seasons earlier, and the large retreat of these glaciers across the TP regions may affect the atmospheric circulation and ecosystem at regional and global scales in multiple ways (Qian et al., 2011; Skiles et al., 2012; Sand et al., 2013). Therefore, the BC content is considered one of the major absorbers to lead great decrease in length and area of TP glaciers (Xu et al., 2006, 2009a; Qian et al., 2015; Li et al., 2016).

15 In addition to BC, organic carbon (OC) and mineral dust (MD) recognized as the other types of ILAPs that –also–substantially contribute to springtime snowmelt and surface warming through the snow darkening effects (Yasunari et al., 2015; Painter et al., 2010, 2012; Huang et al., 2011; ;Painter et al., 2010; Kaspari et al., 2014; Wang et al., 2013, 2014; Yasunari et al., 2015; Wang et al., 2013; Huang et al., 2014). However, the optical properties of OC in snow are still absent due to limited small-scale field campaigns and technical limitations. For instance, the OC concentrations extracted at Antarctic sites are 20 unexpectedly higher ranging from 80 to 360 ng g⁻¹ than those reported for Greenland (10–40 ng g⁻¹) and Alpine (45–98 ng g⁻¹) for pre-industrial ice (Federer et al., 2008; Preunkert et al., 2011). Furthermore, there are still significant uncertainties in estimating the light absorption by different types of OC associated with both the chemical and optical analyses from snow samples across western North America (Dang et al., 2014). Although the 25 contribution of OC to the global warming is generally lower than BC, but still significant

30

mainly over southeastern Siberia, northeastern East Asia, and western Canada (Yasunari et al., 2015). As summarized by Flanner et al. (2009), consideration of OC in snow is a key approach for better estimating the climate effects in global models due to the absorption of solar radiation by other ILAPs from the ultraviolet to visible wavelengths.

5 It is well known that the light absorption capacity of MD mainly depends on the iron oxides (hereafter referred to Fe) (Alfaro et al., 2004; Lafon et al., 2004, 2006; Lafon et al., 2006; Moosmuller et al., 2012). Fe (primarily hematite and goethite) imparted a yellow-red color is a major component, which affects the ability of mineral dust to absorb sunlight at short wavelengths, then alters the dust's radiative properties and may influence the climate
10 (Takahashi et al., 2011; Jeong et al., 2012; Zhou et al., 2017). Cong et al. (2018) indicated that the goethite was predominant form of Fe (81% to 98 % in mass fraction) among the glaciers in the TP regions. Painter et al. (2007) pointed out that (Jeong et al., 2012) snow cover duration in a seasonally snow-covered mountain was shortened by 18 to 35 days due to the deposition of disturbed desert dust. Wang et al. (2013) revealed that the light
15 absorption was major dominated by OC across the grassland of Inner Mongolia across northern China, while the snow particulate light absorption was mainly contributed by local soil and desert dust at the northern boundary of the TP regions.

~~-The Tibetan Plateau (TP), known as the highest plateau in the world, and its surrounding areas contain the largest snow and ice mass outside the polar regions (Qin et al., 2006). Due to the importance of the climate effects by ILAPs, numerous snow surveys have been conducted to investigate the light absorption of ILAPs (Xu et al., 2009a, b; Doherty et al., 2010; Huang et a., 2011; Wang et al., 2013; Dang et al., 2014), and their potential source attribution in snow and ice (Hegg et al., 2010; Zhang et al., 2013a; Doherty et al., 2014 Jenkins et al., 2016; Li et al., 2016; Pu et al., 2017).~~

25 ~~Recently, Li et al. (2016) exhibited that similar contributions from fossil fuel (46±11%) and biomass (54±11%) combustion of the BC sources based on the dual-carbon isotopes technique from aerosol and snowpit samples in the TP regions. Bond et al. (2013) indicated that the best estimate of climate forcing from BC deposition on snow and sea ice in the~~
30 ~~industrial era is +0.13 W m⁻² with 90% uncertainty bounds of +0.04 to +0.33 W m⁻². In~~

addition to BC, organic carbon (OC) and mineral dust (MD) also substantially contribute to springtime snowmelt and surface warming through snow darkening effects (Painter et al., 2010; Huang et al., 2011; Painter et al., 2012; Wang et al., 2013; Kaspari et al., 2014; Wang et al., 2014; Yasunari et al., 2015). Water soluble organic carbon (WSOC) and insoluble organic carbon (ISOC) are the major components of organic carbon in the atmosphere, snow and sea ice. In addition to the strong light absorption of ISOC and WSOC may also influence the regional and global climate through the heating and evaporating of clouds and by acting as cloud condensation nuclei (CCN) (Chen and Bond, 2010; Alexander et al., 2012; Witkowska and Lewandowska, 2016). Moreover, WSOC also plays a key role in affecting human health due to its toxic effects (McConnell and Edwards, 2008; Wang et al., 2015). Although the mass mixing ratio of insoluble organic carbon in the snow and ice has been widely investigated in previous studies (Xu et al., 2006, 2009; Flanner et al., 2009; Wang et al., 2013), Due to the importance of the climate effects by insoluble light absorbing particles (ILAPs), numerous snow surveys have been conducted to investigate the light absorption of ILAPs and their potential source attribution in snow (Xu et al., 2009a, b; Doherty et al., 2010, 2014; Hegg et al., 2010; Wang et al., 2015; Jenkins et al., 2016; Niu et al., 2017; Wang et al., 2017). ~~there are still limited studies that measure the mass mixing ratios of both WSOC and ISOC in ice samples, especially across the TP regions (Li et al., 2016; Yan et al., 2016).~~ It is well known that the light absorption by MD is mostly related to iron oxides. For instance, the increased radiation forcing by MD in snow has affected the timing and magnitude of runoff from the Upper Colorado River Basin (Painter et al., 2007, 2010). ~~Due to the importance of the climate effects by insoluble light absorbing particles (ILAPs), numerous snow surveys have been conducted to investigate the light absorption of ILAPs and their potential source attribution in snow (Xu et al., 2009a, b; Doherty et al., 2010, 2014; Hegg et al., 2010; Wang et al., 2015; Jenkins et al., 2016; Niu et al., 2017; Wang et al., 2017).~~ For instance, Hegg et al. (2009) ~~found out~~ indicated that the light absorption ~~in Arctic snow~~ in Arctic snow by ILAPs is mainly originated from ~~two distinct biomass burning sources, a pollution source, and a marine source~~ based on ~~the a positive matrix factorization (EPA-PMF) receptor model.~~ Huang et al. (2011) conducted the first snow survey over northern China, and the sources

of ILAPs in seasonal snow in the region were explored based on a positive matrix factorization (PMF) with backward trajectory cluster analysis (Zhang et al., 2013a). Wang et al. (2013) indicated that soil dust was found to be the major contributor to snow particulate absorption in Inner Mongolia regions and Qilian mountains over northern China. Doherty et al. (2014) found that the source attribution of particulate light absorption in seasonal snow is dominated by biomass/biofuel burning, soil dust, and fossil fuel pollution based on the chemical and optical data. Recently, vertical profiles of ILAPs in seasonal snow were performed from 67 North American sites, and biomass/biofuel burning, soil and fossil fuel pollution are explored as the major sources of particulate light absorption based on the chemical and optical data (Doherty et al., 2014). However, the assessments of the light absorption and its emission sources of ILAPs on the TP glaciers are sparse due to limited observations.

Up to now, the light absorption and emission sources of ILAPs remain poorly understand. Increasing the in-situ measurements of ILAPs in snow and ice is the most urgent task to explore the glacier retreat, especially in the TP regions. Here, we present performed a snow large survey on collecting the column ice samples on seven high mountain glaciers on in the TP regions during the monsoon and non-monsoon seasons from 2013-2015. By using an integrating sphere/integrating sandwich spectrophotometer (ISSW) system associated with the chemical analysis, the particulate light absorption of by BC, ISOC, and MD in TP glaciers was evaluated. Finally, the relative attribution contributions of their emission sources of the ILAPs in these regions glaciers was explored based on a positive matrix factorization (PMF) receptor model.

2 Site description and methods

2.1 Site description and sample collection

According to the second Chinese glacier inventory dataset, Fig. 1 exhibits the topographical maps in each glacier associated with the sampling locations (Liu et al., 2014). Fig. S1 shows the pictures of the sampling locations in all seven glaciers, and all these glaciers are arranged from north to south according to their latitude and longitude in this study. Basically, the sampling locations are selected to be at least 50 km apart from the main road

and the cities to minimize the effects of local sources. ~67 column ice samples were gathered during monsoon and non-monsoon seasons along a south-north transect over the TP regions from 2013-2015. It is worth noting that the seven glaciers can represent different climate and land surface types gradually from the dry area to wet area along the northern to the southern over the TP regions. To investigate the enrichment of ILAPs via wet and dry deposition on glaciers, we collected 67 ice samples in seven glaciers on the Tibetan Plateau from May 2013 to October 2015 (Fig. 2).

As shown in Fig. 1, the spatial distribution of aerosol optical depth (AOD) retrieved from Moderate-resolution Imaging Spectrometer (MODIS) sensors are ranging from 0.1 to 0.4 from south to north near the high mountain glacier regions over TP regions from 2013-2015. Therefore, the ice samples numbered in chronological order from 1 to 19 was in the Qiyi glacier, while sites 20-22, 23-32, 33-44, 45-49, 50-60, and 61-67 in the Qiumianleiketage, Meikuang, Yuzhufeng, Hariqin, Xiaodongkemadi, and Gurenhekou glaciers, respectively. Samples 1 to 19 were collected from 2013 to 2015 during the monsoon season in the center of the Qiyi glacier (QY, 39°14' N, 97°45' E) (Fig. 1a). The Qiyi glacier (39°14' N, 97°45' E) is a small valley glacier, with the area of 2.98 km² and the length of 3.8 km. It is located in the eastern part of Qilian Mountains on the north border of the TP regions. This with an elevation of 6178 m. It is classified bucket-valley glaciers according to its shape, and is classified subcontinental glacier according to the physical characteristics of glacier. glacier is recognized as a typical "wet island" in arid region due to its multi-land types (e.g. forests, bushes, steppes and meadows).

Samples 20 to 22 were collected during the non-monsoon season in the southeast Qiumianleiketage glacier (QM, 36°70' N, 90°73' E), which is originated from the Kunlun Mountains of the Qinghai-Tibet Plateau (Fig. 1b). The length of the QM glacier is 2.6 km, and the area is 1.73 km².

Samples 23-32 were collected in the northern Meikuang glacier during both monsoon and non-monsoon season (MK, 35°42' N, 94°12' E). The MK glacier is located in the eastern Kunlun Mountains, where is characterized by alluvial deposits and sand dunes. The MK glacier is 1.8 km in length with an area of 1.1 km² (Fig. 1c).

As shown in Fig. 1d, samples 33-44 were collected in the southwest Yuzhufeng glacier (YZF, 35°38' N, 94°13' E). The YZF glacier is adjacent to MK glacier with the highest peak of 6178 m across the eastern Kunlun Mountains at the northern margin of the TP regions. The glacier is surrounded by a small quantity of ferns, forests and some bushes due to the high altitude as well as the cold and arid climate.

Samples 45-49 were collected in the center of Hariqin glacier (HRQ, 33°14' N, 92°09' E), which is located at the headwaters of the Dongkemadi river on the northern slope of the Tanggula Mountains in the central region of the Qinghai-Tibetan Plateau (Fig. 1e). The HRQ glacier face north, with a mountain peak of 5820 m a.s.l. to its terminus of 5400 m a.s.l.

Samples 50-60 were collected in The the southern Xiaodongkemadi glacier (XD, 33°04' N, 92°04' E). The XD glacier is located adjacent to HRQ glacier, with an area of 1.767 km² and 2.8 km in length (Fig. 1f) in the central Qinghai-Tibetan Plateau. It is 2.8 km in length and the average snowline is 5560 m a.s.l. The elevations of the glacier from the peak to its terminus are 5900 and 5500 m a.s.l., respectively. The annual mean air temperature at the equilibrium line altitude is in the range -5~7°C. It has a cold steppe landscape. The surrounding region is mainly surrounded by tundra.

Samples 61-67 were collected in The Yuzhufeng glacier (35°38' N, 94°13' E) is the highest peak across the eastern Kunlun Mountains, with an elevation of 6178 m. The Meikuang and Qiumianleiketage glaciers are also located over the Kunlun Mountains, and these glaciers have an average altitude of 5100 m and 5500 m a.s.l., respectively. The Meikuang glacier is located in the eastern Kunlun Mountains, where is characterized by alluvial deposits and sand dunes, the glacier covers an area of 1.1 km², is 1.8 km in length (Xiao et al., 2002). The Qiumianleiketage glacier is located in the Heyuan District of the Nagora River, the largest river in the Qaidam Basin, which originated in the Kunlun Mountains of the Qinghai-Tibet Plateau. The length of the glacier is 2.6 km, the area is 1.73 km². The glaciers of Hariqin and Meikuang have similar altitudes but are from different mountains. The eastern Gurenhekou glacier (GR, 30°19' N, 90°46' E). The GR glacier is relatively small and cold alpine-type valley glacier located in the central part of the southern TP on the south-eastern margin of the Nyenchen Tanglha Mountains, and which is seated about

90 km northwest of Lhasa, the capital city of Tibet (Fig. 1g) (Liang et al., 1995). The glacier area is 1.4 km², with a length and width of 2.5 km and 0.6 km, and the elevation is in the range of 5600 and 6000 m a.s.l. Kang et al. (2009) and Bolch et al. (2010) indicated that the Gurenhekou glacier is mainly influenced by both the continental climate of central Asia and the Indian monsoon system.

~~To investigate the enrichment of ILAPs via wet and dry deposition on glaciers, we collected 67 ice samples in seven glaciers on the Tibetan Plateau from May 2013 to October 2015 (Fig. 2). The collected ice samples were preserved in 0.5-m pure clean plastic bag with a diameter of 20 cm, and kept frozen at the State Key Laboratory of Cryospheric Sciences, Cold and Arid Regions Environmental and Engineering Research Institute in Lanzhou. Wang et al. (2015) pointed out that the annual accumulation of snow/ice at the drilling site over the TP glaciers was around 2 m on average. Therefore, a 1.2-m pure clean plastic bag with a diameter of 20 cm was put into a vertical tube to collect the ice samples via wet and dry deposition during monsoon and non-monsoon seasons in each sample location from 2013 to 2015 (Fig. 2). Due to the high altitudes of these glaciers, the wet deposition in these areas were predominant by new fallen snow, while much less formed by precipitation. However, most of the samples were gathered by column ice due to the multi-melting processes. Then, the column ice samples were kept frozen under -20 °C and transported to laboratory facilities at the State Key Laboratory of Cryospheric Sciences, Cold and Arid Regions Environmental and Engineering Research Institute in Lanzhou. Then Firstly, each ice sample was cut vertically into small four pieces from the surface top to the bottom as shown in Fig. S2, and only one of the vertical samples was cut at 10 cm resolution following clean protocols, resulting in a total of 189 samples used in this study. It should be noted that if there is a significant dirty layer inside, then, this layer will be cut and analyzed separately. Another key issue is that some of the ice samples in the top layer is not uniform due to the multi-melting processes. Therefore, several samples were cut longer or shorter than the other samples (e.g. sites 13 and 26). To minimize the losses of ILAPs to the container walls, Therefore, 189 pieces of the ice samples were analyzed in this study. In order to analyze light absorption by ILAPs in the ice samples clearly, we arranged seven glaciers from north to south according to their latitude and longitude, and~~

~~samples in each glacier were sorted by sampling time. Therefore, the ice samples numbered in chronological order from 1 to 19 was in the Qiyi glacier, while sites 20-22, 23-32, 33-44, 45-49, 50-60, and 61-67 in the Qiumianleiketage, Meikuang, Yuzhufeng, Hariqin, Xiaodongkemadi, and Gurenhekou glaciers, respectively.~~

~~each~~The ice samples were filtered at laboratories in Lanzhou University. The samples ~~wasere~~ put into a clean glass beaker and ~~quickly~~ melted ~~quickly~~ in a microwave oven, and ~~The melted water then then~~ immediately filtered through a ~~0.2- μm~~ Nuclepore filters ~~with~~ a pore size of ~~0.2- μm~~ , as were used by Doherty et al. (2010). ~~Additional~~ Further details on ~~for filtrate processing~~the ice filtration processes have ~~can be found~~ been previously reported (in Wang et al. (2013)Doherty et al., 2010, 2014 and Doherty et al. (2014); Wang et al., 2013).

2.2 Optical analysis

An updated integrating sphere/integrating sandwich spectrophotometer (ISSW) ~~is~~ ~~was~~ used to calculate the mass mixing ratio of BC in ~~the ice samples~~ ~~snow~~, which is similar with the instrument developed by Grenfell et al. (2011). Compared with the ISSW spectrophotometer developed by Grenfell et al. (2011), the major difference is that we used two integrating spheres ~~to calculate the relative attenuation~~ instead of the integrating sandwich diffuser to reduce the diffuse radiation during the measuring process. This ISSW spectrophotometer measures the light attenuation spectrum from 400 to 700 nm. The total light attenuation spectrum is extended over the full spectral range by linear extrapolation from 400 to 300 and from 700 to 750 nm (~~Grenfell et al., 2011~~). Light attenuation is nominally only sensitive to ILAPs on the filter because of the diffuse radiation field and the sandwich structure of two integrated spheres in the ISSW (Doherty et al., 2014). Briefly, the transmitted light detected by the system for an ice sample, $S(\lambda)$, ~~are~~ ~~is~~ compared with the signal detected for a blank filter, $S_0(\lambda)$, and the relative attenuation (A_{tn}) is expressed as:

$$A_{tn} = \ln[S_0(\lambda)/S(\lambda)] \quad (1)$$

~~The MACs and the absorption Ångström exponents (Å) for BC, OC, and Fe used in this study could be found in Wang et al. (2013). By using this technique, we can estimate the~~

following parameters included equivalent BC (C_{BC}^{equiv}), maximum BC (C_{BC}^{max}), estimated BC (C_{BC}^{est}), fraction of light absorption by non-BC ILAPs (f_{non-BC}^{est}), the absorption Ångström exponent of non-BC ILAPs (A_{non-BC}) and the total absorption Ångström exponent (A_{tot}). These parameters are defined as follows:

5 The following measured parameters included equivalent BC (C_{BC}^{equiv}), maximum BC (C_{BC}^{max}), estimated BC (C_{BC}^{est}), fraction of light absorption by non-BC ILAPs (f_{non-BC}^{est}), the non-BC absorption Ångström exponent (A_{non-BC}) and the absorption Ångström exponent of all ILAPs (A_{tot}), were calculated by using the wavelength dependence of the measured spectral light absorption and by assuming that the MACs of the BC, OC, and Fe are 6.3, 0.3, and
 10 $0.9 \text{ m}^2 \text{ g}^{-1}$, respectively, at 550 nm and that the absorption Ångström exponents (A or AAE) for BC, OC, and Fe are 1.1, 6, and 3, respectively (Doherty et al., 2010, 2014; Grenfell et al., 2011; Wang et al., 2013). These parameters are defined as follows:

1. C_{BC}^{max} (ng g^{-1}): maximum BC is the maximum possible BC mixing ratio in snow by assuming that all light absorption is due to BC at the wavelengths of 650-700 nm.

15 2. C_{BC}^{est} (ng g^{-1}): estimated BC is the estimated snow-true mass of BC mixing ratio in snow derived by separating the spectrally resolved total light absorption and non-BC fractions.

3. C_{BC}^{equiv} (ng g^{-1}): equivalent BC is the amount of BC that would be needed to produce absorption of solar energy by all insoluble particles in snow for the wavelength-integrated
 20 from 300-750 nm.

4. A_{tot} : absorption Ångström exponent is calculated for all insoluble particles deposited on the filter between 450 and 600 nm.

5. A_{non-BC} : non-BC absorption Ångström exponent is defined-derived from the light absorption by non-BC components of the insoluble particles in snow between 450-600 nm.

25 6. f_{non-BC}^{est} (%): fraction of light absorption by non-BC light absorbing particles is the integrated absorption due to non-BC light absorbing particles, which is weighted by the down-welling solar flux from snow at the wavelengths of 300-750 nm.

It is well known that the aerosol composition and the size distribution are key parameters that affect the absorption Ångström exponent. Doherty et al. (2010) reported that the value
 30 of the absorption Ångström exponent of OC was close to 5, which is consistent with

previous studies with values ranging from 4-6 (Kirchstetter et al., 2004). Several studies indicated that the absorption Ångström exponent of mineral dust ranged from 2 to 5 (Fialho et al., 2005; Lafon et al., 2006; [Zhou et al., 2017](#); [Cong et al., 2018](#)). The variation ~~in~~ of the absorption Ångström exponents for urban and industrial fossil fuel emissions is typically in the range of 1.0-1.5 (Millikan, 1961; Bergstrom et al., 2007), which is slightly lower than that of biomass burning aerosols, which primarily falls in the range of 1.5-2.5 (Kirchstetter et al., 2004; Bergstrom et al., 2007). ~~Although the source attribution of the insoluble light absorbing particles in the samples is not a dominant determinant of the value of the absorption Ångström exponent, fossil fuel burning may have a lower absorption Ångström exponent (<2) than 2-5 (Millikan, 1961; Fialho et al., 2005).~~ In this study, we noted that the absorption Ångström exponent (\hat{A}_{tot}) is due to ~~a~~ the mix state of BC and non-BC impurities on ~~our~~ the filters, and the calculations of \hat{A}_{tot} and \hat{A}_{non-BC} could be found in the study of Doherty et al. (2014). ~~The OC mixing ratio was also determined according to Eq. (2) in Wang et al. (2013), and the Fe concentration was determined according to the inductively coupled plasma-mass spectrometry (ICP-MS) measurements. The \hat{A}_{non-BC} is calculated as a linear combination of contributions to light absorption due to OC and Fe, and the equation is listed as follows:~~

$$\hat{A}_{non-BC} = F_{OC} \times \hat{A}_{OC} + F_{Fe} \times \hat{A}_{Fe} \quad (2)$$

2.3 Chemical analysis

~~Previous studies on these parameters have concluded that ILAPs are primarily derived from BC, OC, and Fe (Qian et al., 2015; Wang et al., 2015; Yasunari et al., 2015; Pu et al., 2017). Meanwhile, to quantify WSOC, about 10 ml of the filter liquor was injected into a total carbon analyzer (TOC-V, Shimadzu). The method detection limit (MDL) used was $4 \mu\text{g l}^{-1}$ with a precision of $\pm 5\%$ (Cong et al., 2015). The definition of TOC (Total Organic Carbon) in this study is calculated as the total WSOC measured by carbon analyzer and the ISOC calculated by ISSW instrument.~~

The major metallic elements (Al, Cr, Mn, Fe, Ni, Cu, Zn, Cd, Pb) were analyzed by an inductively coupled plasma-mass spectrometry (ICP-MS, X-7 Thermo Elemental) at the

Institute of Tibetan Plateau Research in Beijing. The detection limits are Al, 0.238 ng ml⁻¹; Cr, 0.075 ng ml⁻¹; Mn, 0.006 ng ml⁻¹; Fe, 4.146 ng ml⁻¹; Ni, 0.049 ng ml⁻¹; Cu, 0.054 ng ml⁻¹; Zn, 0.049 ng ml⁻¹; Cd, 0.002 ng ml⁻¹; Pb, 0.002 ng ml⁻¹. ~~Briefly, we acidified all melted samples directly to pH<2 with ultra-pure HNO₃, then let settled for 48h. Generally speaking, we acidified all ice samples to pH<2 with ultra-pure HNO₃, then let settle for 48h. The instrument adopted national standard materials and standard materials of the United States as the quality monitoring samples.~~ The relative deviation between most of the measured values ~~of and the elements and~~ the standard reference values is within 10%. Details on these procedures are given in Li et al. (2009) and Cong et al. (2010).

Meanwhile, for the filtrated ~~ice-water~~ samples, we measured the major anions (Cl⁻, NO₂⁻, NO₃⁻, SO₄²⁻) and cations (Na⁺, NH₄⁺, K⁺, Mg²⁺, Ca²⁺) with an ion chromatograph (Dionex 320; Dionex, Sunnyvale, CA) using a CS12 column for cations and an AS11 column for anions at the Institute of Tibetan Plateau Research in Beijing. All the detection limit of the ions was 1 ~~μg · l⁻¹~~ ~~μg l⁻¹~~. In addition, except for the anions and cations and trace elements, ~~Cl salt, M-Cl_{salt}, MDD~~ and biosmoke K (K_{Biosmoke}) were determined to assess the mass contributions of the major components in the ice samples. ~~Cl salt, Cl_{salt}~~ was estimated as follows in accordance with Pio et al. (2007), by adding to sodium, chloride, and sea-salt contributions of sodium, magnesium, calcium, potassium, and sulfate, as follows:

$$\begin{aligned}
 CL_{\text{salt}} &= Na_{\text{Ss}}^+ + Cl^- + Mg_{\text{Ss}}^{2+} + Ca_{\text{Ss}}^{2+} + K_{\text{Ss}}^+ + SO_{4\text{Ss}}^{2-} \\
 &= Na_{\text{Ss}}^+ + Cl^- + 0.12Na_{\text{Ss}}^+ + 0.038Na_{\text{Ss}}^+ + 0.038Na_{\text{Ss}}^+ + 0.25Na_{\text{Ss}}^+ \quad (23)
 \end{aligned}$$

$$Na_{\text{Ss}} = Na_{\text{Total}} - Al \cdot (Na/Al)_{\text{Crust}} \quad (34)$$

Where (Na/Al)_{Crust} = 0.33, and represents the Na/Al ratio in the dust materials (Wedepohl, 1995). ~~With 0.12, 0.038, 0.038, and 0.25 being the mass ratios in seawater of magnesium to sodium, calcium to sodium, as well as potassium to sodium and sulfate to sodium, respectively.~~

The MD content was calculated by a straightforward method, and the Al concentration in dust was estimated as ~~st~~ 7% (Zhang et al., 2013b):

$$MD = Al / 0.07 \quad (45)$$

We determined K_{Biosmoke} as follows (Pu et al., 2017):

$$K_{\text{Biosmoke}} = K_{\text{Total}} - K_{\text{Dust}} - K_{\text{Ss}} \quad (56)$$

$$K_{\text{Dust}} = \text{Al} \cdot (K/\text{Al})_{\text{Crust}} \quad (67)$$

$$K_{\text{Ss}} = \text{Na}_{\text{Ss}} \cdot 0.038 \quad (78)$$

Where $(K/\text{Al})_{\text{Crust}}$ is 0.37 ~~and~~ which represents the K/Al ratio in the dust materials
5 (Wedepohl, 1995) and Na_{Ss} is estimated by Eq. (34).

2.4 Enrichment factor (EF)

To evaluate the relative contributions of trace elements from natural (e.g., mineral and soil dust) versus anthropogenic sources (e.g., fossil fuels and vehicle exhaust), an inter-annual
10 comparison of ~~EF~~ EF values, which represent the enrichment of a given element relative to its concentration in the crust of the earth. The primary uncertainty in these calculations is attributed to the differences between chemical compositions in the snow and the reference crustal composition. The EF is defined as the concentration ratio of a given metal to that of Al, which is a reliable measure of crustal dust, normalized to the same
15 concentration ratio characteristic of the upper continental crust (Wedepohl, 1995), calculated with the following equation:

$$\text{EF} = \frac{(X/\text{Al})_{\text{snow}}}{(X/\text{Al})_{\text{crust}}} \quad (89)$$

2.5 Source apportionment

20 The Positive Matrix Factorization (PMF 5.0) is considered as a generally accepted receptor model to determine source apportionment of the ILAPs when source emission profiles are unknown (Paatero and Tapper, 1994). Details of the PMF procedure used in this study are ~~also~~ similar to the previous work as discussed in Hegg et al. (2009, 2010). Generally, the mass concentration ~~of and the uncertainties of~~ the chemical species ~~and the uncertainty~~
25 were used as the input. The final data set used for the PMF analysis contained 189 samples with 18 elements whereby only elements that have high recovery were used. The uncertainty value of each variable in each sample was estimated from an empirical equation. The PMF model was run for 3 to 6 factors with 6 random seeds, but only a three-factor solution ~~of the ILAPs in TP glaciers~~ could provide the most meaningful results of the

ILAPS in TP glaciers. The Q values (modified values) for the 3-factor solution (both robust and true) were closest to the theoretical Q value of any of the factor numbers for which the model was run, suggesting that the 3-factor solution was optimal.

5 **3. Results and Discussion**

3.1 **Aerosol optical depth (AOD)**

As shown in Fig. 43, the QY, QM, MK, YZF glaciers are located in the northern part of Tibetan Plateau, while XD, HRQ, GR glaciers are located in the southern part of Tibetan Plateau. It worth noting that the aerosol optical depth (AOD) can represent the dry aerosol deposition and its transport pathway, which could provide useful information about the possible sources of the ILAPs in the TP glaciers. Therefore, the spatial distribution of the averaged AOD at 500 nm derived from Aqua-MODIS were retrieved over the TP regions and its adjacent areas from 2013 to 2015. Following the work of Ramanathan et al. (2007), the anthropogenic AOD, which is also called as atmospheric brown clouds (ABC), was larger than 0.3 on the southern side of the Himalayas. Therefore, AOD (500 nm) values >0.3 and <0.1 are considered to present the anthropogenic haze and background conditions, respectively. We found that the AOD was much larger across the western TP than that in the central part of TP regions. As a result, the AOD values in the QY, QM, MK, and YZF glaciers were in the range of 0.25 to 0.3 could be highly influenced by human activities. The high values of AOD might thus contribute to the retreat of Himalayan glaciers (Engling and Gelencser, 2010). In contrast, the lower values of AOD (<0.125) were observed near the HRQ, XD, and GR glaciers. However, the AOD over the TP regions was much lower than that over Southern Asia, especially over the Indo-Gangetic Plain during the cold season. This is close to previous measurements over the TP regions (Cong et al., 2009; Ming et al., 2010; Yang et al., 2012; Lüthi et al., 2015(Cong et al., 2009; Yang et al., 2012)).

3.2 **Regional averages of the optical parameters**

Based on our sampling locations shown in Fig. 1, the Qiyi, Qiumianleiketage, Meikuang, Yuzhufeng glaciers were located in the northern part of Tibetan Plateau, while

Xiaodongkemadi, Hariqin, Gurenhekou glaciers were located in the southern part of Tibetan Plateau.

67 ice samples were collected at 7 sites from 2013 to 2015 across the Tibetan plateau field campaign. As shown in Fig. 1, the spatial distribution of aerosol optical depth (AOD) retrieved from Moderate-resolution Imaging Spectrometer (MODIS) sensors are ranging from 0.1 to 0.4 from south to north near the high mountain glacier regions over TP regions from 2013-2015.

The general information of C_{BC}^{est} , C_{BC}^{max} , C_{BC}^{equiv} , f_{non-BC}^{est} , \hat{A}_{tot} , and \hat{A}_{non-BC} of the ice samples are given in Table 1 for each glacier. The lower median values of C_{BC}^{est} could be 23 ng g⁻¹, 26 ng g⁻¹ found during the monsoon season in the Xiaodongkemadi, HariqinHRQ, and Gurenhekou-GR glaciers on the south of the TP regions, while the other glaciers show the a relative higher values of 187 ng g⁻¹ and 165 ng g⁻¹ range (94-172 ng g⁻¹) found in the MK and YZF glaciers on the north-central part edge of the TP regions. Compared with the monsoon season, the concentration of C_{BC}^{est} increased very significantly in all seven glaciers than those values during the non-monsoon season. Details of the vertical profiles of all ice samples collected in each site could also be found in Table S1. Based on the parameters listed in Table 1, we can analyze the major characteristics of the BC and non-BC components in the samples during these field campaigns from 2013-2015 in the TP glaciers. We found that the lowest concentration of BC in the ice samples is found in the Xiaodongkemadi-XD glacier, with a value of $C_{BC}^{est} \sim 10 \text{ ng g}^{-1}$. In contrast, the highest values of C_{BC}^{est} , C_{BC}^{max} , and C_{BC}^{equiv} are were 3100 ng g⁻¹, 3600 ng g⁻¹, and 4700 ng g⁻¹, respectively, taken in the Gurenhekou-GR region glacier. Generally, the median of the absorption Ångström exponent for total particulate constituents (\hat{A}_{tot}) exceeded 1.0 at all locations (Fig. 34, and Table 1). \hat{A}_{tot} and \hat{A}_{non-BC} for all ice samples were in the range of 1.4-3.7 and 1.9-5.8, respectively (Table S1). As shown in Fig. 3a4a, the lowest median values of \hat{A}_{tot} were 2.62, 2.64, 2.18, and 2.46 in the QY, MK, XD, and GR glaciers, associated with the estimated contributions to absorption by non-BC ILAPs in these regions were ~41%, 44%, 36%, and 48%, respectively. Compared with these glaciers, the higher values of median \hat{A}_{tot} were found in the QM (2.76), YZF (2.95), and HRQ (2.87) glaciers. Correspondingly, the estimated f_{non-BC}^{est} values in those regions is ~44%, 48%, and 48%.

respectively. (~2.1) is found in the Xiaodongkemadi glacier, while the other glaciers exhibit much higher values (2.5-2.9). The results indicated that the emission of the ILAPs in the Xiaodongkemadi glacier likely originated from the combustion sources, which is also consistent with the previous studies (Bond et al., 1999, 2001; Schnaiter et al., 2003, 2005; Bergstrom et al., 2007; Clarke et al., 2007). Except the HRQ Hariqin glacier, the other glaciers showed an increased trend of the absorption Ångström exponent for non-BC particulate constituents (A_{non-BC}) from the south to north regions in the TP regions (Fig. 3b4b). A_{tot} and A_{non-BC} for all ice samples were in the range of 1.4-3.7 and 1.9-5.8, respectively (Table S1). Histograms of the A_{tot} absorption Ångström exponent by regions are shown in Fig. 54. We found that there was a large variation of A_{tot} in the XD glacier, not only in the higher values (~2-4), but also for the lower values (<2). The broadness of the A_{tot} distribution is indicative of the complicated sources of particulate light absorption. For instance, Wang et al. (2013) indicated that the higher values of A_{tot} (~3.5-4.5) was highly correlated with the local soil source, while fossil fuel burning may have an absorption Ångström exponent lower than 2 (Millikan, 1961; Fialho et al., 2005). Therefore, In the Yuzhufeng and Xiaodongkemadi glaciers, there is a large variation of the absorption Ångström exponent (~1-4), reflecting a significant fraction of the total absorption was not only attributed to BC (49%, shown in Fig. 7), that the ILAPs are not only dominated by BC in these regions but also influenced/contributed by non-BC absorbers (accounting for 51%) such as due to OC and mineral dust MD in the XD glacier. In contrast, a common feature in the other regions is was that they the major dominated values show a less variable of A_{tot} the absorption Ångström exponent, ranging from from 2.5 to 3. The A_{non-BC} and A_{tot} in each site are also given as red dots and blue triangles, respectively, in Fig. S3.

BC and other ILAPs are integrated into the snowpack and ice surface by dry and wet deposition, such as gravity, turbulence, and precipitation. For instance, Flanner et al. (2012) indicated that BC nucleates ice very poorly via direct deposition of vapor, so most relevant mechanisms involve liquid water. Therefore, the investigation of the mixing ratios of ILAPs in each glacier Figure 6 shows the regional variations of BC, OC, and Fe concentration in each glacier during monsoon and non-monsoon season could be useful to

analyze the emission sources of the air pollutants. As shown in Fig. 5, Although a notable feather is that there were large significant biases differences between the median and the average values of the concentration of ILAPs concentration in the ice samples in each glacier, we found that all kinds of ILAPs exhibited a similar variation from the northern QY glacier to southern GR glacier. In addition, we collected the ice samples during both monsoon and non-monsoon seasons in five glaciers, only except the QY and QM glaciers. On average, the BC and OC concentrations in the HRQ, XD, and GR glacier during non-monsoon season were several orders of magnitude higher than those in monsoon seasons. The result was highly consistent with the previous study by Cong et al. (2015), who found that although the transport pathways of air masses arriving the middle Himalayas during monsoon and non-monsoon were similar, a distinctly higher carbonaceous aerosol level was found only in the non-monsoon season. Lüthi et al. (2015) also exhibited that the atmospheric brown cloud over South Asia can climb across the Himalayan and transport of polluted air mass, which may have serious implications of the cryosphere in the TP regions. However, there appeared to be no apparent difference in the mixing ratios of ILAPs between monsoon and non-monsoon seasons in two adjacent (MK and YZF) glaciers. This can be mainly explained that. We noted that several reasons could lead this discrepency. First of all, all of the ice samples were collected in an individual time. Another major issue is that except the long-range transport of ILAPs, local air pollutants can also affect the ILAPs in the glacier via wet and dry deposition in the central TP regions. For instance, LiHuang et al. (2018) indicated investigated that the Fossil fuel contributions of BC is much higher in the Laohugou No. 12 glacier (close to Qiyi glacier) due to human activities the air masses across the MK and YZF glaciers were originated from the arid western TP and Taklimakan desert regions, and the concentration of trace elements in the YZF glacier was closer to the dust sources indicating that YZF glacier was less influenced by human activities. Based on our sampling locations shown in Fig. 1, the Qiyi, Qiumianleiketage, Meikuang, Yuzhufeng glaciers were located in the northern part of Tibetan Plateau, while Xiaodongkemadi, Hariqin, Gurenhekou glaciers were located in the southern part of Tibetan Plateau. As shown in Fig. 5, the median values of the C_{BC}^{est} and C_{ISOC} (referred as the mass concentration of OC) obviously showed a significant slightly

decreasing trend from the northern TP to the southern TP. The mass concentration of BC in northern TP glaciers was higher than that in southern TP glaciers, which shows a good agreement with Ming et al. (2013). Comparing with Hariqin, Xiaodongkemadi and Gurenhekou glaciers, the relative higher values of the C_{BC}^{ext} and C_{ISOC} in the Qiyi, Qiumianleiketage, Yuzhufeng, and Meikuang glaciers are possibly influenced by human activities. Doherty et al. (2010, 2014) and Wang et al. (2013) indicated that the light absorption of Fe across the Northern Hemisphere is mainly originated from the local mineral dust. Therefore, the concentrations of Fe in ice samples in each glacier are exhibited in Fig. 5c.

The Yuzhufeng glacier is located in the northern part of the Loess Plateau, close to the Meikuang glacier. Twelve ice samples were collected in the Yuzhufeng glacier. The depth of these ice samples collected in the Yuzhufeng glacier are ranging from 15 to 45 cm as Table S1 shown. As shown in Fig. S2, most values of C_{BC}^{ext} in this region range from 100–1000 ng g⁻¹, with a few values lower than 100 ng g⁻¹. One notable feature is that the highest concentrations of C_{BC}^{ext} and ISOC for the surface layer are 1600 ng g⁻¹ and 9160 ng g⁻¹ at site 41. Due to the non-BC fraction of the light absorption (f_{non-BC}^{ext}) is 0.56, we pointed out that the light absorption in the surface glacier at site 41 wasn't only influenced by BC, but also possibly related to the ISOC, and MD. The large variation of the absorption Ångström exponent distribution is an indication of the complicated emission sources of ILAPs in the ice samples. In the Yuzhufeng glacier, A_{non-BC} generally varied between 2 and 3.7, and the average value of f_{non-BC}^{ext} is close to 50%, so these results also reveal that the ILAPs in ice samples are heavily influenced by anthropogenic air pollutants. Large variations of ISOC (measured by ISSW) and WSOC are also observed, with values ranging from 10–17000 ng g⁻¹ and 410–43000 ng g⁻¹, respectively. Except for site 23, the values of C_{BC}^{ext} in the Meikuang glacier are much lower than those in the Yuzhufeng glacier, with values ranging from 20–670 ng g⁻¹ and with a median value of 130 ng g⁻¹. The median value of the mass concentration of ISOC is 600 ng g⁻¹ in the Meikuang glacier. The fraction of total particulate light absorption due to non-BC constituents is typically 16–62%, and A_{non-BC} (5.12) in this region is highly similar to that found in the Yuzhufeng glacier (5.06). In addition, there appears to be no significant difference in the mixing ratios of ILAPs in the

ice samples via dry and wet deposition in these glaciers between the monsoon and non-monsoon seasons (Fig. S2, S3, S4, S5, S6). We noted that several reasons could lead this discrepancy. First of all, all of the ice samples were collected in an individual time. Another major issue is that except the long-range transport of ILAPs, local air pollutants can also affect the ILAPs in the glacier via wet and dry deposition. For instance, Li et al. (2016) indicated that the Fossil fuel contributions of BC is much higher in the Laohugou No. 12 glacier (close to Qiyi glacier) due to human activities. Finally, based the study by Xu et al. (2009), the ILAPs in the TP glacier also can be affected by the European air to reach that location on the eastern plateau, and thus lead the greater proportion of the heavy loading of the BC in the glacier. For instance, the mass concentration of BC in the Muztagh Ata and Xiaodongkemadi glaciers in northern part of Tibetan Plateau is much higher than that in the East Rongbuk, Noijin Kangsang and Zuoqiupo glacier, which are located in the southern part of Tibetan Plateau.

To quantify the regional status of ILAPs in each glacier, the statistics of the ILAPs in snow and ice in the studied TP glaciers and other related glaciers by previous studies are shown in Table 2. The Yuzhufeng glacier is located in the northern part of the Loess Plateau, close to the Meikuang glacier. During this field campaign, twelve ice samples were collected in the Yuzhufeng YZF glacier. The depths of these ice samples collected in the Yuzhufeng YZF glacier were ranging from 15 to 45 cm as (Table S1) shown. As shown in Fig. S24, most values of C_{BC}^{est} in this region ranged from ~ 100 - 1000 ng g^{-1} , with a few values lower than 100 ng g^{-1} . One notable feature is that the highest concentrations of C_{BC}^{max} and $IS_{OC}OC$ for the surface layer were 1600 ng g^{-1} and 9160 ng g^{-1} at site 41. Due to the non-BC fraction of the light absorption (f_{non-BC}^{est}) is 0.56. We pointed out that the light absorption in the surface glacier at site 41 was not only influenced by BC, but also possibly related to the IS_{OC} and MD due to the high value of f_{non-BC}^{est} (0.56). The large variation of the absorption Ångström exponent distribution is an indication of the complicated emission sources of ILAPs in the ice samples. In the Yuzhufeng YZF glacier, \hat{A}_{tot} generally varied between ~ 2 and 3.7, and the average value of f_{non-BC}^{est} is close to 50%, so these results also revealed that the ILAPs in ice samples are heavily influenced by anthropogenic air pollutants. Large variations of $IS_{OC}OC$ (measured by ISSW) and

WSOC ~~are were~~ also observed, with values ranging from ~ 10 to 17000 ng g^{-1} and ~ 410 to 43000 ng g^{-1} , respectively. Except for site 23, the values of C_{BC}^{est} in the Meikuang MK glacier ~~are were~~ much lower than those in the Yuzhufeng YZF glacier, ~~with which were in the values ranging of from~~ ~ 20 to 670 ng g^{-1} and, with a median value of 130 ng g^{-1} (Fig. S5). The median C_{OC} value of the mass concentration of ISOC ~~was is~~ $\sim 600 \text{ ng g}^{-1}$ in the Meikuang MK glacier. The fraction of total particulate light absorption due to non-BC constituents ~~is was~~ typically ~ 16 to 62% , and A_{non-BC} (5.12) in this region ~~is was~~ highly similar to that found in the Yuzhufeng YZF glacier (5.06).

In the Qiyi QY glacier (Fig. S4S6), the C_{BC}^{est} ~~are were~~ much similar ~~with than~~ those in the Meikuang MK glacier, with values ranging from ~ 20 to 720 ng g^{-1} , which ~~does did~~ not include the highest value of 1900 ng g^{-1} at site 13. The fraction of total particulate light absorption due to non-BC constituent f_{non-BC}^{est} ~~is was~~ typically ~ 20 to 70% , with a median value of 41% . This information along with the lower A_{tot} (2.6) indicateds that BC playeds the dominant role in influencing the light absorption in this region. ~~Compared with the other TP glaciers, we noted that the vertical profiles of ILAPs in the QY glacier were collected in the monsoon season from 2014 to 2015 (Table S1). The mixing ratios of OC and Fe ranged from 80-10100 ng g^{-1} and 20-340 ng g^{-1} , respectively. Fig. S7 shows that the vertical profiles of the mass mixing ratios of BC, OC, and Fe for the ice samples in the XD glacier were more variable than those for the other regions. With the exception of the surface layer at sites 53 and 54, most values of C_{BC}^{est} ranged from 10 to 280 ng g^{-1} in the XD glacier; therefore, this glacier was the cleanest region among all the studied glaciers. At sites 56-58, f_{non-BC}^{est} was lower than 38% , and A_{tot} ranged from 1-2.5. These results are were consistent with the fossil fuel combustion source due to industrial activities.~~

3.3 Scavenging and washing efficiencies

Previous studies have ~~also~~ illustrated that the ILAPs could become trapped and integrated at the surface of the snowpack due to melting and sublimation to enrich the surface concentrations (Conway et al., 1996; Painter et al., 2012; Doherty et al., 2013). ~~For instance, Doherty et al. (2013) found that the ILAPs could be scavenged with the snow meltwater to lead to a much higher concentration of BC in the surface snow. Flanner et al. (2007, 2009) indicated that the melt amplification due to concentrated BC in melted snow would amplify~~

snow-albedo reduction, and therefore provide a positive feedback to radiative forcing. However, it still remains unclear what happens to the vertical ILAPs in the deeper layer of snow and ice during the multi-melting processes due to limited in-situ observations.

In this study, Compared with the other TP glaciers, we noted that the vertical profiles of ILAPs in the Qiyi glacier were collected in the monsoon season from 2014 to 2015 (Table S1). In the monsoon season, the mixing ratios of ISOC and Fe ranged from 80-10100 ng g⁻¹ and 20-340 ng g⁻¹, respectively, and t

the mixing ratios of ILAPs in most of the ice samples increased remarkably from the top to the bottom in QY glacier. TThis result is-seemed highly in

consistent with a previous study by Doherty et al. (2013). However, Xu et al. (2012) observed that the concentrations of BC were higher not only at the snow surface, but also found at the bottom due to the percolation time of meltwater and superimposed ice by the temperature decline in the snowpack. Fig. S5 shows that the vertical profiles of

the mass mixing ratios of BC, ISOC, and Fe for the ice samples in the Xiaodongkemadi glacier were more complicated than those for the other regions. With the exception of the

surface layer at sites 53 and 54, most values of C_{BC}^{est} ranged from 10 to 280 ng g⁻¹ in the Xiaodongkemadi glacier; therefore, this glacier was the cleanest region of all the studied

glaciers. At sites 52-54, Anothera notable feature is-was that the surface mixing ratios of C_{BC}^{est} at sites 52-54 in the XD glacier are-were significantly larger than those in the sub-

surface layers, possibly because of the accumulation of BC via dry/wet deposition on the surface samples. Doherty et al. (2013) also found that the ILAPs could be scavenged with

the snow meltwater, therefore leading to a much higher concentration of BC in the surface snow. At sites 56-58, f_{non-BC}^{est} was lower than 38%, and A_{ice} ranged from 1-2.5. These

results are consistent with the fossil fuel combustion source due to industrial activities. We found that the mechanism of the ILAPs in the vertical ice samples in the QY and XD glacier

could be difference. The ice samples in the QY glacier were collected in the monsoon season. Due to the higher temperature in the monsoon season, the strong melting processes

could wash out the ILAPs in ice samples to lead a higher concentration in the bottom layer in QY glaciers. In contrast, the ice samples were collected in XD glacier in both monsoon

and monsoon seasons. Therefore, it can be seen clearly that a decreasing trend of the ILAPs in the ice samples was found from the top to the bottom in XD glacier due to the high

scavenging effect during the non-monsoon season (Fig. S7a-S7f, only except Fig. S7e and S7g), while a opposite trend due to the washing effect during the monsoon season (Fig. S7h and Fig. S7j). Because the single layer samples are not shown, the vertical profiles of C_{BC}^{est} are plotted in Fig. S6-S8 for all ice samples, which were collected in the QiumianleiketageQM, HariqinHRQ, and Gurenhekou-GR glaciers. Except for the sites in Fig. S6dS8d, S6eS8e, S6iS8i, and S6hS8h, the other sites revealed the trapping and scavenging effects of a higher mass concentration of BC in the surface layer due to the melting processes. ~~Previous studies have also illustrated that the ILAPs could become trapped and integrated at the surface of the snowpack due to melting and sublimation to enrich the surface concentrations (Conway et al., 1996; Painter et al., 2012; Doherty et al., 2013).~~

~~3.2 Water-soluble organic carbon~~

It is well known that the WSOC component has a large variation ranging from 20% to 99% of total carbonaceous particles (Saxena and Hildemann, 1996; Mayol-Bracero et al., 2002). There is a very large fraction representing the average WSOC (>80%) to TOC, which can absorb solar light and enhance cloud formation through their direct and indirect climate effects (Ram et al., 2010). These results are highly consistent with previous studies showing that fossil fuel combustion plays a key role in leading to the higher fraction of WSOC to total organic carbon (TOC) (Zhang et al., 2012). The concentration of WSOC during the field campaign varied from 400 to 43600 ng g⁻¹, with a median of 1400 ng g⁻¹ (Table 1). The median values of the WSOC/TOC ratio were 0.85 for the monsoon season and 0.9 for the non-monsoon season during this field campaign (Fig. 6). No remarkable correlation was observed between WSOC and ISOC in both monsoon and non-monsoon seasons. As WSOC is considered as a stable indicator of the primary biomass burning, with a small contribution of fossil fuel combustion, we indicate that a mixture emission sources from the biomass burning and fossil fuel combustion might be contributing significantly to the TOC concentrations in these TP glacier regions.

—

~~3.43 Contributions to particulate light absorption by ILAPs~~

BC and OC were mainly emitted from biomass burning and biofuel and fossil fuel combustion, while mineral dust was emitted from the local soil or desert regions (Bond et al., 2013; Kaspari et al., 2014; Painter et al., 2007; Chen and Bond, 2010; Streets et al., 2001; Pu et al., 2017). The contributions to particulate light absorption by BC, OC, and Fe have been investigated using the ISSW measurements across northern China and North America (Wang et al., 2013; Doherty et al., 2014). The fractional contributions to total absorption by BC, ISOC, and Fe (assumed to be in the form of goethite) at 450 nm in surface each glaciers are shown in Fig. 7, and further details of the concentrations of BC, ISOC, and Fe are given in Table S1. BC plays a dominant role in particulate light absorption with average values ranging from ~20.44%-54.87% in all glacier regions. ISOC is the second highest absorber in glacier regions, and there are large variations of light absorption of ISOC during the field campaign (with values ranging from ~0.525%-46.58% on average). The contributions to total absorption due to BC and OC were relatively comparable in the QY, YZF and HRQ, which are located in the eastern TP regions. The highest fraction of BC was accounting for 54% in the QM glaciers, which is located in the western TP regions. So the light absorption due to ILAPs in the TP glacier regions is not only from industrial and biomass burning BC and OC, but also with a small contribution from local soil dust Fe. Note that the median average fraction of total light absorption due to Fe is ~11.3%-31% in all seven glaciers, with the highest light absorption of Fe being higher than 40% in the Gurenhekou GR glacier. The relative contributions to total light absorption by BC, OC, and Fe for surface ice samples in each sampling location are also shown in Fig. S9 and Table 1. This result was an indication that mineral dust played a key role in affecting the spectral absorption properties of ILAPs in ice samples from the TP glaciers. This result is an indication that mineral dust plays a key role in affecting the spectral absorption properties due to the soil and mineral dust at site 67. Although the total light absorption was dominated by BC and ISOC in all selected glaciers, we note that the relative spatial distribution of the total light absorption due to Fe (>17%) also play key roles to affected the snowmelt in the southern glaciers than that of northern glaciers across the TP regions (Fig. S7).

30

3.54 Enrichment factor (EF)

Briefly, ~~the~~ EF values ranging from 0.1 to 10 indicate significant input from crustal sources. Conversely, EF values that larger than 10 exhibit a major contribution from anthropogenic activities. Referring to the EF analysis (Fig. 8), the mean EF of Fe < 5 in each glacier can be assumed to customarily originate from crustal sources. Recent studies have also indicated that light-absorbing particles in snow are dominated by local soil dust in some typical regions over northern China (Wang et al., 2013), and northern America (Doherty et al., 2014). Comparable with Fe, the other trace metals with the mean EF of ≥ 5.0 were moderately to highly enriched ~~predominantly~~ from anthropogenic emissions (Hsu et al., 2010). For example, Pacyna ~~and Pacyna~~ (2001) reported that fossil fuel combustion is a major source of Cr. Cu primarily originates from emissions from fossil fuel combustion and industrial processes, while Pb and Zn are known to be drawn from the traffic-related activities and coal burning (Christian et al., 2010; Contini et al., 2014). ~~Together with~~ Hence, ~~the~~ high EF values observed for Cu, Zn, and Cd in our ice samples clearly suggested that the TP glaciers have already been polluted by human activities, such as biomass burning, fossil fuel burning, and the coal burning. ~~For instance, high level of Pb and Cr have demonstrated a link to coal combustion (Zhang et al., 2013a, 2013b; Mokhtar et al., 2014), abundant Cu and Cd were associated with traffic-related dusts (Cheng et al., 2010). Therefore, we concluded that the natural dust source and anthropogenic emission source are both non-negligible to the ILAPs in the TP glaciers.~~

3.65 Source apportionment

Given the importance of the climate effect in our understanding of the ILAPs in TP glaciers, we ~~present~~ applied a PMF receptor model to analyze the source attribution of ILAPs light absorption in these glaciers. In this study, ~~two datasets including~~ the mass concentrations of the chemical components and the ILAPs in ice ~~and the~~ associated with the uncertainty datasets were used to run the PMF 5.0 model. The details of the techniques have already been illustrated by Hegg et al. (2009, 2010) and Pu et al. (2017). The factor loadings (apportionment of species mass to individual factors) for the 3-factor solution of the source profiles based on the PMF 5.0 model are given in Fig. 9 (in both measured mass

concentration and the % total mass allocated to each factor). It ~~is~~ was evident that the first factor (top panel) was obviously characterized by high loadings of Cl^- , ~~Cl salt, Cl_{salt} ,~~ SO_4^{2-} , and NO_3^- , which are well known markers for the urban or local industrial pollutions (Alexander et al., 2015). Although Cl^- to Na^+ are usually considered as a potential product of emission source of sea salt, but also a high loading of Cl^- to ~~Cl salt~~ Cl_{salt} reflecting another source in addition to sea salt such as industrial emission and coal combustion (Hailin et al., 2008; Kulkarni, 2009) ~~indicated another source in addition to sea salt such as industrial emission and coal combustion (Hailin et al., 2008; Kulkarni, 2009)~~. Additionally, the highest loading of NH_4^+ is also suggested as an indicator of coal combustion (Pang et al., 2007). Compared with the first factor, ~~the highest loading of Al (90.3%) and Fe (87.3%) usually regarded are well known as major indicators markers~~ for the urban or regional mineral dust (Pu et al., 2017). Therefore, the second factor ~~or source profile is~~ was easily interpretable as a natural mineral dust source. ~~But a~~ It was notable ~~feature is~~ that ~~the relative high mass loading of C_{BC}^{max} (76.4%) showed a high mass loading in this factor to that of the previously identified mineral dust source as reported by Pu et al. (2017)~~. It is well known ~~that~~ K^+ and $\text{K}_{\text{Biosmoke}}$ are the major indicators of biomass burning ~~source~~ (Zhang et al., 2013a). Therefore, it ~~is~~ was easily interpretable that the highest loadings of K^+ and $\text{K}_{\text{Biosmoke}}$ ~~are~~ were well representative for the biomass burning source (Fig. 9c). However, ~~it is also important to note that~~ the lowest mass loading of C_{BC}^{max} in this factor is a bit unexpected. Indeed, the C_{BC}^{max} is not only attributed to the biomass burning emission, but also associated with the industrial activities associated with the local mineral dust (Bond et al., 2006). Therefore, we interpreted the third factor normally considered a predominantly biomass burning product. ~~However, the major emission of BC in TP glaciers originated from the local mineral dust source instead of the biomass burning and industrial pollution than previous studies (Zhang et al., 2013a; Pu et al., 2017)~~.

Finally, the chemical composition and mean source apportionment of the ILAPs to the three sources in the TP glaciers were given in Fig. 10. Note that the apportionment ~~is~~ was of the light absorption by insoluble particles in the surface glaciers. On average, the source apportionment of the ILAPs in all TP glaciers by mineral dust ~~is~~ was close to 37.5%, while the industrial emission and biomass burning contributed ~~s~~ 33% and 29.4%, respectively.

Specifically, the largest biomass burning contribution of the light-absorption of ILAPs was found in the Qiyi-QY glacier, which is close to the human activity regions (Guan et al., 2009; Li et al., 2016). In the Meikuang-MK, Qiumianleiketage-QM, Gurenhekou-GR, and Xiaodongkemadi-XD glaciers, the mineral dust contribution of light absorption ~~is~~ was much larger (>47.9%) than that of industrial pollution and biomass burning, especially in the Meikuang-MK glacier. In these regions, the percent of the ~~MD~~-light absorption due to soil dust ~~is~~ is ranged from 20.4-31.1%, while the light absorption by biomass burning ~~is~~ was in the range of 18.5-35.8%. Industrial pollution ~~constitutes~~ constituted a major fraction in the Yuzhufeng-YZF glacier. Chemical analysis ~~showed~~ shows that the percentages of the chemical species in the Yuzhufeng-YZF and Meikuang-MK glaciers ~~are~~ were much similar. The attribution of the total anions by chloride, nitrate, and sulphate ~~is~~ were higher ~~52% and 48%~~ than the other chemical species in the Yuzhufeng-YZF and Meikuang-MK glaciers. In the Hariqin-HRQ glacier, the largest ~~attribution~~ contribution of the sulphate ~~is~~ was up to 45.4%. As shown in Fig. 10, the source ~~apportionment~~ of the light absorption by insoluble particles in the surface glaciers ~~is~~ was dominated by mineral dust and the industrial pollution in most glaciers. ~~The~~, only exception was the YZF glacier ~~wherewith~~ a large fraction of the light absorption was due to biomass burning in the Yuzhufeng-YZF glacier. These results ~~are~~ were highly consistent with the previous studies (Andersson et al., 2015). They found that the contributions of coal-combustion-sourced BC are the most significant for the TP glaciers. ~~Based on the model simulations, Zhang et al. (2015) revealed that the largest contribution to annual mean BC burden and surface deposition in the entire TP regions is from biofuel and biomass (BB) emissions in South Asia, followed by fossil fuel (FF) emissions from South Asia.~~

4 Conclusions

In this study, the ILAPs observations in ~~7~~ seven glacier regions across the Tibetan Plateau ~~are~~ were presented using the ISSW technique along with chemical analysis. 67 vertical profiles of ice samples ~~are~~ analyzed ~~collected~~ during the monsoon and non-monsoon seasons from 2013-2015 were analyzed. On average, the BC and OC concentrations in the HRQ XD, and GR glacier during non-monsoon season were several orders of magnitude

~~higher than those in monsoon seasons. There are no apparent differences in the mixing ratios of ILAPs in the ice samples during seasonal transitions. However, it remains unclear that the ILAPs in the MK and YZF glaciers were comparable during the monsoon and non-monsoon seasons, which could be investigated by future survey studies across these regions.~~

5 ~~The results indicate that the variations of A_{tot} and A_{non-BC} for all ice samples range from 1.4-3.7 and 1.9-5.8, respectively, excluding site 16. The lower absorption Ångström exponent ($A_{tot} < 2$) suggested that the sites 30, 51, and 56-58, 65 were primarily influenced by fossil fuel emission, whereas the rest of the sites were heavily influenced by mineral dust and biomass burning. Another notable feature is the large variation of the ILAPs in the ice~~

10 ~~samples. By excluding some of the highest ILAPs values in the ice samples, the values mass concentration of C_{BC}^{est} , C_{ISOC} , and C_{Fe} , BC, OC, and Fe, ranged from 100-1000 ng g⁻¹, 10-2700 ng g⁻¹, and 10-1000 ng g⁻¹, respectively. Among the samples, the lower concentrations of BC were found in the~~

~~Xiaodongkemadi XD, Hariqin HRQ and Gurenhekou GR glaciers, with the median concentrations of 33 ng g⁻¹, 24 ng g⁻¹, and 28 ng~~

15 ~~g⁻¹, respectively. We found that the ILAPs in the ice samples was decreased from the top to the bottom in XD glacier due to the scavenging effect during the non-monsoon season, while a opposite trend due to the washing effect by high temperature during the monsoon season.~~

20 ~~BC played a dominant role in particulate light absorption with average values ranging from ~44%-54% in these glaciers, while ~25%-46% for OC.~~

~~We also present By using a PMF receptor model, to analyze the source attributions of ILAPs in these glaciers. We found that the anthropogenic air pollution ILAPs across the northern~~

~~glaciers is much heavy polluted across the northern glaciers due to human activities, but the major emissions of the light absorption by insoluble particles in TP glaciers originated~~

25 ~~from the local mineral dust and industrial pollution sources, followed by the biomass burning source. We note that the C_{BC}^{max} is not only attributed to the biomass burning emission, but also associated with the industrial activities associated with the local mineral~~

~~dust. Therefore, the natural mineral dust source and anthropogenic emission source are both non-negligible to the ILAPs in the TP glaciers.~~

~~Therefore, we concluded that the natural dust source and anthropogenic emission source are both non-negligible to the ILAPs in the TP glaciers.~~

5

5 Data availability

All datasets and codes used to produce this study can be obtained by contacting Xin Wang (wxin@lzu.edu.cn).

10

Competing interests. The authors declare that they have no conflicts of interest.

Acknowledgements. This research was supported by the Foundation for Innovative Research Groups of the National Natural Science Foundation of China (41521004), the National Natural Science Foundation of China under grant (41775144 and 41522505), and the Fundamental Research Funds for the Central Universities (lzujbky-2018-k02).

15

Table 1. Statistics of the ~~ice variables~~ ILAPs in each glacier measured using an ISSW spectrophotometer associated with the chemical analysis for each glacier.

Region	Latitude	Longitude		C_{BC}^{equiv}	C_{BC}^{max}	C_{BC}^{est}	f_{non-BC}^{est}	A_{tot}	ISOC	WSOC	Fe
	(N)	(E)		(ng g ⁻¹)	(ng g ⁻¹)	(ng g ⁻¹)	(%)		(ppm)	(ppm)	(ppm)
Qiyi glacier	39°14'28"	97°45'27"	average	414	299	238 (116, 313)	42 (15, 66)	2.59	1.21	0.195 <u>0.43</u>	0.18 <u>0.18</u>
			median	176	128	94 (29, 124)	41 (17, 70)	2.62	0.66	0.082 <u>0.25</u>	0.099 <u>0.93</u>
			minimum	26	29	25 (13, 35)	21 (—, 53)	0.8	0.08	0.010 <u>0.62</u>	0.02 <u>0.19</u>
			maximum	2651	2230	1877 (1182, 2109)	73 (41, —)	3.73	11.59	3.35 <u>43.5</u>	2.4 <u>124</u>
Qiumianleiketage	36°41'47"	90°43'44"	average	421	296	238 (139, 402)	44 (24, 81)	2.80	1.43	0.21 <u>0.99</u>	0.23 <u>0.23</u>
			median	307	215	172 (64, 218)	44 (24, 81)	2.76	1.06	0.152 <u>0.23</u>	0.18 <u>0.18</u>
			minimum	139	93	62 (19, 93)	37 (12, 64)	2.45	0.54	0.09 <u>0.17</u>	0.11 <u>0.10</u>
			maximum	995	662	558 (143, 678)	56 (27, 86)	3.08	3.97	0.552 <u>0.56</u>	0.63 <u>0.62</u>
Meikuang glacier	35°40'24"	94°11'10"	average	493	328	260 (119, 331)	42 (15, 37)	2.65	2.14	0.192 <u>0.80</u>	0.222 <u>0.21</u>
			median	197	156	133 (76, 153)	44 (16, 69)	2.64	0.61	0.093 <u>0.05</u>	0.13 <u>0.12</u>
			minimum	24	23	19 (17, 24)	16 (—, 17)	1.37	0.13	0.020 <u>0.62</u>	0.033 <u>0.32</u>
			maximum	4696	2817	2292 (109, 2938)	62 (23, 85)	3.56	16.89	1.368 <u>0.06</u>	1.22 <u>0.12</u>
Yuzhufeng glacier	35°38'43"	94°13'36"	average	457	312	233 (94, 295)	51 (—, 37)	2.84	1.51	0.172 <u>0.85</u>	0.444 <u>0.43</u>
			median	317	201	160 (116, 204)	48 (26, 87)	2.95	1.02	0.102 <u>0.76</u>	0.212 <u>0.21</u>
			minimum	52	35	24 (8, 35)	15 (—, 37)	1.82	0.07	0.020 <u>0.8</u>	0.054 <u>0.545</u>
			maximum	2630	1608	1169 (72, 1603)	110 (6, 49)	3.7	9.16	0.815 <u>0.92</u>	3.51 <u>0.35</u>
Hariqin glacier	33°08'23"	92°05'34"	average	476	327	256 (100, 385)	48 (26, 82)	2.79	1.59	0.17 <u>0.67</u>	0.17 <u>0.17</u>
			median	54	37	23 (9, 30)	48 (26, 82)	2.87	0.22	0.04 <u>0.08</u>	0.055 <u>0.52</u>
			minimum	36	24	13 (4, 22)	19 (—, 41)	1.96	0.08	0.010 <u>0.72</u>	0.032 <u>0.26</u>
			maximum	3990	2702	2131 (682, 2784)	64 (32, 84)	3.52	9.64	1.114 <u>0.92</u>	1.05 <u>0.10</u>

Region	Latitude	Longitude		C_{BC}^{equiv}	C_{BC}^{max}	C_{BC}^{est}	f_{non-BC}^{est}	\dot{A}_{tot}	ISOC	$\frac{Al}{WS}$	$\frac{Fe}{Fe}$
	(N)	(E)		(ng g ⁻¹)	(ng g ⁻¹)	(ng g ⁻¹)	(%)		(ppm)	(ppm)	(ppm)
Xiaodongkemadi	33°04'08"	92°04'24"	average	253	171	152 (76, 177)	37 (15, 63)	2.28	0.95	0.131-82	0.1747
			median	62	47	53 (37, 65)	36 (13, 59)	2.18	0.19	0.031-41	0.0662
			minimum	13	12	9 (6, 18)	8 (—, 19)	1.08	0.01	0.010-45	0.0140
			maximum	2770	1849	1637 (596, 2031)	86 (25, 90)	3.63	6.97	2.405-91	2.1324
Gurenhekou glacier	30°11'17"	90°27'23"	average	382	292	247 (212, 591)	46 (16, 71)	2.42	0.62	0.151-24	0.1818
			median	61	46	30 (19, 44)	48 (18, 75)	2.46	0.13	0.050-85	0.1097
			minimum	28	23	15 (10, 24)	27 (7, 52)	1.34	0.02	0.010-44	0.0334
			maximum	4674	3634	3080 (1876, 3884)	61 (26, 85)	2.92	5.22	1.354-65	0.9194

Table 2. Statistics of the ILAPs in snow and ice in the studied TP glaciers and other related glaciers.

<u>Glacier name</u>	<u>Sampling time</u>	<u>Season</u>	<u>Altitude/ m a.s.l.</u>	<u>BC (ng g⁻¹)</u>	<u>OC (ng g⁻¹)</u>	<u>MD (μg g⁻¹)</u>	<u>Sample type</u>	<u>References</u>
<u>Qiyi</u>	<u>2005.7</u>	<u>Monsoon</u>	<u>4850</u>	<u>22±2</u>	<u>—</u>	<u>—</u>	<u>Snow pit</u>	<u>Ming et al., 2009</u>
	<u>2001.7-8</u>	<u>Monsoon</u>	<u>4600</u>	<u>6.65±3.3</u>	<u>87.52±37.59</u>	<u>—</u>	<u>Fresh snow</u>	<u>Xu et al., 2006</u>
	<u>2001.7-8</u>	<u>Monsoon</u>	<u>4600</u>	<u>52.64±17.83</u>	<u>195.5±85</u>	<u>—</u>	<u>Aged snow</u>	<u>Xu et al., 2006</u>
	<u>2013.8-9</u>	<u>Monsoon</u>	<u>4700</u>	<u>238±349</u>	<u>1210±2023</u>	<u>1.42±1.17</u>	<u>Ice</u>	<u>This study</u>
<u>Qiumianleiketage</u>	<u>2014.5</u>	<u>Non-monsoon</u>	<u>5300</u>	<u>238±168</u>	<u>1431±1130</u>	<u>2.92±2.09</u>	<u>Ice</u>	<u>This study</u>
<u>Meikuang</u>	<u>2001.7-8</u>	<u>Monsoon</u>	<u>5200</u>	<u>446</u>	<u>124</u>	<u>—</u>	<u>Surface snow</u>	<u>Xu et al., 2006</u>
	<u>2015.10</u>	<u>Monsoon</u>	<u>5050</u>	<u>290±241</u>	<u>3745±5100</u>	<u>5.27±6.81</u>	<u>Ice</u>	<u>This study</u>
	<u>2015.5</u>	<u>Non-monsoon</u>	<u>5050</u>	<u>250±468</u>	<u>1718±3639</u>	<u>1.85±2.38</u>	<u>Ice</u>	<u>This study</u>
<u>Yuzhufeng</u>	<u>2014,2015.10</u>	<u>Monsoon</u>	<u>5350</u>	<u>265±270</u>	<u>1596±2052</u>	<u>2.93±3.19</u>	<u>Ice</u>	<u>This study</u>
	<u>2014.5</u>	<u>Non-monsoon</u>	<u>5350</u>	<u>213±188</u>	<u>1421±1173</u>	<u>1.9±1.77</u>	<u>Ice</u>	<u>This study</u>
<u>Hariqin</u>	<u>2015.10</u>	<u>Monsoon</u>	<u>5650</u>	<u>91±126</u>	<u>930±1880</u>	<u>1.23±1.77</u>	<u>Ice</u>	<u>This study</u>
	<u>2015.5</u>	<u>Non-monsoon</u>	<u>5650</u>	<u>1077±1489</u>	<u>4860±6759</u>	<u>8.38±10.59</u>	<u>Ice</u>	<u>This study</u>
<u>Xiaodongkemadi</u>	<u>2014.8-2015.7</u>	<u>Monsoon</u>	<u>5400-5750</u>	<u>41.77±6.36</u>	<u>157.97±42.3</u>	<u>1.89±0.92</u>	<u>Fresh snow</u>	<u>Li et al., 2017</u>
		<u>Monsoon</u>	<u>5400-5750</u>	<u>246.84±118.3</u>	<u>611.45±467.7</u>	<u>39.43±24.35</u>	<u>Aged snow</u>	<u>Li et al., 2017</u>
		<u>Monsoon</u>	<u>5400-5750</u>	<u>3335±3767</u>	<u>9857±10923</u>	<u>880±1038</u>	<u>Granular ice</u>	<u>Li et al., 2017</u>

	<u>2015.10</u>	<u>Monsoon</u>	<u>5600</u>	<u>57+37</u>	<u>250+233</u>	<u>0.68+0.3</u>	<u>Ice</u>	<u>This study</u>
	<u>2013-2015.5</u>	<u>Non- monsoon</u>	<u>5600</u>	<u>178+381</u>	<u>1174+2014</u>	<u>2.18+6.15</u>	<u>Ice</u>	<u>This study</u>
<u>Gurenhekou</u>	<u>2015.10</u>	<u>Monsoon</u>	<u>5610</u>	<u>85+177</u>	<u>330+648</u>	<u>1.17+1.49</u>	<u>Ice</u>	<u>This study</u>
	<u>2014.5</u>	<u>Non-monsoon</u>	<u>5610</u>	<u>1116+1700</u>	<u>2148+2668</u>	<u>7.7+9.99</u>	<u>Ice</u>	<u>This study</u>
<u>Palong-Zanbu-</u>	<u>1998-2005</u>	<u>Monsoon</u>	<u>4800-5600</u>	<u>5.27+2.23</u>	<u>70.8+39.3</u>	<u>==</u>	<u>Ice core</u>	<u>Xu et al., 2009a</u>
<u>No. 4</u>		<u>Non-monsoon</u>	<u>4800-5600</u>	<u>11.51+4.7</u>	<u>97.5+49.9</u>	<u>==</u>	<u>Ice core</u>	<u>Xu et al., 2009a</u>
<u>Zuoqiupu</u>	<u>1956-2006</u>	<u>Monsoon</u>	<u>5100-5400</u>	<u>2.37+1.55</u>	<u>11.55+11.5</u>	<u>==</u>	<u>Ice core</u>	<u>Xu et al., 2009b</u>
		<u>Non-monsoon</u>	<u>5100-5400</u>	<u>8.33+3.29</u>	<u>26.71+13.74</u>	<u>==</u>	<u>Ice core</u>	<u>Xu et al., 2009b</u>
<u>Zhadang</u>	<u>2012.8</u>	<u>Monsoon</u>	<u>5500-5800</u>	<u>51.9+7.2</u>	<u>==</u>	<u>6.38+1.54</u>	<u>Snow pit</u>	<u>Qu et al., 2014</u>
<u>—</u>	<u>2014.6</u>	<u>Monsoon</u>	<u>5800</u>	<u>79</u>	<u>515.08</u>	<u>==</u>	<u>Snow pit</u>	<u>Li et al., 2016</u>
<u>—</u>	<u>2015.5</u>	<u>Non-monsoon</u>	<u>5790</u>	<u>303</u>	<u>822</u>	<u>==</u>	<u>Snow pit</u>	<u>Li et al., 2018</u>
<u>—</u>	<u>2015.6-9</u>	<u>Monsoon</u>	<u>5570-5790</u>	<u>281</u>	<u>743</u>	<u>==</u>	<u>Surface snow</u>	<u>Li et al., 2018</u>
<u>Urumqi No.1</u>	<u>2004.7-8</u>	<u>Monsoon</u>	<u>4130</u>	<u>500</u>	<u>1200</u>	<u>==</u>	<u>Surface snow</u>	<u>Xu et al., 2012</u>
	<u>2013.8</u>	<u>Monsoon</u>	<u>3800-4100</u>	<u>30+5</u>	<u>==</u>	<u>17+6</u>	<u>Fresh snow</u>	<u>Ming et al., 2016</u>
<u>Muji</u>	<u>2012.6-10</u>	<u>Monsoon</u>	<u>4700-5500</u>	<u>375+3</u>	<u>175+15</u>	<u>==</u>	<u>Snow pit</u>	<u>Yang et al., 2015</u>
<u>Qiangyong</u>	<u>2001</u>	<u>==</u>	<u>5400</u>	<u>43.1</u>	<u>117.3</u>	<u>==</u>	<u>Surface snow</u>	<u>Xu et al., 2006</u>
<u>Kangwure</u>	<u>2001</u>	<u>==</u>	<u>6000</u>	<u>21.8</u>	<u>161.1</u>	<u>==</u>	<u>Surface snow</u>	<u>Xu et al., 2006</u>
<u>Namunani</u>	<u>2004</u>	<u>==</u>	<u>5780-6080</u>	<u>4.4+2.1</u>	<u>51.1+20.6</u>	<u>==</u>	<u>Surface snow</u>	<u>Xu et al., 2006</u>
<u>Demula</u>	<u>2014.5</u>	<u>Non-monsoon</u>	<u>5404</u>	<u>17</u>	<u>185</u>	<u>==</u>	<u>Snow pit</u>	<u>Li et al., 2016</u>
<u>Yulong</u>	<u>2015.5</u>	<u>Non-monsoon</u>	<u>4400-4800</u>	<u>372+58</u>	<u>2003+308</u>	<u>9.47+2.36</u>	<u>Aged snow</u>	<u>Niu et al., 2017</u>

	2015.8	Monsoon	4400-4800	2309+125	3211+168	97.12+50.78	Aged snow	Niu et al., 2017
Laohugou No. 12	2015.8	Monsoon	4400-4800	2198+1004	2190+1203	114+67	Aged snow	Zhang et al., 2017
	2015.10	Non-monsoon	4400-4800	1218+212	504+50	63+2	Aged snow	Zhang et al., 2017

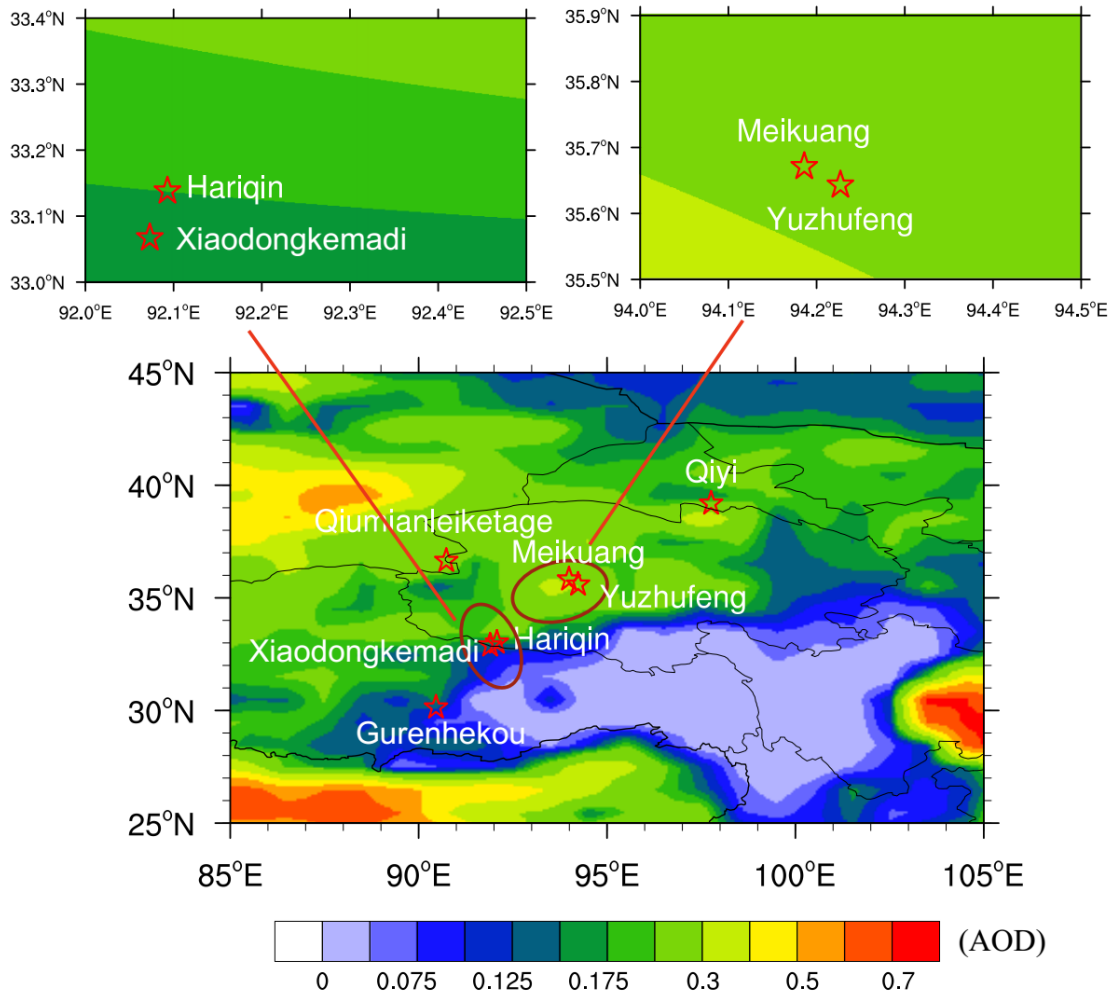


Figure 1. Spatial distribution of the averaged AOD retrieved from Aqua MODIS over Tibetan Plateau from 2013 to 2015, and larger values represent higher optical depth and smaller values represent smaller optical depth. The red stars are the sampling locations (see also Table 1): 1, Qiyi glacier (97.76° E, 39.24° N, 4850 m a.s.l.); 2, Qiumianleiketage glacier (90.73° E, 36.70° N, 5240 m a.s.l.); 3, Meikuang glacier (94.19° E, 35.67° N, 4983 m a.s.l.); 4, Yuzhufeng glacier (94.23° E, 35.65° N, 5200 m a.s.l.); 5, Hariqin glacier (92.09° E, 33.14° N, 5100 m a.s.l.); 6, Xiaodongkemadi glacier (92.07° E, 33.07° N, 5600 m a.s.l.); 7, Gurenhekou glacier (90.46° E, 30.19° N, 5655 m a.s.l.).

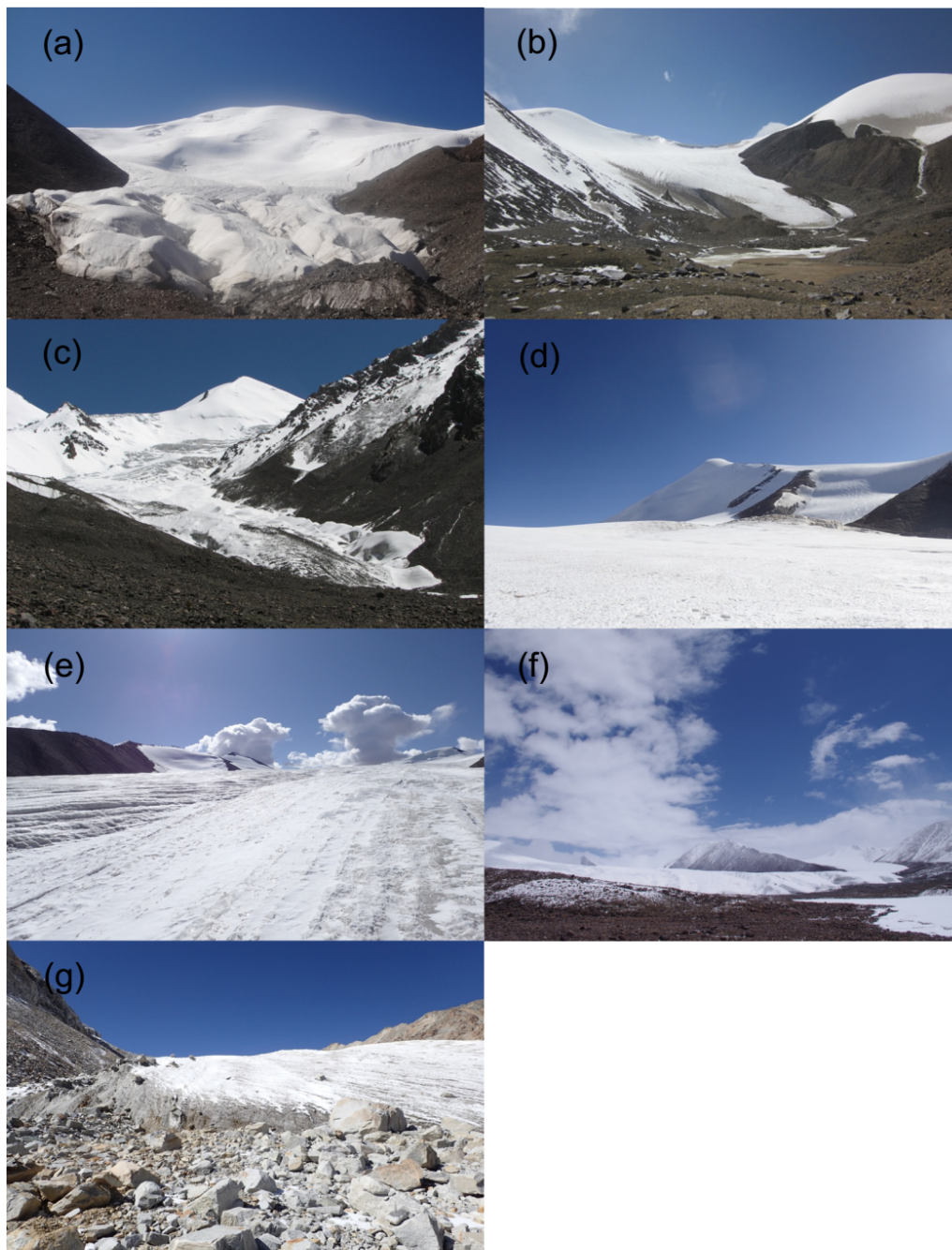


Figure 2. Pictures of ice sampling location in the (a) Qiyi, (b) Qiumianleiketage, (c) Meikuang, (d) Yuzhufeng, (e) Hariqin, (f) Xiaodongkemadi, (g) Gurenhekou glaciers, respectively.

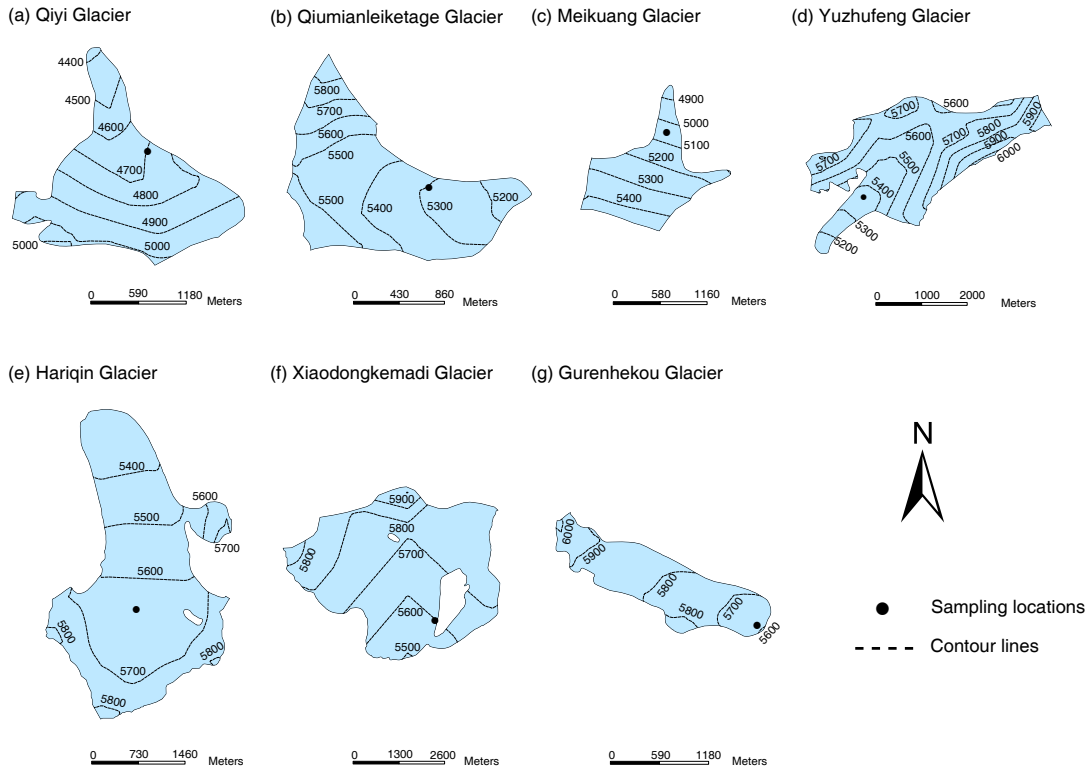


Figure 1. Geographical locations of (a) Qiyi glacier (97.76° E, 39.24° N), (b) Qimianleiketage glacier (90.73° E, 36.70° N), (c) Meikuang glacier (94.19° E, 35.67° N), (d) Yuzhufeng glacier (94.23° E, 35.65° N), (e) Hariqin glacier (92.09° E, 33.14° N), (f) Xiaodongkemadi glacier (92.07° E, 33.07° N), (g) Gurenhekou glacier (90.46° E, 30.19° N). The black dot is the sampling locations.



Figure 2. The equipment for collecting new snow samples in seven TP glaciers.

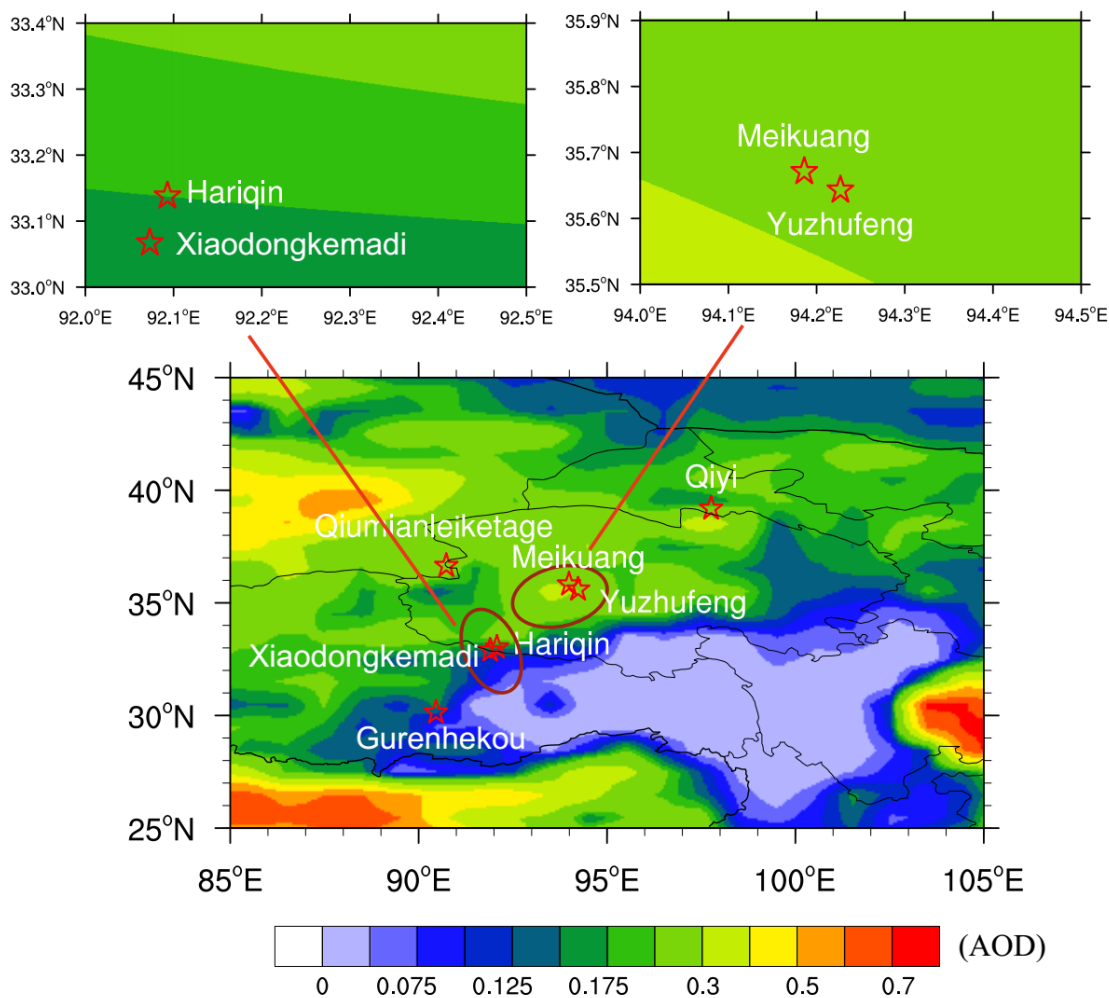


Figure 31. Spatial distribution of the averaged AOD retrieved from Aqua-MODIS at 500 nm over Tibetan Plateau from 2013 to 2015, and larger values represent higher optical depth and smaller values represent smaller optical depth. The red stars are the sampling locations (see also Table 1): 1, Qiyi glacier (97.76° E, 39.24° N, 4850 m a.s.l); 2, Qiumianleiketage glacier (90.73° E, 36.70° N, 5240 m a.s.l); 3, Meikuang glacier (94.19° E, 35.67° N, 4983 m a.s.l); 4, Yuzhufeng glacier (94.23° E, 35.65° N, 5200 m a.s.l); 5, Hariqin glacier (92.09° E, 33.14° N, 5100 m a.s.l); 6, Xiaodongkemadi glacier (92.07° E, 33.07° N, 5600 m a.s.l); 7, Gurenhekou glacier (90.46° E, 30.19° N, 5655 m a.s.l).

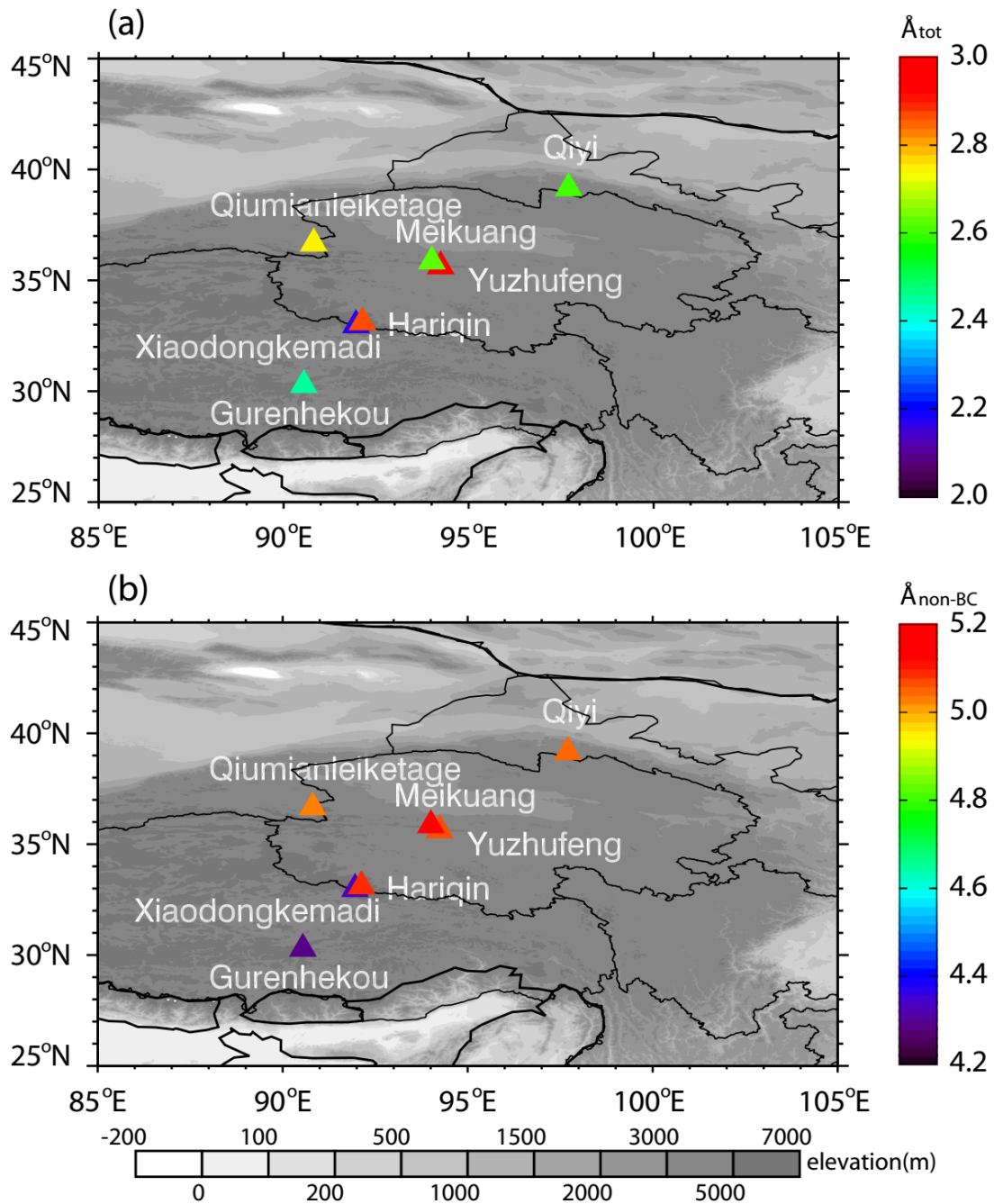


Figure 43. The spatial distribution of the median absorption Ångström exponent for (a) total particulate constituents (\hat{A}_{tot}), and (b) non-BC particulate constituents (\hat{A}_{non-BC}) in each glacier (see Fig. 1).

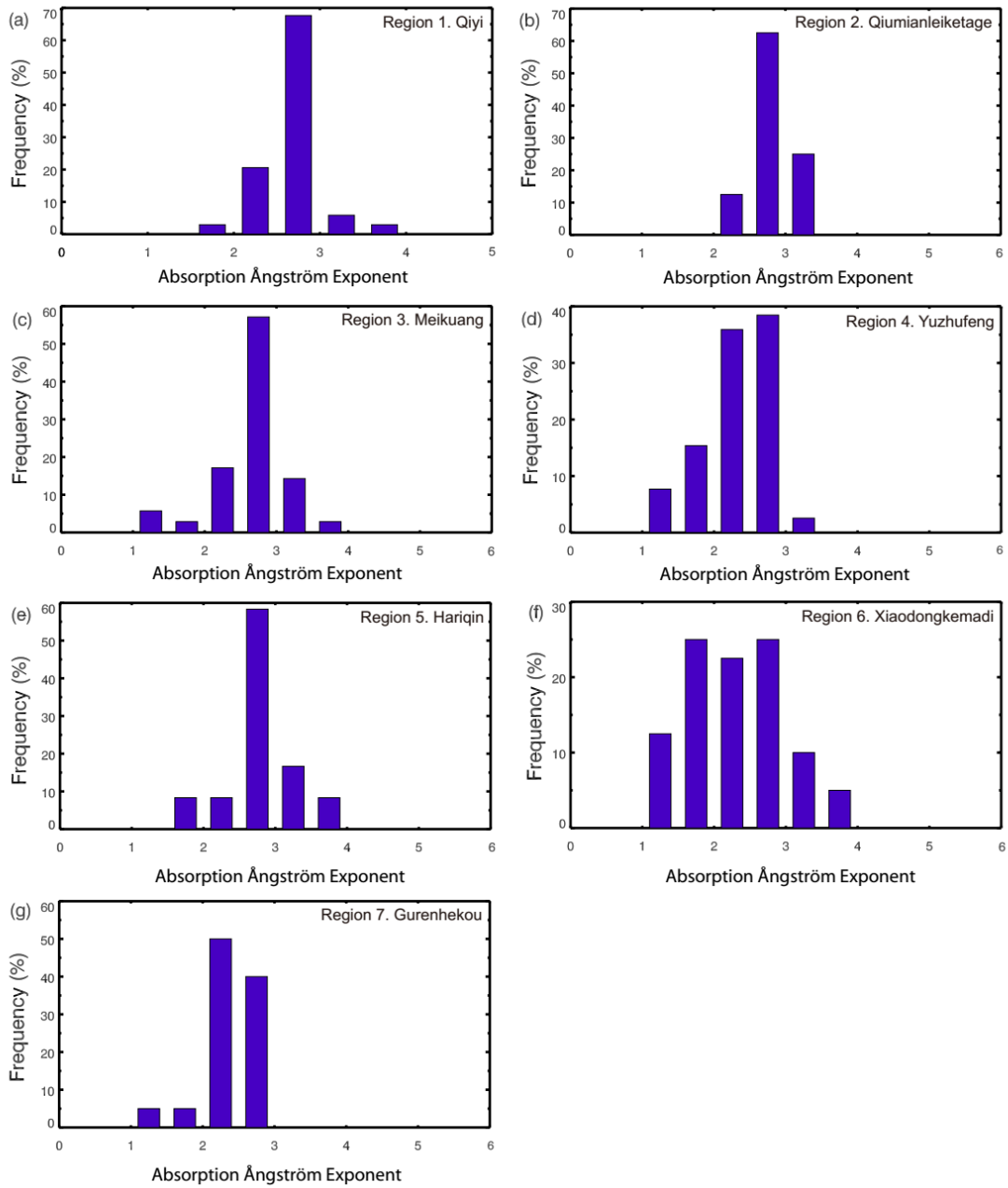
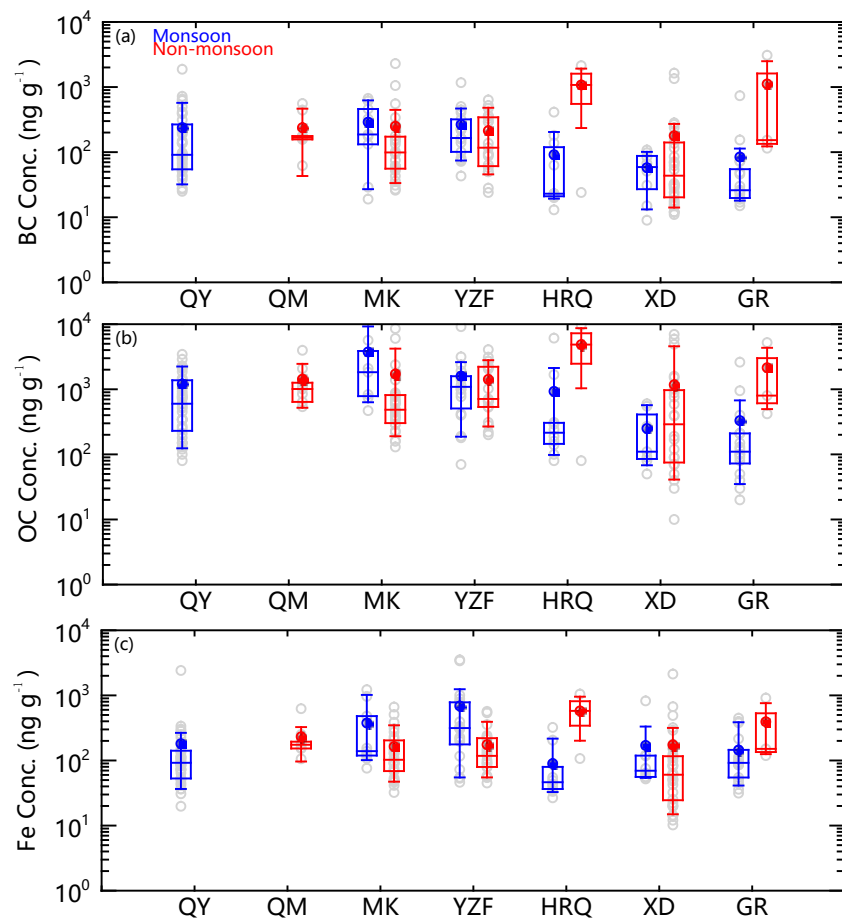


Figure 54. Histograms of the frequency of A_{tot} (450-600 nm) for ice samples in each of the glacier region. Samples from all vertical profiles are included.



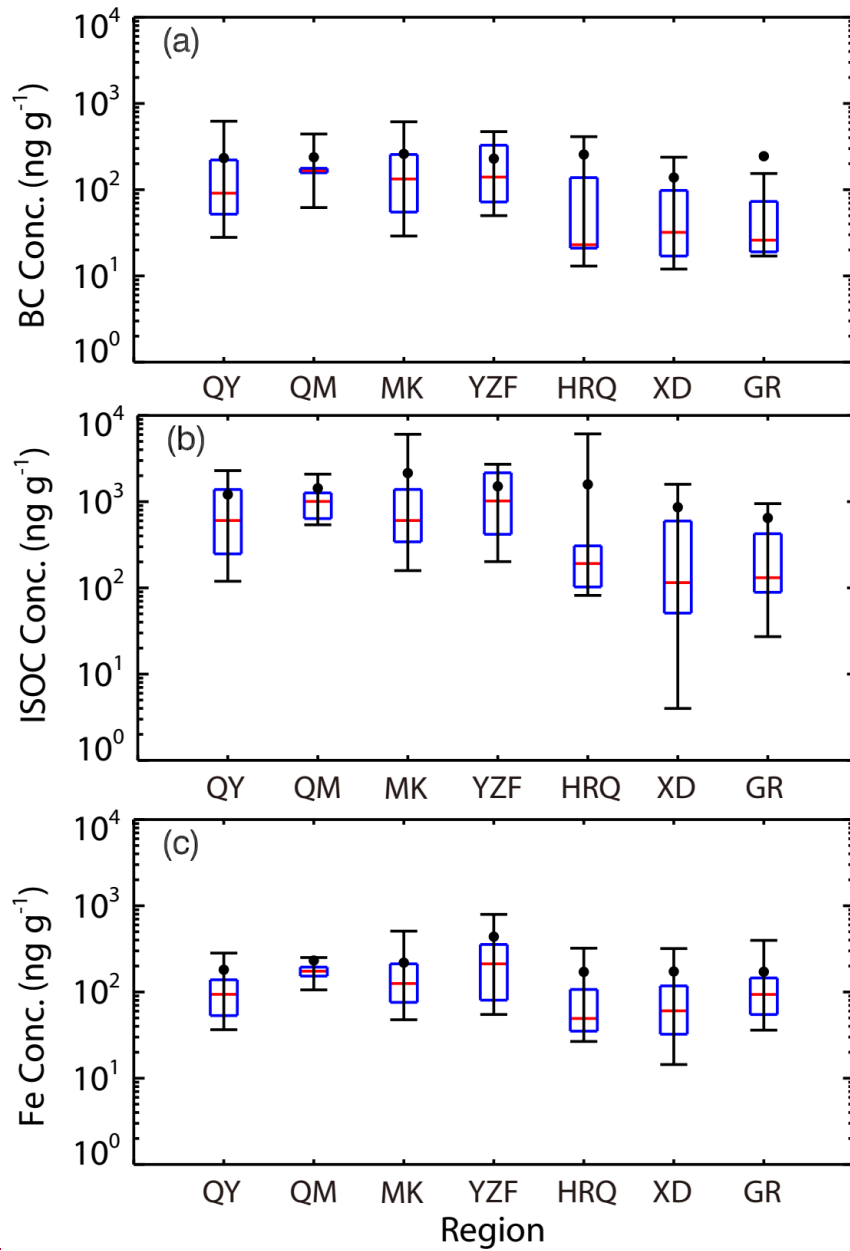


Figure 65. Box plots of the regional variations in (a) BC concentration, (b) ISOC concentration, and (c) Fe concentration of the seven glaciers. QY, QM, MK, YZF, HRQ, XD, and GR represent the following glaciers: Qiyi, Qiumianleiketage, Meikuang, Yuzhufeng, Hariqin, Xiaodongkemadi, Gurenhekou glaciers, respectively. Error bars are 10th, 25th, median, 75th, and 90th percentiles of the data. The dot symbol represents the average concentrations of the ILAPs in ice samples in each glacier.

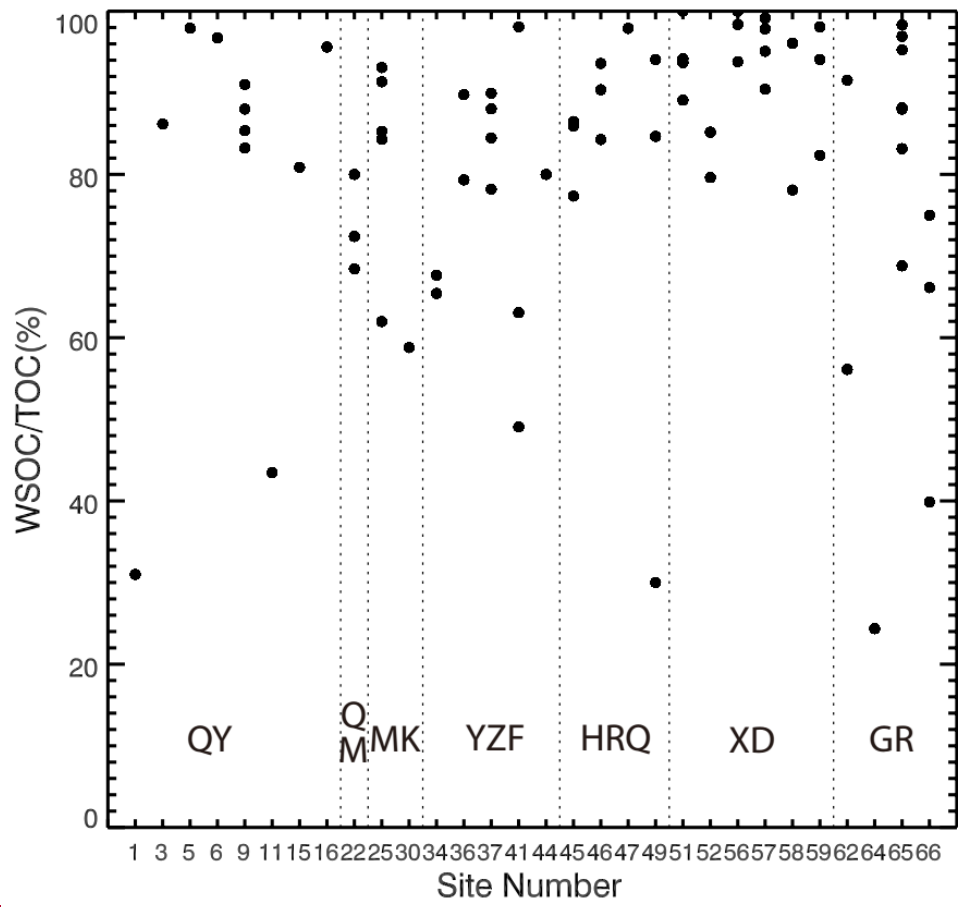


Figure 6. The mass fraction of WSOC to TOC of each ice sample.

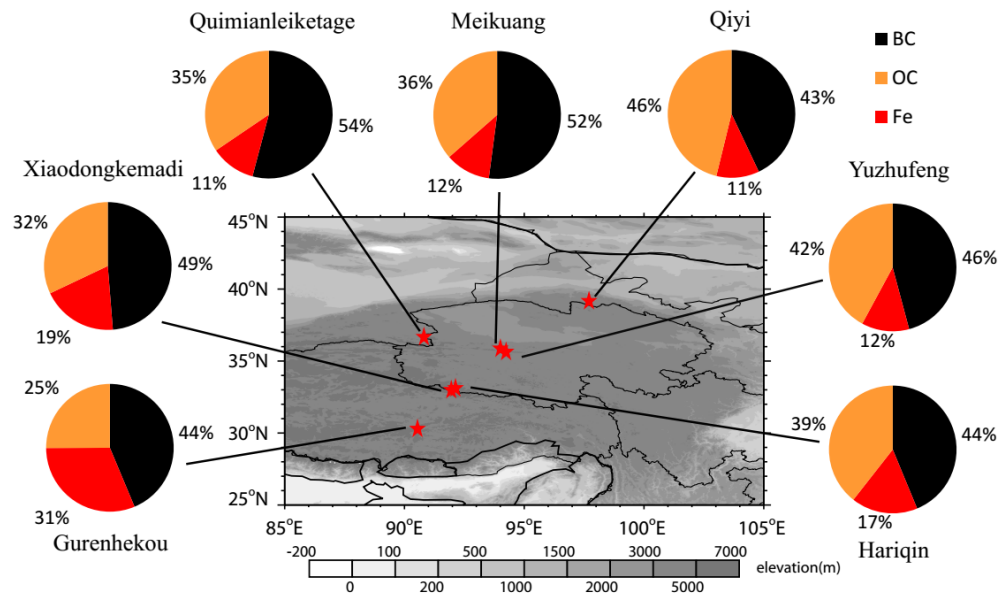


Figure 7. The median of relative contributions to total light absorption by BC, OC, and Fe for ice samples in each glacier.

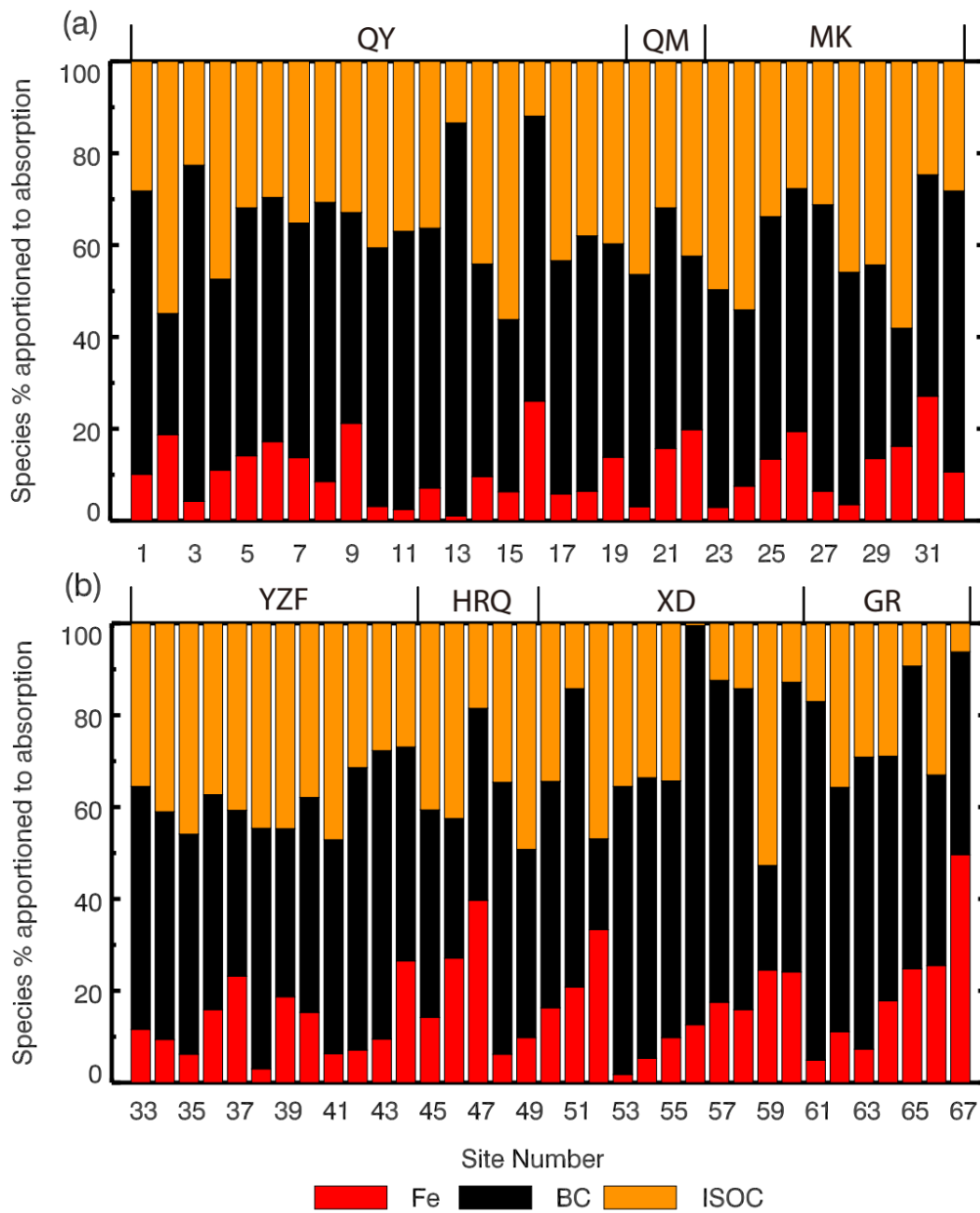


Figure 7. Relative contributions to total light absorption by BC, ISOC, and Fe oxide (assumed to be in the form of goethite) for surface ice samples in each sampling site (See Table 1).

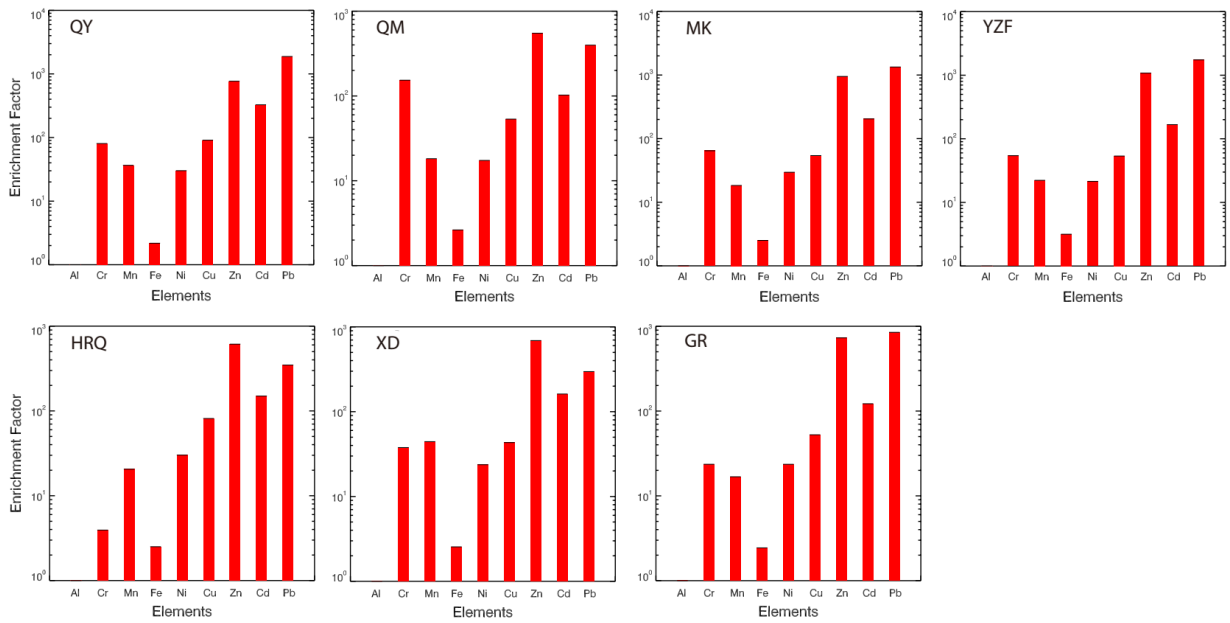


Figure 8. Average enrichment factors of trace metals in surface ice samples at each region.

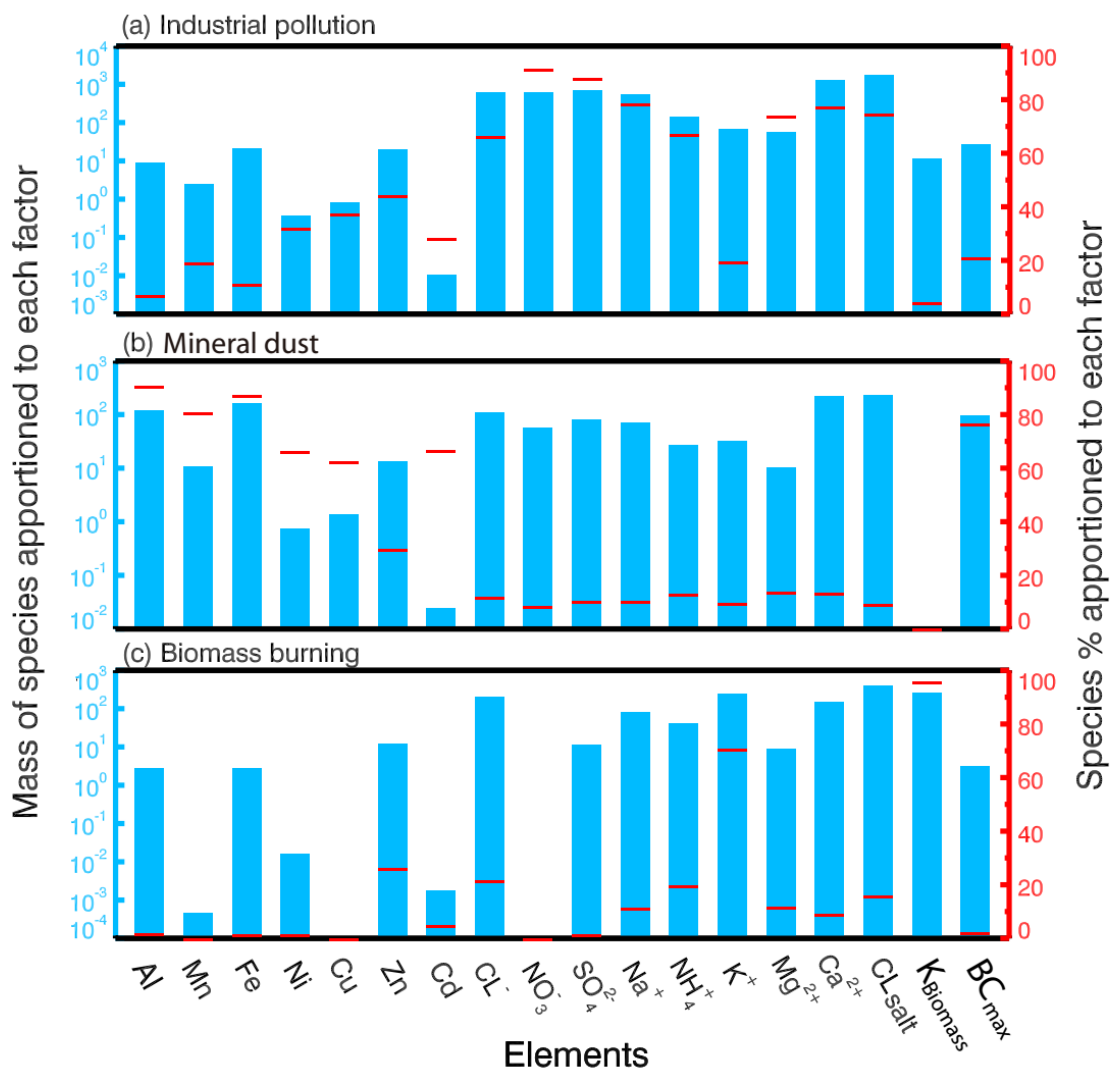


Figure 9. Source profiles for the three factors/sources that were resolved by the PMF 5.0 model.

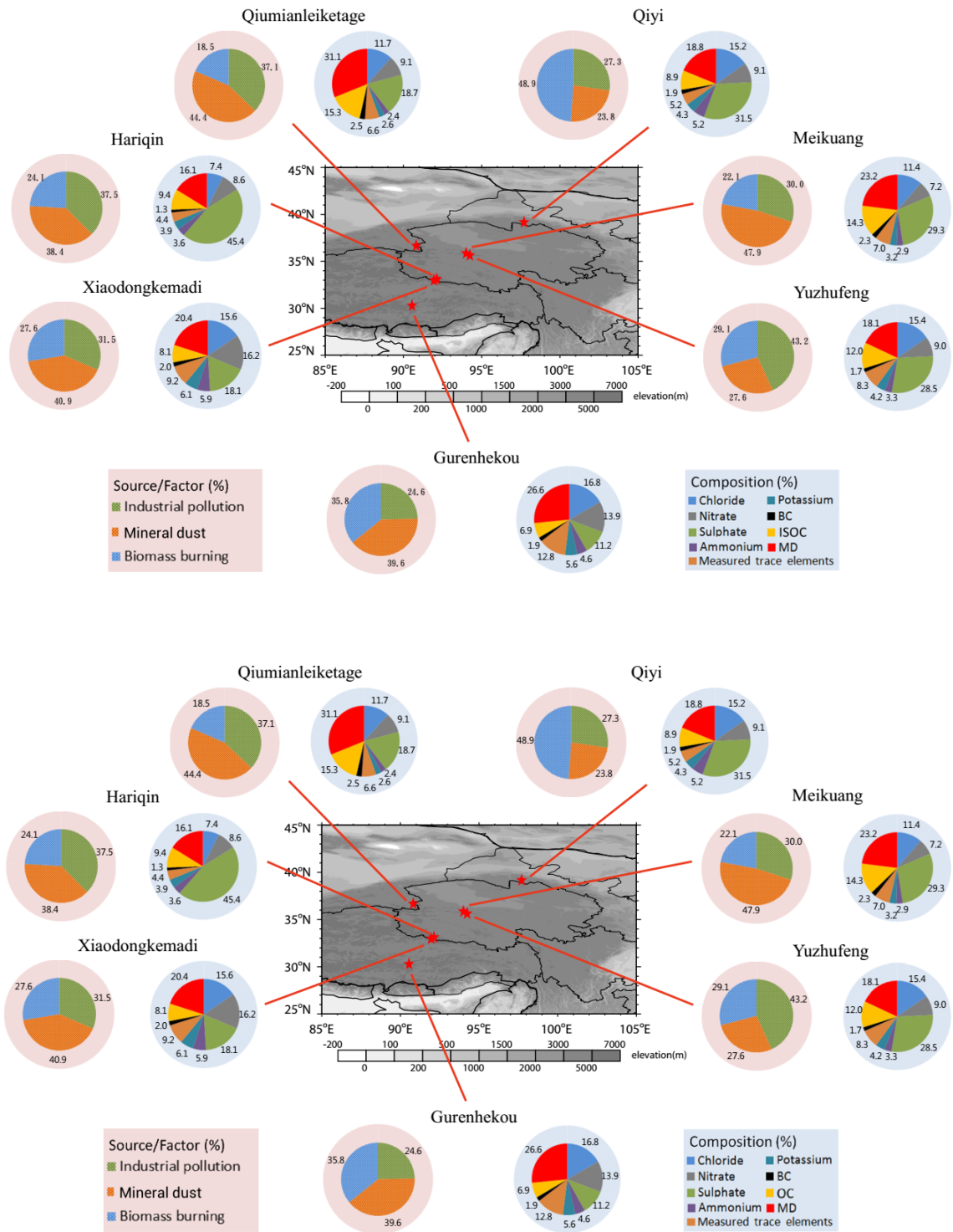


Figure 10. Chemical composition and source apportionment for the seven glaciers in the TP_ regions. Note that the apportionment is of the light absorption by insoluble particles in the surface_

glaciers.

References

- Alexander, B., and Mickley, L. J.: Paleo-perspectives on potential future changes in the oxidative capacity of the atmosphere due to climate change and anthropogenic emissions, Current Pollution Reports, 1, 57-69, 2015.
- Alfaro, S. C., Lafon, S., Rajot, J. L., Formenti, P., Gaudichet, A., and Maille, M.: Iron oxides and light absorption by pure desert dust: An experimental study, J. Geophys. Res.-Atmos., 109, Artn D08208, 10.1029/2003jd004374, 2004.
- Bergstrom, C.: Measuring the value and prestige of scholarly journals, College and Research Libraries News, 68, 314-316, 2007.
- Bolch, T., Yao, T., Kang, S., Buchroithner, M. F., Scherer, D., Maussion, F., Huintjes, E., and Schneider, C.: A glacier inventory for the western Nyainqentanglha Range and the Nam Co Basin, Tibet, and glacier changes 1976–2009, The Cryosphere, 4, 419-433, <https://doi.org/10.5194/tc-4-419-2010>, 2010.
- Bond, T. C., and Bergstrom, R. W.: Light absorption by carbonaceous particles: An investigative review, Aerosol Sci. Technol., 40, 27-67, 2006.
- Bond, T. C., Doherty, S. J., Fahey, D. W., et al.: Bounding the role of black carbon in the

- [climate system: A scientific assessment, J. Geophys. Res.-Atmos., 118, 5380-5552, 2013.](#)
- [Brandt, R. E., Warren, S. G., and Clarke, A. D.: A controlled snowmaking experiment testing the relation between black carbon content and reduction of snow albedo, J. Geophys. Res.-Atmos., 116, Artn D08109, 10.1029/2010jd015330, 2011.](#)
- [Christian, T. J., Yokelson, R. J., Cárdenas, B., Molina, L. T., Engling, G., and Hsu, S. C.: Trace gas and particle emissions from domestic and industrial biofuel use and garbage burning in Central Mexico, Atmos. Chem. Phys., 10, 565-584, 2010.](#)
- [Chylek, P., Ramaswamy, V. & Srivastava, V.: Graphitic carbon content of aerosols, clouds and snow, and its climatic implications, Sci. Total Environ., 36, 117–120, 1984.](#)
- [Cong, Z., Gao, S., Zhao, W., Wang, X., Wu, G., Zhang, Y., Kang, S., Liu, Y., and Ji, J.: Iron oxides in the cryoconite of glaciers on the Tibetan Plateau: abundance, speciation and implications, The Cryosphere, 12, 3177-3186, 10.5194/tc-12-3177-2018, 2018.](#)
- [Cong, Z. Y., Kang, S. C., Smirnov, A., and Holben, B.: Aerosol optical properties at Nam Co, a remote site in central Tibetan Plateau, Atmos. Res., 92, 42-48, 10.1016/J.Atmosres.2008.08.005, 2009.](#)
- [Cong, Z. Y., Kang, S. C., Zhang, Y. L., and Li, X. D.: Atmospheric wet deposition of trace elements to central Tibetan Plateau, Appl. Geochem., 25, 1415-1421, 2010.](#)
- [Cong, Z., Kang, S., Kawamura, K., Liu, B., Wan, X., Wang, Z., Gao, S., and Fu, P.: Carbonaceous aerosols on the south edge of the Tibetan Plateau: concentrations, seasonality and sources, Atmos. Chem. Phys., 15, 1573-1584, 2015.](#)
- [Contini, D., Cesari, D., Genga, A., Siciliano, M., Ielpo, P., and Guascito, M. R.: Source apportionment of size-segregated atmospheric particles based on the major water-soluble components in Lecce \(Italy\), Sci. Total Environ., 472, 248-261, 2014.](#)
- [Conway, H., Gades, A., and Raymond, C. F.: Albedo of dirty snow during conditions of melt, Water Resour. Res., 32, 1713-1718, 10.1029/96wr00712, 1996.](#)
- [Dang, C., and Hegg, D. A.: Quantifying light absorption by organic carbon in Western North American snow by serial chemical extractions, J. Geophys. Res.-Atmos., 119, 10.1002/2014jd022156, 2014.](#)
- [Doherty, S. J., Warren, S. G., Grenfell, T. C., Clarke, A. D., and Brandt, R. E.: Light-absorbing impurities in Arctic snow, Atmos. Chem. Phys., 10, 11647-11680, 2010.](#)

- Doherty, S. J., Grenfell, T. C., Forsström, S., Hegg, D. L., Brandt, R. E., and Warren, S. G.: Observed vertical redistribution of black carbon and other insoluble light-absorbing particles in melting snow, *J. Geophys. Res.-Atmos.*, 118, 5553-5569, 2013.
- Doherty, S. J., Dang, C., Hegg, D. A., Zhang, R. D., and Warren, S. G.: Black carbon and other light-absorbing particles in snow of central North America, *J. Geophys. Res.-Atmos.*, 119, 12807-12831, 2014.
- Engling, G. and Gelencser, A.: Atmospheric Brown Clouds: From Local Air Pollution to Climate Change, *Elements*, 6, 223-228, 2010.
- Federer, U., Kaufmann, P. R., Hutterli, M., Schüpbach, S., and Stocker, T. F.: Continuous flow analysis of total organic carbon in polar ice cores, *Environ. Sci. Technol.*, 42, 8039–8043, 2008.
- Fialho, P., Hansen, A. D. A., and Honrath, R. E.: Absorption coefficients by aerosols in remote areas: a new approach to decouple dust and black carbon absorption coefficients using seven-wavelength Aethalometer data, *J. Aerosol Sci.*, 36, 267-282, 2005.
- Flanner, M. G., Zender, C. S., Randerson, J. T., and Rasch, P. J.: Present-day climate forcing and response from black carbon in snow, *J. Geophys. Res.-Atmos.*, 112, D11202, doi: 10.1029/2006jd008003, 2007.
- Flanner, M. G., Zender, C. S., Hess, P. G., Mahowald, N. M., Painter, T. H., Ramanathan, V., and Rasch, P. J.: Springtime warming and reduced snow cover from carbonaceous particles, *Atmos. Chem. Phys.*, 9, 2481-2497, 2009.
- Grenfell, T. C., Doherty, S. J., Clarke, A. D., and Warren, S. G.: Light absorption from particulate impurities in snow and ice determined by spectrophotometric analysis of filters, *Appl. Opt.*, 50, 2037-2048, 2011.
- Guan, X., Huang, J., Guo, N., Bi, J., and Wang, G.: Variability of soil moisture and its relationship with surface albedo and soil thermal parameters over the Loess Plateau, *Adv. Atmos. Sci.*, 26, 692-700, 2009.
- Hadley, O. L., and Kirchstetter, T. W.: Black-carbon reduction of snow albedo, *Nat. Clim. Change*, 2, 437-440, 2012.
- Hansen, J., and Nazarenko, L.: Soot climate forcing via snow and ice albedos, *P. Natl. Acad. Sci. USA*, 101, 423-428, 2004.

- Hegg, D. A., Warren, S. G., and Grenfell, T. C.: Source attribution of black carbon in Arctic snow, Environ. Sci. Technol., 43, 4016-4021, 2009.
- Hegg, D. A., Warren, S. G., and Grenfell, T. C.: Sources of light-absorbing aerosol in arctic snow and their seasonal variation, Atmos. Chem. Phys., 10, 10923-10938, 2010.
- Hsu, S. C., Liu, S. C., Arimoto, R., et al.: Effects of acidic processing, transport history, and dust and sea salt loadings on the dissolution of iron from Asian dust, J. Geophys. Res.-Atmos., 115, 2010.
- Huang, J., Li, Y. F., Li, Z., and Xiong, L. F.: Spatial variations and sources of trace elements in recent snow from glaciers at the Tibetan Plateau, Environ. Sci. Pollut. R., 25, 7875-7883, 2018.
- Huang, J. P., Fu, Q., Zhang, W., Wang, X., Zhang, R. D., Ye, H., and Warren, S. G.: Dust and Black Carbon in Seasonal Snow across Northern China, Bull. Amer. Meteor. Soc., 92, 175-181, 2011.
- Jenkins, M., Kaspari, S., Kang, S. C., Grigholm, B., and Mayewski, P. A.: Tibetan plateau geladaindong black carbon ice core record (1843-1982): recent increases due to higher emissions and lower snow accumulation, Advances in Climate Change Research, 7(3), 132-138, 2016.
- Jeong, D., Kim, K., and Choi, W.: Accelerated dissolution of iron oxides in ice, Atmos. Chem. Phys., 12, 11125-11133, 10.5194/acp-12-11125-2012, 2012.
- Kang, S., Chen, F., Gao, T., Zhang, Y., Yang, W., Yu, W., and Yao, T.: Early onset of rainy season suppresses glacier melt: a case study on Zhadang glacier, Tibetan Plateau, J. Glaciol., 55(192), 755-758, 2009.
- Kaspari, S., Painter, T. H., Gysel, M., Skiles, S. M., and Schwikowski, M.: Seasonal and elevational variations of black carbon and dust in snow and ice in the Solu-Khumbu, Nepal and estimated radiative forcings, Atmos. Chem. Phys., 14, 8089-8103, 2014.
- Kirchstetter, T. W., Novakov, T., Hobbs, P. V.: Evidence that the spectral dependence of light absorption by aerosols is affected by organic carbon, J. Geophys. Res.-Atmos., 109, D21, 10.1029/2004JD004999, 2004.
- Kulkarni, S.: Assessment of source-receptor relationships of aerosols: an integrated forward and backward modeling approach, Dissertations and Theses-Gradworks, 2009.

- [Lafon, S., Rajot, J. L., Alfaro, S. C., and Gaudichet, A.: Quantification of iron oxides in desert aerosol, Atmos. Environ., 38, 1211-1218, 10.1016/J.Atmosenv.2003.11.006, 2004.](#)
- [Lafon, S., and Lee, A. B.: Diffusion maps and coarse-graining: a unified framework for dimensionality reduction, graph partitioning and data set parameterization, IEEE T. Pattern anal., 28, 1393-1403, 2006.](#)
- [Li C. L., Kang S. C., Zhang Q.: Elemental composition of Tibetan Plateau top soils and its effect on evaluating atmospheric pollution transport, Environ. Pollut., 157, 8-9, 2009.](#)
- [Li, C. L., Bosch, C., Kang, S. C., Andersson, A., Chen, P. F., Zhang, Q. G., Cong, Z. Y., Chen, B., Qin, D. H., and Gustafsson, O.: Sources of black carbon to the Himalayan-Tibetan Plateau glaciers, Nat. Commun., 7, 12574, 10.1038/ncomms12574, 2016.](#)
- [Li, X. F., Kang, S. C., He, X. B., Qu, B., Tripathee, L., Jing, Z. F., Paudyal, R., Li, Y., Zhang, Y. L., Yan, F. P., Li, G., and Li, C. L.: Light-absorbing impurities accelerate glacier melt in the Central Tibetan Plateau, Sci. Total Environ., 587, 482-490, 2017.](#)
- [Li, X. F., Kang, S. C., Zhang, G. S., Qu, B., Tripathee, L., Paudyal, R., Jing, Z. F., Zhang, Y. L., Yan, F. P., Li, G., Cui, X. Q., Xu, R., Hu, Z. F., and Li, C. L.: Light-absorbing impurities in a southern Tibetan Plateau glacier: Variations and potential impact on snow albedo and radiative forcing, Atmos. Res., 200, 77-87, 2018.](#)
- [Liou, K. N., Takano, Y., and Yang, P.: Light absorption and scattering by aggregates: Application to black carbon and snow grains, J. Quant. Spectrosc. Ra., 112, 1581-1594, 10.1016/J.Jqsrt.2011.03.007, 2011.](#)
- [Liu S. Y., Guo, W. Q., Xu J. L., et al.: The Second Glacier Inventory Dataset of China \(Version 1.0\), Cold and Arid Regions Science Data Center at Lanzhou, 10.3972/glacier.001.2013.db, 2014.](#)
- [Lüthi, Z. L., Škerlak, B., Kim, S.-W., Lauer, A., Mues, A., Rupakheti, M., and Kang, S.: Atmospheric brown clouds reach the Tibetan Plateau by crossing the Himalayas, Atmos. Chem. Phys., 15, 6007-6021, <https://doi.org/10.5194/acp-15-6007-2015>, 2015.](#)
- [Millikan, R. C.: Optical properties of soot, J. Opt. Soc. Am., 51, 698-699, 1961.](#)
- [Ming, J., Xiao, C. D., Cachier, H., Qin, D. H., Qin, X., Li, Z. Q., and Pu, J. C.: Black](#)

- [Carbon \(BC\) in the snow of glaciers in west China and its potential effects on albedos, Atmos. Res., 92, 114-123, 2009.](#)
- [Ming, J., Xiao, C. D., Du, Z. C., and Yang, X. G.: An overview of black carbon deposition in High Asia glaciers and its impacts on radiation balance, Adv. Water Resour., 55, 80-87, 2013.](#)
- [Ming, J., Xiao, C. D., Sun, J. Y., Kang, S. C., and Bonasoni, P.: Carbonaceous particles in the atmosphere and precipitation of the Nam Co region, central Tibet, J. Environ. Sci., 22, 1748-1756, 10.1016/S1001-0742\(09\)60315-6, 2010.](#)
- [Ming, J., Xiao, C. D., Wang, F. T., Li, Z. Q., and Li, Y. M.: Grey Tienshan Urumqi Glacier No.1 and light-absorbing impurities, Environ. Sci. Pollut. R., 23, 9549-9558, 2016.](#)
- [Moosmuller, H., Engelbrecht, J. P., Skiba, M., Frey, G., Chakrabarty, R. K., and Arnott, W. P.: Single scattering albedo of fine mineral dust aerosols controlled by iron concentration, J. Geophys. Res.-Atmos., 117, Artn D11210, 10.1029/2011jd016909, 2012.](#)
- [Niu, H. W., Kang, S. C., Zhang, Y. L., Shi, X. Y., Shi, X. F., Wang, S. J., Li, G., Yan, X. G., Pu, T., and He, Y. Q.: Distribution of light-absorbing impurities in snow of glacier on Mt. Yulong, southeastern Tibetan Plateau, Atmos. Res., 197, 474-484, 2017.](#)
- [Paatero, P., and Tapper, U.: Positive matrix factorization: a non-negative factor model with optimal utilization of error estimates of data values, Environmetrics, 5, 111-126, 1994.](#)
- [Pacyna, J. M. and Pacyna, E. G.: An assessment of global and regional emissions of trace metals to the atmosphere from anthropogenic sources worldwide, Environ. Rev., 9, 269-298, 2001.](#)
- [Painter, T. H., Barrett, A. P., Landry, C. C., Neff, J. C., Cassidy, M. P., Lawrence, C. R., McBride, K. E., and Farmer, G. L.: Impact of disturbed desert soils on duration of mountain snow cover, Geophys. Res. Lett., 34, L12502, 10.1029/2007gl030284, 2007.](#)
- [Painter, T. H., Deems, J. S., Belnap, J., Hamlet, A. F., Landry, C. C., and Udall, B.: Response of Colorado River runoff to dust radiative forcing in snow, P. Natl. Acad. Sci. USA, 107, 17125-17130, 2010.](#)
- [Painter, T. H., Bryant, A. C., and Skiles, S. M.: Radiative forcing by light absorbing impurities in snow from MODIS surface reflectance data, Geophys. Res. Lett., 39, L17502, 10.1029/2012gl052457, 2012.](#)

- Pang, H., He, Y., Theakstone, W. H., and Zhang, D. D.: Soluble ionic and oxygen isotopic compositions of a shallow firn profile, Baishui glacier No. 1, southeastern Tibetan Plateau, *Ann. Glaciol.*, 46, 325-330, 2007.
- Pio, C. A., Legrand, M., Oliveira, T., Afonso, J., Santos, C., Caseiro, A., Fialho, P., Barata, F., Puxbaum, H., Sanchez-Ochoa, A., Kasper-Giebl, A., Gelencser, A., Preunkert, S., and Schock, M.: Climatology of aerosol composition (organic versus inorganic) at nonurban sites on a west-east transect across Europe, *J. Geophys. Res.*, 112, D23S02, 10.1029/2006JD008038, 2007.
- Preunkert, S., Legrand, M., Stricker, P., Bulat, S., Alekhina, I., Petit, J. R., Hoffmann, H., May, B., and Jourdain B.: Quantification of Dissolved Organic Carbon at very low levels in natural ice samples by a UV induced oxidation method, *Environ. Sci. Technol.*, 45, 673–678, 2011.
- Pu, W., Wang, X., Wei, H. L., Zhou, Y., Shi, J. S., Hu, Z. Y., Jin, H. C., and Chen, Q. L.: Properties of black carbon and other insoluble light-absorbing particles in seasonal snow of northwestern China, *The Cryosphere*, 11, 1213-1233, 2017.
- Qian, Y., Flanner, M. G., Leung, L. R., and Wang, W.: Sensitivity studies on the impacts of Tibetan Plateau snowpack pollution on the Asian hydrological cycle and monsoon climate, *Atmos. Chem. Phys.*, 11, 1929-1948, 2011.
- Qian, Y., Yasunari, T. J., Doherty, S. J., Flanner, M. G., Lau, W. K. M., & Jing, M.: Light-absorbing particles in snow and ice: measurement and modeling of climatic and hydrological impact, *Adv. Atmos. Sci.*, 32, 64-91, 2015.
- Qin, D. H., Liu, S. Y., and Li, P. J.: Snow cover distribution, variability, and response to climate change in western China, *J. Climate*, 19, 1820-1833, 2006.
- Qiu, J.: The third pole, *Nature*, 454, 393-396, 10.1038/454393a, 2008.
- Qu, B., Ming, J., Kang, S. C., Zhang, G. S., Li, Y. W., Li, C. D., Zhao, S. Y., Ji, Z. M., and Cao, J. J.: The decreasing albedo of the Zhadang glacier on western Nyainqentanglha and the role of light-absorbing impurities, *Atmos. Chem. Phys.*, 14, 11117-11128, 2014.
- Ramanathan, V., Li, F., Ramana, M. V., et al.: Atmospheric brown clouds: Hemispherical and regional variations in long-range transport, absorption, and radiative forcing, *J. Geophys. Res.*, 112, D22S21, 10.1029/2006JD008124, 2007.

- [Sand, M., Berntsen, T. K., Seland, O., and Kristjansson, J. E.: Arctic surface temperature change to emissions of black carbon within Arctic or midlatitudes, J. Geophys. Res.-Atmos., 118, 7788-7798, 10.1002/Jgrd.50613, 2013.](#)
- [Skiles, S. M., Painter, T. H., Deems, J. S., Bryant, A. C., and Landry, C. C.: Dust radiative forcing in snow of the Upper Colorado River Basin: 2. Interannual variability in radiative forcing and snowmelt rates, Water Resour. Res., 48, 10.1029/2012wr011986, 2012.](#)
- [Takahashi, Y., Higashi, M., Furukawa, T., and Mitsunobu, S.: Change of iron species and iron solubility in Asian dust during the long-range transport from western China to Japan, Atmos. Chem. Phys., 11, 11237-11252, 10.5194/acp-11-11237-2011, 2011.](#)
- [Wang, M., Xu, B., Cao, J., et al.: Carbonaceous aerosols recorded in a southeastern Tibetan glacier: analysis of temporal variations and model estimates of sources and radiative forcing, Atmos. Chem. Phys., 15, 1191-1204, 10.5194/Acp-15-1191-2015, 2015.](#)
- [Wang, X., Doherty, S. J., and Huang, J. P.: Black carbon and other light-absorbing impurities in snow across Northern China, J. Geophys. Res.-Atmos., 118, 1471-1492, 2013.](#)
- [Wang, X., Xu, B. Q., and Ming, J.: An overview of the studies on Black Carbon and Mineral Dust deposition in Snow and Ice Cores in East Asia, J. Meteorol. Res., 28, 354-370, 2014.](#)
- [Wang, X., Pu, W., Ren, Y., Zhang, X., Zhang, X., Shi, J., Jin, H., Dai, M., and Chen, Q.: Observations and model simulations of snow albedo reduction in seasonal snow due to insoluble light-absorbing particles during 2014 Chinese survey, Atmos. Chem. Phys., 17, 2279-2296, 2017.](#)
- [Warren, S. G., and Wiscombe, W. J.: A Model for the Spectral Albedo of Snow. II: Snow Containing Atmospheric Aerosols, J. Atmos. Sci., 37, 2734-2745, 1980.](#)
- [Warren, S. G.: Optical-Properties of Snow, Rev. Geophys., 20, 67-89, 1982.](#)
- [Warren, S. G., and Wiscombe, W. J.: Dirty Snow after Nuclear-War, Nature, 313, 467-470, 10.1038/313467a0, 1985.](#)
- [Wedepohl, K. H.: The Composition of the Continental-Crust, Geochim. Cosmochim. Ac., 59, 1217-1232, 1995.](#)
- [Xu, B. Q., Yao, T. D., Liu, X. Q., and Wang, N. L.: Elemental and organic carbon](#)

- [measurements with a two-step heating-gas chromatography system in snow samples from the Tibetan Plateau, *Ann. Glaciol.*, 43, 257-262, 2006.](#)
- [Xu, B. Q., Cao, J. J., Hansen, J., Yao, T. D., Joswia, D. R., Wang, N. L., Wu, G. J., Wang, M., Zhao, H. B., Yang, W., Liu, X. Q., and He, J. Q.: Black soot and the survival of Tibetan glaciers, *P. Natl. Acad. Sci. USA*, 106, 22114-22118, 2009a.](#)
- [Xu, B. Q., Wang, M., Joswiak, D. R., Cao, J. J., Yao, T. D., Wu, G. J., Yang, W., and Zhao, H. B.: Deposition of anthropogenic aerosols in a southeastern Tibetan glacier, *J. Geophys. Res.-Atmos.*, 114, D17209, 10.1029/2008jd011510, 2009b.](#)
- [Xu, B. Q., Cao, J. J., Joswiak, D. R., Liu, X. Q., Zhao, H. B., and He, J. Q.: Post-depositional enrichment of black soot in snow-pack and accelerated melting of Tibetan glaciers, *Environ. Res. Lett.*, 7, 014022, 10.1088/1748-9326/7/1/014022, 2012.](#)
- [Yang, K., Ding, B., Qin, J., Tang, W., Lu, N., and Lin, C.: Can aerosol loading explain the solar dimming over the Tibetan Plateau?, *Geophys. Res. Lett.*, 39, 10.1029/2012GL053733, 2012.](#)
- [Yang, S., Xu, B. Q., Cao, J. J., Zender, C. S., and Wang, M.: Climate effect of black carbon aerosol in a Tibetan Plateau glacier, *Atmos. Environ.*, 111, 71-78, 2015.](#)
- [Yao, T. D., Thompson, L., Yang, W., Yu, W. S., Gao, Y., Guo, X. J., Yang, X. X., Duan, K. Q., Zhao, H. B., Xu, B. Q., Pu, J. C., Lu, A. X., Xiang, Y., Kattel, D. B., and Joswiak, D.: Different glacier status with atmospheric circulations in Tibetan Plateau and surroundings, *Nat. Clim. Change*, 2, 663-667, 2012.](#)
- [Yasunari, T. J., Koster, R. D., Lau, W. K. M., and Kim, K. M.: Impact of snow darkening via dust, black carbon, and organic carbon on boreal spring climate in the Earth system, *J. Geophys. Res.-Atmos.*, 120, 5485-5503, 2015.](#)
- [Zhang, R., Hegg, D. A., Huang, J., and Fu, Q.: Source attribution of insoluble light-absorbing particles in seasonal snow across northern China, *Atmos. Chem. Phys.*, 13, 6091-6099, 2013a.](#)
- [Zhang, R., Jing, J., Tao, J., Hsu, S. C., Wang, G., Cao, J., Lee, C. S. L., Zhu, L., Chen, Z., Zhao, Y., and Shen, Z.: Chemical characterization and source apportionment of PM_{2.5} in Beijing: seasonal perspective, *Atmos. Chem. Phys.*, 13, 7053-7074, 2013b.](#)

Zhang, Y. L., Kang, S. C., Li, C. L., Gao, T. G., Cong, Z. Y., Sprenger, M., Liu, Y. J., Li, X. F., Guo, J. M., Sillanpaa, M., Wang, K., Chen, J. Z., Li, Y., and Sun, S. W.: Characteristics of black carbon in snow from Laohugou No. 12 glacier on the northern Tibetan Plateau, *Sci. Total Environ.*, 607, 1237-1249, 2017.

Zhou, Y., Wang, X., Wu, X., Cong, Z., Wu, G., and Ji, M.: Quantifying light absorption of iron oxides and carbonaceous aerosol in seasonal snow across northern China, *Atmosphere*, 8, 63, 10.3390/atmos8040063, 2017. **References**

~~Agarwal, S., Aggarwal, S. G., Okuzawa, K., and Kawamura, K.: Size distributions of dicarboxylic acids, ketoacids, α -dicarbonyls, sugars, wsoe, oe, ec and inorganic ions in atmospheric particles over northern japan: implication for long-range transport of siberian biomass burning and east asian polluted aerosols, *Atmos. Chem. Phys.*, 10, 5839-5858, 2010.~~

~~Akagi, S. K., Yokelson, R. J., Wiedinmyer, C., and Alvarado, M. J.: Emission factors for open and domestic biomass burning for use in atmospheric models, *Atmos. Chem. Phys.*, 11, 27523-27602, 2011.~~

~~Alexander, B., Allman, D. J., Amos, H. M., Fairlie, T. D., Dachs, J., and Hegg, D. A.: Isotopic constraints on the formation pathways of sulfate aerosol in the marine boundary layer of the subtropical northeast atlantic ocean, *J. Geophys. Res.-Atmos.*, 117, D06304, doi: 10.1029/2011JD016773, 2012.~~

~~Alexander, B., and Mickley, L. J.: Paleo-perspectives on potential future changes in the oxidative capacity of the atmosphere due to climate change and anthropogenic emissions, *Current Pollution Reports*, 1, 57-69, 2015.~~

~~Andersson, A., Deng, J., Du, K., Zheng, M., Yan, C., and Sköld, M.: Regionally-varying combustion sources of the January 2013 severe haze events over eastern China, *Environ. Sci. Technol.*, 49, 2038-2043, 2015.~~

~~Andreae, M. O., and Rosenfeld, D.: Aerosol-cloud-precipitation interactions. Part 1. The nature and sources of cloud-active aerosols, *Earth Sci. Rev.*, 8, 13-41, 2008.~~

~~Banta, J. R., McConnell, J. R., Frey, M. M., Bales, R. C., and Taylor, K.: Spatial and temporal variability in snow accumulation at the West Antarctic Ice Sheet Divide over recent centuries, *J. Geophys. Res.*, 113, D23102, doi: 10.1029/2008JD010235,~~

2008.

- Begum, B. A., Nasiruddin, M., Biswas, S. K.: Trend and spatial distribution of air particulate matter pollution in Dhaka city, *Journal of Bangladesh Academy of Sciences*, 34, 151-157, 2010a.
- Begum, B. A., Biswas, S. K., Hopke, P. K.: Identification of sources of fine and coarse particulate matter in Dhaka, Bangladesh, *Aerosol and Air Qual. Res.*, 10, 345-353, 2010b.
- Bergstrom, C.: Measuring the value and prestige of scholarly journals, *College and Research Libraries News*, 68, 314-316, 2007.
- Bond, T. C., Charlson, R. J., and Heintzenberg, J.: Quantifying the emission of light-absorbing particles: Measurements tailored to climate studies, *Geophys. Res. Lett.*, 25, 337-340, 1998.
- Bond, T. C.: Spectral dependence of visible light absorption by carbonaceous particles emitted from coal combustion, *Geophys. Res. Lett.*, 28, 4075-4078, 2001.
- Bond, T. C., Streets, D. G., Yarber, K. F., Nelson, S. M., Woo, J. H., and Klimont, Z.: A technology based global inventory of black and organic carbon emissions from combustion, *J. Geophys. Res. Atmos.*, 109, D14203, doi: 10.1029/2003JD003697, 2004.
- Bond, T. C., and Bergstrom, R. W.: Light absorption by carbonaceous particles: An investigative review, *Aerosol Sci. Technol.*, 40, 27-67, 2006.
- Alfaro, S. C., Lafon, S., Rajot, J. L., Formenti, P., Gaudichet, A., and Maille, M.: Iron oxides and light absorption by pure desert dust: An experimental study, *J. Geophys. Res. Atmos.*, 109, Artn D08208
Doi 10.1029/2003jd004374, 2004.
- Brandt, R. E., Warren, S. G., and Clarke, A. D.: A controlled snowmaking experiment testing the relation between black carbon content and reduction of snow albedo, *J. Geophys. Res. Atmos.*, 116, Artn D08109
Doi 10.1029/2010jd015330, 2011.
- Cong, Z. Y., Kang, S. C., Smirnov, A., and Holben, B.: Aerosol optical properties at Nam Co, a remote site in central Tibetan Plateau, *Atmos. Res.*, 92, 42-48, Doi

- 10.1016/J.Atmosres.2008.08.005, 2009.
- Federer, U., Kaufmann, P. R., Hutterli, M. A., Schupbach, S., and Stocker, T. F.: Continuous Flow Analysis of Total Organic Carbon in Polar Ice Cores, *Environ. Sci. Technol.*, 42, 8039–8043, 10.1021/es801244c, 2008.
- Hadley, O. L., and Kirchstetter, T. W.: Black-carbon reduction of snow albedo, *Nat. Clim. Chang.*, 2, 437–440, 10.1038/Nclimate1433, 2012.
- Huang, J. P., Fu, Q. A., Zhang, W., Wang, X., Zhang, R. D., Ye, H., and Warren, S. G.: Dust and Black Carbon in Seasonal Snow across Northern China, *Bull. Amer. Meteor. Soc.*, 92, 175–181, 10.1175/2010bams3064.1, 2011.
- Jeong, D., Kim, K., and Choi, W.: Accelerated dissolution of iron oxides in ice, *Atmos. Chem. Phys.*, 12, 11125–11133, DOI 10.5194/acp-12-11125-2012, 2012.
- Kaspari, S., Painter, T. H., Gysel, M., Skiles, S. M., and Schwikowski, M.: Seasonal and elevational variations of black carbon and dust in snow and ice in the Solu-Khumbu, Nepal and estimated radiative forcings, *Atmos. Chem. Phys.*, 14, 8089–8103, Doi 10.5194/Acp-14-8089-2014, 2014.
- Lafon, S., Rajot, J. L., Alfaro, S. C., and Gaudichet, A.: Quantification of iron oxides in desert aerosol, *Atmos. Environ.*, 38, 1211–1218, Doi 10.1016/J.Atmosenv.2003.11.006, 2004.
- Lafon, S., Sokolik, I. N., Rajot, J. L., Caquineau, S., and Gaudichet, A.: Characterization of iron oxides in mineral dust aerosols: Implications for light absorption, *J. Geophys. Res.-Atmos.*, 111, Artn D21207 Doi 10.1029/2005jd007016, 2006.
- Moesmuller, H., Engelbrecht, J. P., Skiba, M., Frey, G., Chakrabarty, R. K., and Arnott, W. P.: Single scattering albedo of fine mineral dust aerosols controlled by iron concentration, *J. Geophys. Res.-Atmos.*, 117, Artn D11210 10.1029/2011jd016909, 2012.
- Painter, T. H., Deems, J. S., Belnap, J., Hamlet, A. F., Landry, C. C., and Udall, B.: Response of Colorado River runoff to dust radiative forcing in snow, *Proc Natl Acad Sci U S A*, 107, 17125–17130, doi:10.1073/pnas.0913139107, 2010.
- Painter, T. H., Bryant, A. C., and Skiles, S. M.: Radiative forcing by light absorbing

- impurities in snow from MODIS surface reflectance data, *Geophys. Res. Lett.*, **39**, n/a–n/a, doi:10.1029/2012gl052457, 2012.
- Preunkert, S., Legrand, M., Stricker, P., Bulat, S., Alekhina, I., Petit, J. R., Hoffmann, H., May, B., and Jourdain, B.: Quantification of Dissolved Organic Carbon at Very Low Levels in Natural Ice Samples by a UV-Induced Oxidation Method, *Environ. Sci. Technol.*, **45**, 673–678, 10.1021/es1023256, 2011.
- Qiu, J.: The third pole, *Nature*, **454**, 393–396, Doi 10.1038/454393a, 2008.
- Takahashi, Y., Higashi, M., Furukawa, T., and Mitsunobu, S.: Change of iron species and iron solubility in Asian dust during the long-range transport from western China to Japan, *Atmos. Chem. Phys.*, **11**, 11237–11252, DOI 10.5194/acp-11-11237-2011, 2011.
- Wang, X., Doherty, S. J., and Huang, J. P.: Black carbon and other light-absorbing impurities in snow across Northern China, *J. Geophys. Res.-Atmos.*, **118**, 1471–1492, 10.1029/2012jd018291, 2013.
- Wang, X., Xu, B. Q., and Ming, J.: An Overview of the Studies on Black Carbon and Mineral Dust Deposition in Snow and Ice Cores in East Asia, *J Meteorol Res Pre*, **28**, 354–370, Doi 10.1007/S13351-014-4005-7, 2014.
- Wang, X., Pu, W., Ren, Y., Zhang, X., Zhang, X., Shi, J., Jin, H., Dai, M., and Chen, Q.: Observations and model simulations of snow albedo reduction in seasonal snow due to insoluble light-absorbing particles during 2014 Chinese survey, *Atmos. Chem. Phys.*, **17**, 2279–2296, 10.5194/acp-17-2279-2017, 2017.
- Warren, S. G., and Wiscombe, W. J.: A Model for the Spectral Albedo of Snow .2. Snow Containing Atmospheric Aerosols, *J. Atmos. Sci.*, **37**, 2734–2745, 10.1175/1520-0469(1980)037<2734:Amftsa>2.0.Co;2, 1980.
- Warren, S. G.: Optical Properties of Snow, *Rev. Geophys.*, **20**, 67–89, Doi 10.1029/Rg020i001p00067, 1982.
- Warren, S. G., and Wiscombe, W. J.: Dirty Snow after Nuclear War, *Nature*, **313**, 467–470, 10.1038/313467a0, 1985.
- Yang, K., Ding, B., Qin, J., Tang, W., Lu, N., and Lin, C.: Can aerosol loading explain the solar dimming over the Tibetan Plateau?, *Geophys. Res. Lett.*, **39**,

~~10.1029/2012GL053733, 2012.~~

~~Yao, T. D., Thompson, L., Yang, W., Yu, W. S., Gao, Y., Guo, X. J., Yang, X. X., Duan, K. Q., Zhao, H. B., Xu, B. Q., Pu, J. C., Lu, A. X., Xiang, Y., Kattiel, D. B., and Joswiak, D.: Different glacier status with atmospheric circulations in Tibetan Plateau and surroundings, *Nat. Clim. Chang.*, 2, 663–667, Doi 10.1038/Nclimate1580, 2012.~~

~~Yasunari, T. J., Koster, R. D., Lau, W. K. M., and Kim, K. M.: Impact of snow darkening via dust, black carbon, and organic carbon on boreal spring climate in the Earth system, *J. Geophys. Res. Atmos.*, 120, 5485–5503, 10.1002/2014jd022977, 2015.~~

~~Zhao, Z., Cao, J., Shen, Z., Xu, B., Zhu, C., Su, X., Liu, S., Han, Y., Wang, G., and Kinfa, Ho.: Aerosol particles at a high-altitude site on the Southeast Tibetan Plateau, China: Implications for pollution transport from South Asia, *J. Geophys. Res. Atmos.*, 118, 11360–11375, 2013.~~

~~Zhang, R., Hegg, D. A., Huang, J., and Fu, Q.: Source attribution of insoluble light-absorbing particles in seasonal snow across northern China, *Atmos. Chem. Phys.*, 13, 6091–6099, 2013a.~~

~~Zhang, R., Jing, J., Tao, J., Hsu, S. C., Wang, G., Cao, J., Lee, C. S. L., Zhu, L., Chen, Z., Zhao, Y., and Shen, Z.: Chemical characterization and source apportionment of PM_{2.5} in Beijing: seasonal perspective, *Atmos. Chem. Phys.*, 13, 7053–7074, 2013b.~~

~~Zhang Y. L., Kang, S., Li, C., Gao, T., Cong, Z., Sprenger, M., Liu, Y., Li, X., Guo, J., Sillanpää, M., Wang, K., Chen, J., Li, Y., Sun, S.: Characteristics of black carbon in snow from Laohugou No. 12 glacier on the northern Tibetan Plateau, *Sci. Total Environ.*, 607–608, 1237–1249, 2017.~~

~~Zhang Y., Kang, S., Sprenger, M., Cong, Z., Gao, T., Li, C., Tao, S., Li, X., Zhong, X., Xu, M., Meng, W., Neupane, B., Qin, X., Sillanpää, M.: Black carbon and mineral dust in snow cover on the Tibetan Plateau, *The Cryosphere*, 12, 413–431, 2018.~~

~~Zhou, Y., Wang, X., Wu, X., Cong, Z., Wu, G., and Ji, M.: Quantifying light absorption of iron oxides and carbonaceous aerosol in seasonal snow across northern China, *Atmosphere*, 8, 63, doi: 10.3390/atmos8040063, 2017.~~

~~Zhang, X., Liu, Z., Hecobian, A., Zheng, M., Frank, N. H., and Edgerton, E. S.: Spatial and seasonal variations of fine particle water-soluble organic carbon (wsoc) over the southeastern united states: implications for secondary organic aerosol formation, Atmos. Chem. Phys., 12, 6593-6607, 2012.~~